JOURNAL OF THE Electrochemical Society

UNIV. OF UTAH
1951
Engineering Library

Vol. 98, No. 6 June, 1951

Published Monthly by

THE ELECTROCHEMICAL SOCIETY

Journal of the

Electrochemical Society

JUNE, 1951 VOLUME 98 • NUMBER 6

CONTENTS

Anodic Corrosion of Lead in H_2SO_4 Solutions. *J. J. Lander* 213
Some Preliminary Studies of Positive Grid Corrosion in the Lead-Acid Cell. *J. J. Lander* 220
Bright Nickel Plating on Metallic Single Crystals in the Absence of Addition Agent. *Henry Leidheiser, Jr., and Allan T. Gwathmey* 225
Amperometric Titrations of Sn^{IV} and Hg^{II} with Tetraphenyl arsonium Chloride. *I. M. Kolthoff and Ralph A. Johnson* 231
The Mechanism and Rate of Dissolution of Titanium in Hydrofluoric Acid. *M. E. Straumanis and P. C. Chen* 234
The Kinetics of the Oxidation of Cobalt. *Earl A. Gulbransen and Kenneth F. Andrew* 241
Discussion Section 252

Feature Section

The Ideal Phosphor. *Roland Ward* 75C

Current Affairs

Washington Meeting Report 78C
Activities of the Board of Directors 79C
Hunter to Propose Nominating Committee 79C
Divisions Elect Officers in Washington 80C
News Notes 81C
Section News 82C
Personals 82C
Meetings of Other Organizations 82C
New Members 83C
Notes from Industry 83C
Recent Patents 83C
Constitution of The Electrochemical Society, Inc. 84C

EDITORIAL STAFF

R. M. Burns, *Chairman*

Norman Hackerman, *Technical Editor* Eleanor Reid, *Managing Editor* F. L. Laque, *Business Manager*
Cecil V. King, *Associate Editor* Mary F. Murray, *Assistant Editor* U. B. Thomas, *News Editor*

DIVISIONAL EDITORS: J. M. Bialosky, *Corrosion*; Abner Brenner, *Electrodeposition*; N. C. Cahoon, *Battery*; H. C. Froelich, *Electronics*; W. C. Gardiner, *Industrial Electrolytic*; S. J. Sindeband, *Electrothermic*; R. R. Ralston, *Electric Insulation*; L. B. Rogers, *Theoretical*; Sherlock Swann, Jr., *Electro-Organic*

REGIONAL EDITORS: Joseph A. Schulein, *Pacific Northwest*; J. C. Schumacher, *Los Angeles*; O. W. Storey, *Chicago*; G. W. Heise, *Cleveland*; Paul S. Brallier, *Niagara Falls*; Oliver Osborn, *Houston*; Earl A. Gulbransen, *Pittsburgh*; J. W. Cuthbertson, *Great Britain*; T. L. Rama Char, *India*

Advertising: Richard Rimbach Associates—James Condon, 36 Myrtle St., *Boston;* Richard Rimbach, Jr., 551 Fifth Ave., *New York;* William J. Gallagher, 3701 N. Broad St., *Philadelphia;* C. F. Goldcamp, 921 Ridge Ave., *Pittsburgh;* Harold Haskett, 360 N. Mich. Ave., *Chicago;* James R. Wright, 411 N. Tenth St., *St. Louis;* M. D. Pugh, 2721 N. Marengo Ave., *Altadena (Los Angeles).*

Published monthly by The Electrochemical Society, Inc., Mt. Royal and Guilford Aves., Baltimore 2, Md., combining the Journal and Transactions of The Electrochemical Society. Editorial Office: 235 W. 102nd St., New York 25, N. Y. Business Office: Mt. Royal and Guilford Aves., Baltimore 2, Md., or 235 W. 102nd St., New York 25, N. Y. Statements and opinions given in articles and papers in the Journal of The Electrochemical Society are those of the contributors, and The Electrochemical Society assumes no responsibility for them. Subscription: $8.50 to members, $12.00 to nonmembers. Single copies $1.00 to members, $1.25 to nonmembers. Copyright 1951 by The Electrochemical Society. Entered as second-class matter November 15, 1947, at the Post Office at Baltimore, Md., under the act of August 24, 1912.

Editorial

Aims for the Coming Year

AT THE BEGINNING of each year, we make new resolutions. In this spirit the Editor has asked the incoming President to state his resolutions, desires, and aims. Naturally, such resolutions and aims should be toward the constant advance of our Society, and the industry it represents.

For several years, there has been a growing feeling among your officers that the importance of electrochemistry is not recognized by the profession itself, or by the colleges that should prepare the future leaders in electrochemistry.

The statistics of production eloquently bespeak the rapid growth of the electrochemical industry. Whereas general industrial production has doubled in about 30 years, the chemical process industries have doubled every 10 years, the petroleum industry every 13 years, the electroprocess industries, as represented by chlorine, aluminum, magnesium, electric steel, and furnace alloys, have doubled in every 4 to 8 years. This rate of increase is matched only by the glamorous synthetic resins industry which has doubled every 6 years.

As further proof of the importance of electrochemical products, we might quote the fact that in considering the expansion of the chemical industry for the war emergency, chlorine was the chemical first studied, and its importance may be gauged by the fact that it was the first chemical in which the manufacturers as a group were given amortization certificates. Our Society is indeed fortunate in being the representative of so healthy and important a part of the American manufacturing economy.

Of course, such growth, volume, and expansion require men trained in the theory and practice of the industry. We hope the colleges will recognize this, and that they are not overlooking the demand for men trained in this field. We hope the members of the industry, as represented by our Society, will urge educational institutions to supply us with an adequate number of well-trained men, since the improvement of processes depends upon modern advancing technology.

Let it be an aim of the coming year, and for many to follow, to be proud of our profession, and of its past accomplishments, ever remembering that its future can only be assured by our present efforts and the preparation of the leaders who follow us.

R. M. HUNTER

Practical Methods for Determining Impurities in Nickel Plating Baths

SILICA can be easily determined by either gravimetric or colorimetric methods.

Colorimetrically, soluble silica is determined by measuring the amount of incident light absorbed by yellow silico-molybdate complex—the reaction product of ammonium molybdate and silicic acid.

The gravimetric method requires that silica be dehydrated with perchloric acid, filtered, ignited and weighed. After being volatilized with hydrofluoric acid and reweighed, difference in weight shows the true amount.

SODIUM and POTASSIUM are revealed by using flame photometry. The diluted bath sample is atomized in the flame photometer. Intensity of the characteristic light of either sodium or potassium is measured with respect to a standard. Concentration of the ion in the diluted sample is read off a calibration curve.

CADMIUM can be determined after copper and iron are removed by precipitation with cupferron and extraction with amyl acetate. Cadmium is precipitated with 2-mercaptobenzothiazole in an ammoniacal solution and extracted with chloroform. Then it is returned to an aqueous medium by shaking the extract with hydrochloric acid. The solution is made strongly alkaline with sodium hydroxide solution and the cadmium is extracted with a carbon tetrachloride solution of dithizone. After dilution, the extinction of the colored system is measured.

ALUMINUM may be determined colorimetrically after removing interfering metals. Color of the aluminon lake is developed by adding aluminon and a buffer to adjust pH to 5.5 and transmittancy of the lake is measured with a colorimeter.

AMMONIUM is separated from the bath by alkali treatment and steam distillation with a micro Kjeldahl apparatus. The ammonia is treated with Nessler's reagent, and the color developed is measured photometrically.

CHROMIUM: To determine chromate chromium, any reducing agents are oxidized with nitric acid. Diphenylcarbazide is added, the transmittancy of the solution is measured, and the amount of CrO_3 present as chromate read off a calibration curve.

For total chromium, any iron, organic compounds, reducing agents, and chlorides are removed, after which the chromium is oxidized with ammonium persulfate. Transmittancy of the solution is measured and the amount of CrO_3 read off a calibration curve.

ZINC is determined colorimetrically. Copper and iron are first removed; then heavy metal impurities including nickel are complexed with sodium di(B-hydroxyethyl)dithiocarbomate. Zinc dithizonate is formed in the presence of these complexes, when a carbon tetrachloride solution of dithizone is added. After removal of excess dithizone, zinc is determined colorimetrically.

CALCIUM is determined by precipitating the heavy metals as hydroxides, and then separating the calcium from the filtrate by precipitating it as the oxalate at a controlled pH. The calcium oxalate is converted to oxalic acid, and the acid is allowed to reduce a known amount of potassium permanganate. Transmittancy of the residual potassium permanganate solution is then measured.

A.E.S. RESEARCH PROGRAM

The American Electroplaters' Society is conducting a comprehensive research program and has developed useful information on current plating problems. International Nickel, in addition to its other support of this program, feels that it will be a further service to make copies of these A.E.S. Research Reports available.

For an authoritative, detailed, 84-page study of this subject, we offer you a free copy of the A.E.S. Research Report, Serial No. 6, entitled *"Determination of Impurities in Electroplating Solutions."* Use the coupon now.

EMBLEM OF INCO SERVICE

The International Nickel Company, Inc.
Dept. JES, 67 Wall Street
New York 5, N. Y.

Please send me a copy of A.E.S. Research Report, Serial No. 6, entitled "Determination of Impurities in Electroplating Solutions."

Name.....Title.....

Company.....

Address.....

City.....State.....

THE INTERNATIONAL NICKEL COMPANY, INC. 67 WALL STREET NEW YORK 5, N.Y.

Anodic Corrosion of Lead in H_2SO_4 Solutions[1]

J. J. Lander

Naval Research Laboratory, Washington, D. C.

ABSTRACT

Pure lead was anodized at various constant potentials in sulfuric acid solutions. At potentials below those for PbO_2 formation, a layer of tetragonal PbO is formed near the lead. $PbSO_4$ is formed as an outer layer. The rate of corrosion of Pb was found to increase with increasing temperature and decreasing acid concentration and is given by the equation: $w = ct^n$. At constant time, weight loss is related to potential by the equation: $\log w = A + BV$. At higher potentials a protective film, presumably PbO_2, is formed.

Introduction

This experimental work was conducted in an attempt to obtain fundamental information which might be applied in retarding corrosion of the positive grid in the lead-acid battery. This grid is subjected to severe anodic corrosion which may result in disintegration of the grid structure and failure of the battery. It is a problem of primary importance, especially because some recent applications require thinner grids in order to obtain greater high-rate capacities.

Previous investigators have usually used constant current methods in corrosion studies, but because there are at least three possible corrosion products of lead, depending on potential, and because the positive grids of batteries which are on float in telephone service operate under essentially different potential conditions and are much less rapidly corroded than the positives of those in cycling service, it was decided to study rates at constant potentials under various conditions of temperature and acid concentration. It was hoped that the data could be analyzed and compared with the various theoretical equations for rate processes, thus deriving some knowledge about the corrosion mechanism.

Similar work has been reported (1) previously which involved potentials different from the range studied here.

Experimental

"Baker's Analyzed" granular lead (about 99.97% pure) was melted in a clean glass beaker, cast into slugs in a steel mold, and cold-rolled to a thickness of 0.051 cm (0.02 in.) between polished steel rolls. Samples, cut always to the same dimensions giving a total area of 34 cm^2 (13.4 $in.^2$) were maintained at several constant potentials in sulfuric acid solutions in the range covering about one volt below the reversible potentials for the PbO_2-$PbSO_4$ couple. Some work was also done at potentials above that for PbO_2 formation. The sulfuric acid was used in concentrations of 40, 30, and 10 per cent by weight, and two constant temperatures: 30° and 50°C (86° and 122°F) were employed. The rates of attack were followed either by stripping the film in ammonium acetate solution and determining weight loss directly or by recording the currents flowing through the samples. By checking measured weight losses against those calculated from Faraday's law, it was established that the law, calculated for the reaction: $Pb \rightarrow Pb^{++} + 2e$, applies at potentials below those for PbO_2 formation. X-ray analyses of the film substance were obtained by methods previously used (2).

The circuit diagram of the apparatus used for maintaining constant potential is shown in Fig. 1. A resistor R_1, consisting of several feet of copper wire, was connected in series with the variable resistors R_3 and R_4, so that currents producing potential drops up to 1.1 volts across R_1 could be made to flow. B, the sample to be anodized, was contained in a beaker of sulfuric acid electrolyte, and could be connected to any position on R_1 through R_2, a two-ohm resistor, from which leads ran to a G.E. potentiometer recorder. A and A′ were sections of positive plate from a lead-acid cell, having a capacity such that currents of the magnitude drawn by the samples produced no polarization. They were connected by switches S_1 and S_2 to either end of the slide wire so that a given potential, anodic or cathodic to that of the PbO_2 plate, could be applied to the sample. C was a mercury-mercurous sulfate reference electrode, the tip of which was kept within 1 mm of the sample. The contribution to the potential by the ohmic resistance between sample and reference electrode was estimated to be considerably less than 1 mv for a current of 10 ma. The reference

[1] Manuscript received June 15, 1950. This paper prepared for delivery before the Buffalo Meeting, October 11 to 13, 1950.

electrode and the sample were connected to a Rubicon Null-point potentiometer. The sample potential was adjusted manually by sliding the contact from R_2 along R_1 and by adjusting the resistors R_3 and R_4. Potentials were controlled to within ±0.01 volt and variations within this range did not introduce significant errors. Current-time curves were plotted from the record, and weight-loss vs. time curves were then calculated using small increments of the area under the curve and Faraday's law.

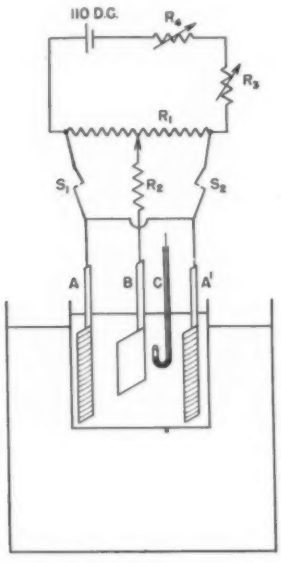

FIG. 1. Diagram of apparatus

Nernst equation for the reactions:

$$Pb + H_2O \rightarrow PbO + 2H^+ + 2e$$

and

$$Pb + 2H_2O \rightarrow Pb(OH)_2 + 2H^+ + 2e.$$

RESULTS AND DISCUSSION

The first experiment was preliminary in nature. Weighed samples were run at a series of potentials from 0.70 to 1.55 volts in 40 per cent by weight acid at 30°C (86°F). Individual samples were removed at various times up to seven hours, the films stripped off, and the weight loss determined. The results are shown in Fig. 2. About half the points recorded are mean values for two or more samples. The samples began to gas oxygen visibly at 1.40 volts.

These results show that the rate of attack increases rapidly with potential and reaches a maximum at about 1.0–1.1 volts, after which it falls off giving a broad minimum from about 1.2 to 1.5 volts. At 1.55 volts the rate begins to increase rapidly again. This behavior is shown in Fig. 3, where weight losses at the end of three and seven hours are plotted against the potential. It is noteworthy that the reversible potential for the PbO_2, $PbSO_4$ couple lies at 1.18 for this solution. X-ray patterns obtained for these samples showed that the heavier coats (1.0 volts, seven hours) consisted primarily of $PbSO_4$ on the surface, even though the samples were reddish brown in color. No pattern could be obtained for the films formed at the higher voltages, possibly because they were too thin.

TABLE I. *Potentials of various electrodes referred to the Hg, Hg_2SO_4 electrode in 40.8% H_2SO_4 at 20°C*

Electrode	$E°$	Concentration of H_2SO_4					
		10%		30%		40%	
		30°C	50°C	30°C	50°C	30°C	50°C
PbO_2, $PbSO_4$	+1.685	+1.063	+1.058	+1.135	+1.131	+1.181	+1.177
Hg, Hg_2SO_4	+0.615	+0.104	+0.099	+0.038	+0.031	+0.000	−0.004
Pb, PbO	+0.250	−0.348	−0.351	−0.306	−0.306	−0.280	−0.277
Pb, $Pb(OH)_2$	+0.242	−0.357	−0.360	−0.312	−0.312	−0.280	−0.277
Pb, $PbSO_4$	−0.355	−0.865	−0.873	−0.933	−0.942	−0.970	−0.979

All voltages are referred to the mercury-mercurous sulfate electrode in 40.8 per cent sulfuric acid at 20°C, which has a potential of +0.566 to the standard hydrogen electrode. For purposes of orientation the reversible potentials of the several couples under the various experimental conditions with respect to this electrode are given in Table I. Standard potentials are also included. These values were all calculated from the data of Harned and Hamer (3) except for the Pb, PbO, and Pb, $Pb(OH)_2$ couples for which $E°$'s were calculated using the free energy data from Latimer (4) and the other values using the

The minimum[2] in the weight-loss vs. potential curve shows that the film formed above the PbO_2, $PbSO_4$ reversible potential is protective. Several samples were run for periods up to 16 and 24 hours. The weight losses were still very low as shown in Table II, where the data for 3 and 7 hours are also given for comparison. Based on weight losses these films may be estimated to be 300–3000 Å thick. Oxygen must be discharged either at the lead surface

[2] This minimum is also exhibited at lower concentrations and higher temperatures. See the data for 1.3 volts, 10% acid, and 50°C (122°F), Fig. 7.

or the film surface, and since the films are protective, the latter situation is quite likely. If this is true, the film is a good electronic conductor and probably

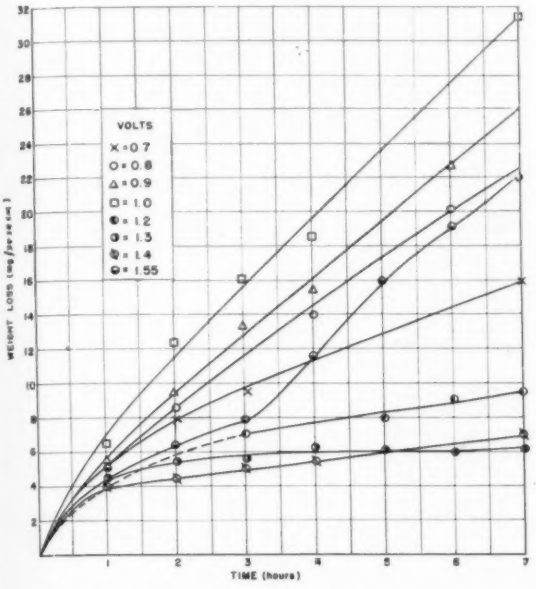

FIG. 2. Rate of attack of Pb anodes at constant potential in 40% H_2SO_4 at 30°C.

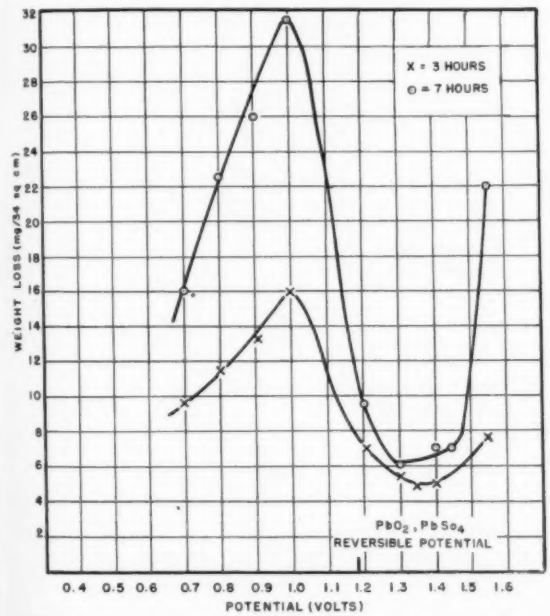

FIG. 3. Total attack of Pb anodes after 3 and after 7 hours in 40% H_2SO_4 at 30°C.

consists of PbO_2 which has a conductivity approaching that of metals.

Next a few samples were anodized for 25 hours at several potentials in the range 1.0 to 0.0 volt in several concentrations of acid at several temperatures. X-ray analysis showed that the grayish-white surface film obtained was almost entirely $PbSO_4$.

TABLE II. *Weight losses for Pb anodes (mg/34 cm²) in 40% H_2SO_4 at 30°C (86°F)*

Time (hours)	Potential (volts)		
	1.2	1.3	1.4
3	7.1	5.7	5.0
7	9.5	6.2	7.0
16	9.5	9.4	9.1
24	11.8		9.9

It was loosely adherent and could be wiped off with cotton or a soft wooden wedge, whereupon a brown to black underfilm was exposed, which x-ray analysis proved to be tetragonal PbO. This film is either very unreactive or is protected to a considerable degree by the covering $PbSO_4$ film from chemical reaction with the electrolyte. The PbO film was observed at potentials as low as 0.1 volt and under all conditions of temperature and concentration. This potential corresponds approximately to the maximum oxidizing potential employed by Wolf and Bonilla (1).

Most of the experimental work was concerned with corrosion rate studies at constant potentials in the range 1.0 to −0.1 volt. Rate curves were determined for periods up to 25 hours for 30 per cent and 10 per cent acid both at 30° and 50°C (86° and 122°F). The weight-loss data calculated from the current-time curves for the four sets of conditions are given in Fig. 4, 5, 6, and 7. From a study of the data two results are apparent: increase in temperature and decrease in concentration both appreciably increase the rate of attack.

On the basis of the facts that corrosion decreases with increasing acid concentration and that it is thermodynamically possible for water to furnish the oxygen for PbO formation, it might be considered that the water molecule itself could be the attacking agent from solution (i.e., not OH^- or other ions which may be furnished by water). If the weight losses for four and seven hours for the three concentrations at 30°C (86°F) are plotted against the square of the activity of the water [calculated from vapor pressure data (5)], an approximately linear[3] relationship is found, as shown in Fig. 8. This analysis is by no means proof that the water molecule itself is directly involved but it is presented to indicate such a possibility.

[3] An alternative method of plotting, i.e., log w vs. log a, may be used to indicate more nicely that the relationship is w vs. a^2. This may be interpreted to mean that the electrochemical part of the corrosion reaction is: $Pb + 2H_2O \rightarrow Pb(OH)_2 + 2H^+ + 2e$, followed by a chemical decomposition: $Pb(OH)_2 \rightarrow PbO + H_2O$.

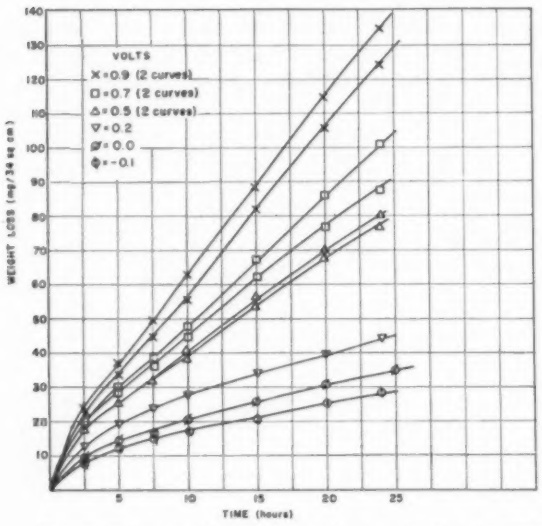

FIG. 4. Rate of attack at constant potential in 30% H_2SO_4 at 30°C.

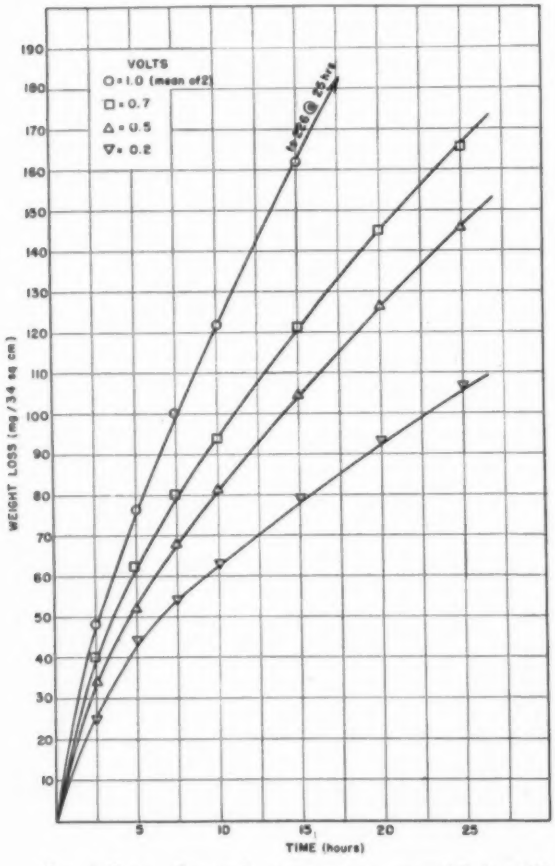

FIG. 5. Rate of attack at constant potential in 30% H_2SO_4 at 50°C.

If the weight-loss vs. time data are plotted on log-log paper it is found that the curves are approximately linear after about two to five hours, the slopes of the curves varying from about 0.90 at the high potentials to about 0.55 at the low potentials. This is illustrated in Fig. 9, where the curves of Fig. 6 are replotted. Thus the relationship between weight loss and time is approximately described by the equation: $w = ct^n$, where n may take on values of 0.55 to 0.90 under the various conditions and c also takes on different values depending on conditions.

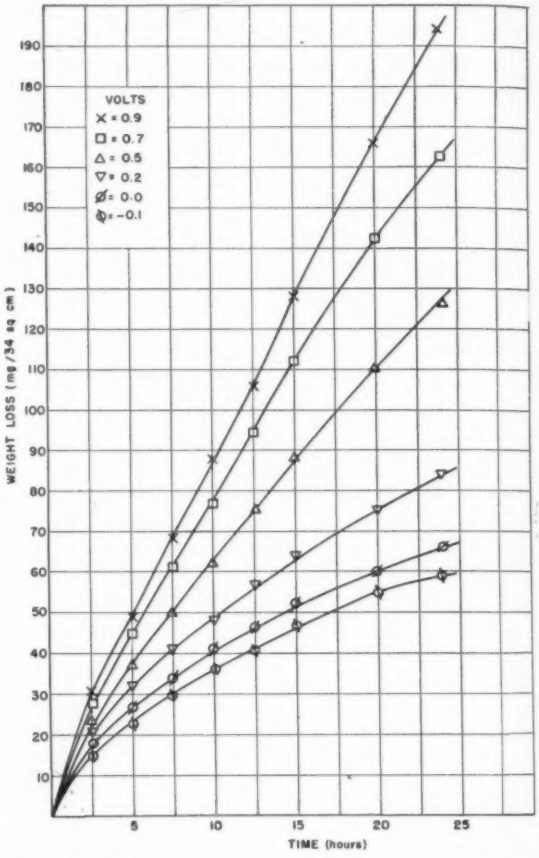

FIG. 6. Rate of attack at constant potential in 10% H_2SO_4 at 30°C.

A result which is probably more significant is obtained when log w at constant time is plotted against V. Fig. 10 shows such a plot at various times, again using the data from the curves of Fig. 6. These curves are linear within experimental error and those illustrated are typical of the whole data. Consequently weight loss in the voltage range studied may further be described by the empirical relation: $\log w = A + BV$. The activation equation, which has been applied (6–10) to various other electrochemical systems, can be indicated to be of the same form. We may use a simple form of the equation:

$$i = ke^{\alpha z\mathbf{F}V/RT}, \qquad \text{(I)}$$

where: i = the true current density;
k = a constant which is related to the specific reaction velocity constant, and may contain other terms;
α = a constant, the nature of which is still problematical;
$\mathbf{F}$ = the Faraday;
R = the gas constant;
T = the absolute temperature;
z = the electron change for the reaction; and
V = the voltage.

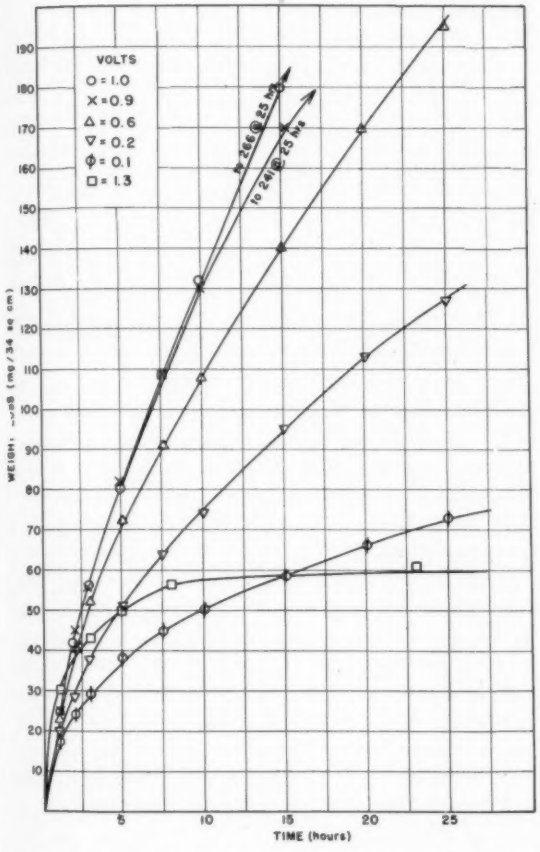

FIG. 7. Rate of attack at constant potential in 10% H_2SO_4 at 50°C.

The total current, I, is equal to the current density times the true area, A, so:

$$I = Ake^{\alpha z\mathbf{F}V/RT}. \qquad \text{(II)}$$

If a film is formed and Faraday's law applies, we may use:

$$w = n\int_0^t Idt, \qquad \text{(III)}$$

where w is the weight of metal attacked, and n is the equivalent weight divided by the Faraday, to obtain for constant voltage:

$$w = nke^{\alpha z\mathbf{F}V/RT}\int_0^t Adt. \qquad \text{(IV)}$$

This may be expressed in the log form:

$$\log w = \log n + \log k + \log\int_0^t Adt + \frac{\alpha z\mathbf{F}V}{2.3RT}. \qquad \text{(V)}$$

Evidently this equation contains both the elements by which w is described experimentally. Although the integral term is not evaluated, it could

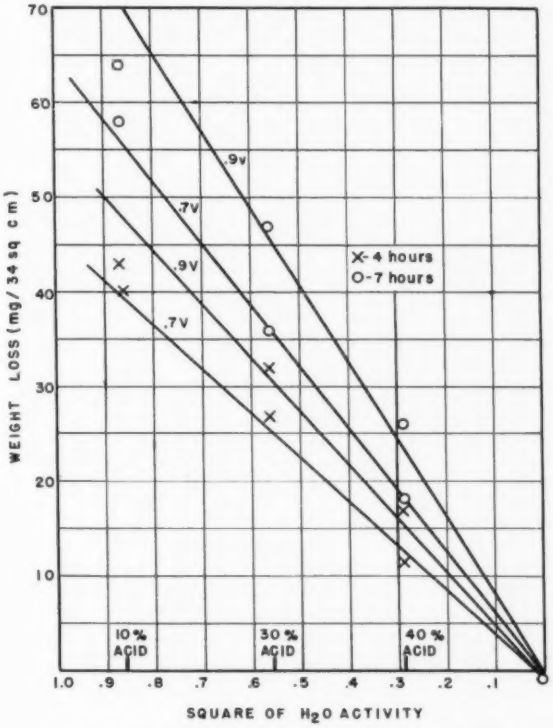

FIG. 8. Weight-loss vs. square of activity of water

be concluded that the activation equation expresses the data, and that rates of attack of lead depend upon the activation energy[4] for the reaction itself[5]. The rates, however, are modified by modes of nucleation and growth of the film substance.

Now the question may be examined as to whether such knowledge as has been obtained indicates lines

[4] If certain assumptions are made, the activation energy can be calculated to be of the order of 6000–8000 calories/mole.

[5] For the process $Fe \rightarrow Fe(OH)_2$ in alkaline solutions this conclusion has been extended to infer that the film is porous and that the reaction is taking place at the metal-solution interface at the bottom of pores. See Kabanov and Leikis, *Acta Physicochim. U.R.S.S.*, **21**, 799 (1946).

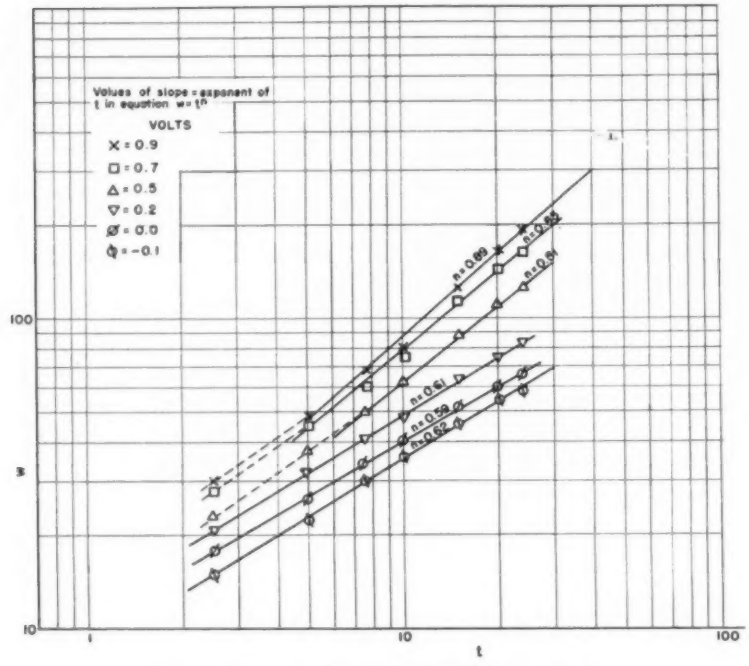

FIG. 9. Log w vs. log t for 10% H_2SO_4 at 30°C

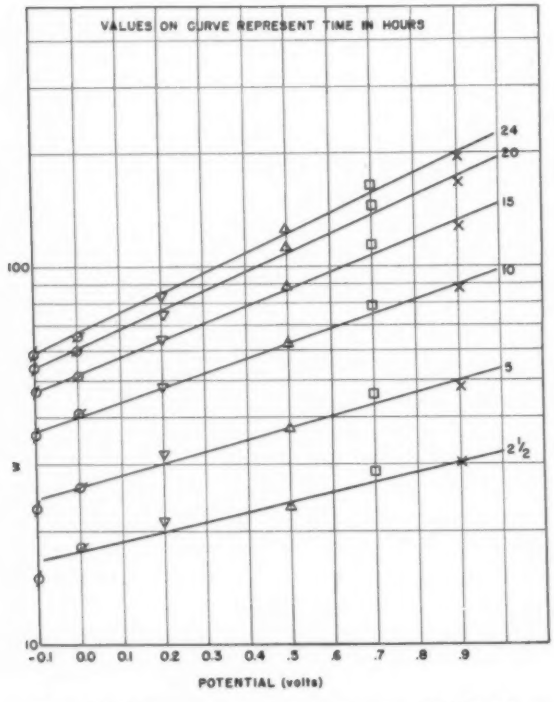

FIG. 10. Log w vs. V at constant t for 10% H_2SO_4 at 30°C.

of attack for further investigation of the corrosion problem. If it can be assumed that corrosion of the positive grids in a battery will depend on the variables, potential, concentration, and temperature, in a way which is at least generally similar to the results found here, then evidently anything which can be done to keep the temperature down will slow down the corrosion rate. The concentration effect should be thoroughly investigated. However, if it were found that increasing the concentration resulted in appreciably better performance in a working battery as far as corrosion of the positive grid is concerned, the factors of self-discharge, charging efficiency, and capacity vs. life and rate would have to be investigated, particularly at the negative plate. Finally, a broader problem may also be indicated: determination and evaluation of the factors which affect the activation energy, because rates are dependent on the activation energy in an exponential fashion and it is conceivable that even a small increase in its value might bring about an appreciable decrease in the corrosion rate.

SUMMARY

At constant potentials in the range investigated, 1.0 to −0.1 volt, tetragonal PbO is formed in contact with lead in sulfuric acid solutions. An outer layer of $PbSO_4$ is formed, probably by chemical reaction between H_2SO_4 and the PbO layer.

The corrosion rate in this voltage range increases with increase in temperature and with decreasing acid concentration. The latter effect is explained by showing a linear relation between rate and the square of the activity of water in the electrolyte.

The weight-loss data are generally linear with time on a log-log plot and the following relation was found between weight loss in a given time and voltage:

$$\log w = A + BV.$$

This is shown to be similar in form to the activation equation.

At potentials from 1.20 to about 1.50 a protective film is formed, presumably consisting of PbO_2.

ACKNOWLEDGMENT

The author gratefully acknowledges permission of the Naval Research Laboratory to publish this paper.

Any discussion of this paper will appear in a Discussion Section, to be published in the December 1951 issue of the JOURNAL.

REFERENCES

1. E. WOLF AND C. BONILLA, *Trans. Electrochem. Soc.*, **79,** 307 (1941).
2. J. J. LANDER, *J. (and Trans.) Electrochem. Soc.*, **95,** 174 (1949).
3. H. S. HARNED AND W. J. HAMER, *J. Am. Chem. Soc.*, **57,** 33 (1935).
4. W. M. LATIMER, "Oxidation Potentials," pp. 304 and 305, Prentice-Hall Inc., New York (1938).
5. H. CROCKFORD, Naval Research Laboratory Report No. P-1113, January 18, 1935, Unclassified.
6. S. GLASSTONE, "Introduction to Electrochemistry," Van Nostrand Co., Inc., New York (1942).
7. R. AUDUBERT, *Disc. Faraday Soc.*, **1,** 73 (1947).
8. J. E. B. RANDLES, *Disc. Faraday Soc.*, **1,** 13 (1947).
9. YA. V. DURDIN, *Uchenye Zapiski Leningrad. Gosudarst.-Univ., Ser. Khim. Nauk*, No. 4 (40), 3 (1939); through *C.A.*, **43,** 506d (1949).
10. D. ROGERS AND A. BURR, *J. Electrochem. Soc.*, **97,** 92 (1950).

Some Preliminary Studies of Positive Grid Corrosion in the Lead-Acid Cell[1]

J. J. Lander

Naval Research Laboratory, Washington, D. C.

ABSTRACT

Preliminary experiments in connection with positive grid corrosion in the lead-acid cell show: (*a*) PbO_2 and Pb undergo the solid phase reaction: $PbO_2 + Pb \rightarrow 2PbO$; (*b*) an intermediate film of PbO_2 is formed at the positive plate which does not cycle to $PbSO_4$; (*c*) the existence of an experimental relationship between grid growth and film formation; and (*d*) electrolyte concentration and time of cycle are important factors in corrosion under cycling conditions in constant-concentration acid. Explanations for these effects and the discharge and self-discharge reactions at the positive plate are offered.

Certain problems concerning the negative plate in connection with the concentration effect are briefly reviewed.

Introduction

This paper is an account of some preliminary experiments on positive grid corrosion. The experiments were not a complete study of any of the phenomena encountered; however, the results and discussion included may be of value in stimulating further thought and research on the problem.

The Solid Phase Reaction: $PbO_2 + Pb \rightarrow 2PbO$

During the course of work on the determination of the conductivity of PbO_2, it was observed that Pb-PbO_2 contacts gave poor and erratic conductivity. Because of this the following experiment was performed: powdered Baker's Analyzed PbO_2 was sandwiched between two freshly abraded, weighed lead sheets with proper contacts made to the lead so that the resistance of the combination could be determined. During the time necessary for making a measurement of the potential drop only, currents of about 15 ma/cm^2 (100 ma/in.^{2}) were passed. The resistance was found to increase with time in a fashion shown in Fig. 1. After about 400 hours, the lead sheets were boiled in ammonium acetate solution and were found to have lost 8 and 19 mg/5.15 cm^2 (0.8 in.^{2}). The experiment was repeated several times and although the reproducibility of the results was poor, resistance was always found to increase with time and the lead sheets always gave a weight loss of the same order of magnitude. It was considered that these results might be due to a solid phase reaction. In another experiment, granulated lead, freshly made by filing a lead block, was sealed in a glass bottle with the powdered PbO_2 and glass beads and rotated several days in a ball mill. The amount of lead used was in about two to one weight excess over the PbO_2 based on the above reaction. A sample of the starting material was subjected to x-ray analysis. The patterns of both components were easily identified. After six days the bottle was opened and the contents again subjected to x-ray analysis. The PbO_2 pattern was almost completely gone from the trace, while a very strong pattern for tetragonal PbO was present along with the Pb pattern somewhat reduced in intensity. It is concluded that PbO_2 undergoes a solid phase reaction with Pb, whereby the PbO_2 is reduced to tetragonal PbO while the Pb is oxidized to the same product.

A possible mechanism for this reaction based on the Volta effect is offered. Since PbO_2 has a conductivity approaching that of metals a contact potential may exist between the phases which is set up by migration of electrons from Pb to PbO_2. These electrons satisfy some of the Pb^{++} valence, releasing O^{--} for reaction. Reaction of Pb^{++} and O^{--} takes place at the interface and the PbO film continues to build up until its resistance becomes too high for passage of Pb^{++}, O^{--}, or electrons. This reaction offers a possibility for the corrosion mechanism at the positive grid in a lead-acid cell and could account for some of the self-discharge at the positive plate.

The process also offers a mechanism for the discharge reaction at the positive plate. During the discharge electrons are available from the negative plate as well as from the positive grid. They cross the Pb-PbO_2 interface and are distributed throughout the mass of the PbO_2 since it is a good conductor. At the solution interface O^{--} is released for the reaction with H^+ ions in the solution to form water, while the PbO formed at the surface of the particles reacts chemically with the H_2SO_4 of the electrolyte.

[1] Manuscript received June 15, 1950. This paper prepared for delivery before the Buffalo Meeting, October 11 to 13, 1950.

At the negative plate Pb^{++} ions are released for reaction with the electrolyte.

Such a PbO_2-Pb contact potential could be an important part of the total cell potential.

Grid Growth

As a part of another investigation, corrosion studies were made on certain alloys by cycling samples in sulfuric acid solution about the positive plate potential. It was always observed, whenever the corrosion film had been built up for a week or so, that even after long discharge periods there existed a black, shiny, hard, brittle, adherent film underneath the outer $PbSO_4$ film. This film is a good electrical conductor and was shown by x-ray analysis to be PbO_2 containing small amounts of PbO. Evidently this intermediate film was not being completely converted to $PbSO_4$ during the cycling process.

It has been suggested (1) that, since the PbO_2 film has a higher specific volume than the underlying metal, it may be subjecting the grid members to a tensile stress which might result in growth if the grid metal did not have enough strength or creep resistance. The hardness and adherence of the film is additionally indicative of the operation of such a mechanism which would be expected to be especially effective on soft alloys or pure lead[2].

The corrosion tests referred to above had been run on binary alloys of lead with tin and antimony. They showed that under the experimental conditions used a 4.5 per cent by weight tin alloy exhibited better corrosion resistance than either the antimony alloy (6% by weight) or pure lead. Assuming that the mechanism given is responsible for growth, short-term tests were run in an effort to determine if there is a relation between corrosion and growth. These alloys were selected because the tin alloy corrodes at somewhat more than one half the rate for the antimony alloy and it has a tensile strength which is about one half that of the antimony alloy.

Samples of each alloy were cold-rolled to different thicknesses and cut into strips of two different widths. These strips were weighed and shorted to a positive plate and immersed to a depth of 17 cm (6.69 in.) in sulfuric acid (30 and 40% by weight). The system was cycled automatically twice daily for 20 days and the growth was measured from time to time. The percentage elongation is plotted against time in Fig. 2. At the end of the period the films were stripped and their weight losses determined. Assuming uniform corrosion over the whole length, the depth of corrosion of the samples was calculated. This figure was divided by the cross-sectional area of the sample and the result plotted against the per cent final elongation as shown in Fig. 3. This plot resulted in a straight line for the 4.5 per cent Sn alloy and may be roughly linear for the Sb alloy. A more careful study should establish the nature of these curves.

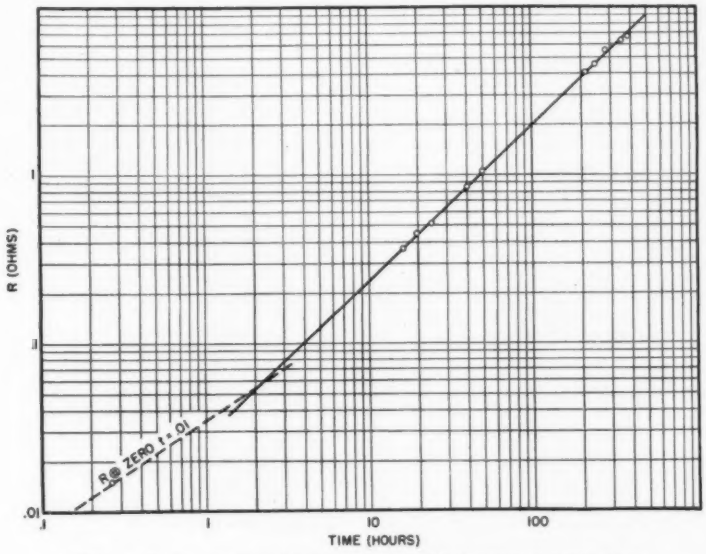

FIG. 1. Increase in resistance of a Pb-PbO_2 contact with time

For purposes of discussion let it be assumed that the relationship is linear. Then by extrapolating the curves to zero per cent elongation it is found that the lines do not pass through the origin but have an intercept on the depth of corrosion per unit cross-sectional area axis. This is quite reasonable because

[2] See, for example, the results of tests made on pure lead grids (W. H. Power, *et al.*, Naval Research Laboratory Report No. P-2908, January 9, 1947, Unclassified).

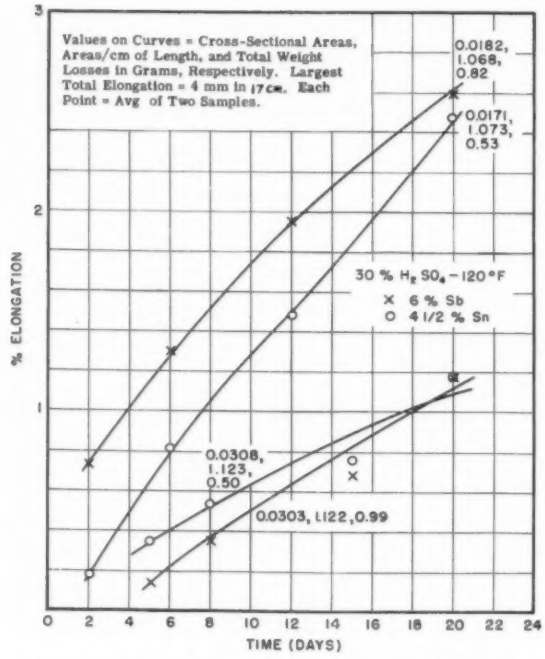
Values on Curves = Cross-Sectional Areas, Areas/cm of Length, and Total Weight Losses in Grams, Respectively. Largest Total Elongation = 4 mm in 17 cm. Each Point = Avg of Two Samples.
0.0182, 1.068, 0.82
0.0171, 1.073, 0.53
30 % H_2SO_4 – 120°F
× 6 % Sb
○ 4 1/2 % Sn
0.0308, 1.123, 0.50
0.0303, 1.122, 0.99
% ELONGATION
TIME (DAYS)

FIG. 2. Rate of growth of 4.5% Sn alloy and 6% Sb alloy

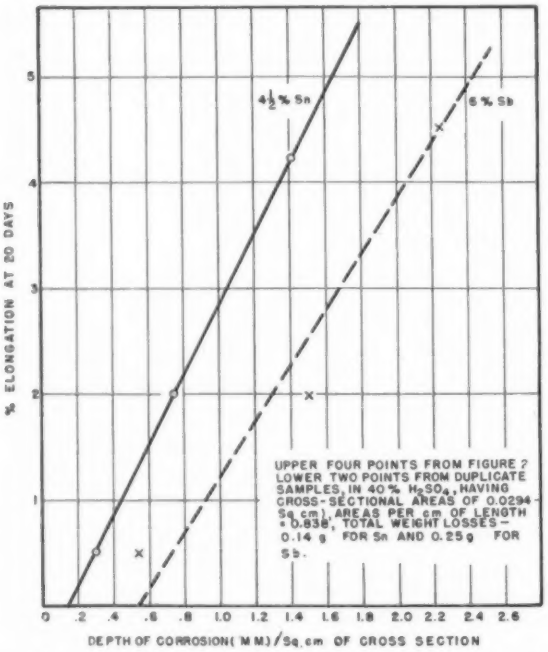
4½ % Sn
6 % Sb
UPPER FOUR POINTS FROM FIGURE 7
LOWER TWO POINTS FROM DUPLICATE SAMPLES, IN 40 % H_2SO_4, HAVING CROSS-SECTIONAL AREAS OF 0.0294 Sq cm, AREAS PER cm OF LENGTH = 0.838, TOTAL WEIGHT LOSSES – 0.14 g FOR Sn AND 0.25 g FOR Sb.
% ELONGATION AT 20 DAYS
DEPTH OF CORROSION (MM)/Sq cm OF CROSS SECTION

FIG. 3. Relation between growth and film thickness and cross-sectional area.

there is a minimum tensile strength for elongation of metals and also a minimum load to induce creep. Furthermore, the slope of the Sn alloy line is greater than that drawn for the Sb alloy, which is again reasonable because these slopes should be related to the tensile strength or the creep resistance of the alloys.

The growth factor should also be considered in conjunction with film thickening. Experimental cells sometimes fail in spite of the fact that corrosion of the positive grid has progressed to a relatively small extent. This could be due to lack of contact between the grid and the active material caused by grid growth and lack of film formation. Antimonial grids not only grow at a slower rate but form the grid film faster so that contact is maintained between the active material and the grid. Thus a grid of the 4.5 per cent Sn alloy should have its grid members spaced about twice as close as one made of the antimony alloy, because while it grows at about the same rate, the film thickens at about one half the rate. It should be pointed out that telephone batteries which had been on float for nine years exhibited appreciable looseness of the pellets in the positive grid structure, but actually gave satisfactory discharge characteristics (1), so that there may be other important factors involved. Nevertheless, further studies along these lines might be of considerable value in grid design.

The Effect of Electrolyte Concentration and Time of Cycle

The previous paper (2) has shown the importance of electrolyte concentration in the rate of PbO formation at lead anodes under constant potential conditions. To determine whether the effect also obtains under conditions of cycling potential, and to see if corrosion rates depend on potential conditions on charge and discharge, and time of cycle, the following work was done. An apparatus was constructed by means of which samples could be maintained, during cycling, at various constant charge potentials and various constant discharge potentials relative to a positive plate immersed in the electrolyte. The positive plates employed had sufficient capacity so that they were not polarized by currents of the magnitude drawn by the samples. The duration of the cycle could be varied between three minutes and forty-eight hours, and the ratio of charge to discharge time could be set at any desired value. The results of these tests will not be covered in detail. It is sufficient to state that considerable variation in corrosion rates was obtained under different conditions. In general, a combination of high charge and high discharge potentials and shorter cycling times favored more rapid corrosion.

Fig. 4 shows the results at various total times for different time cycles as a function of concentration for 4.5 per cent Sn alloy, Pb, and 6 per cent Sb alloy, all cold-rolled. This test was conducted at room temperature with charge potential at +0.25 and

discharge potential at −0.10 and 55 per cent of the time on the charge part of the cycle. These potentials are referred to the potential of the positive plate in the solutions concerned.

The tin alloy is shown to be more corrosion resistant than either Pb or Sn alloy under the conditions of the experiment. However, the most significant feature of these results is the effect of acid concentration on the corrosion rate. Increasing acid concentration from 10 per cent to 40 per cent results in decreased corrosion by a factor from 3 to 7 times. Thus it is shown, under certain cycling conditions

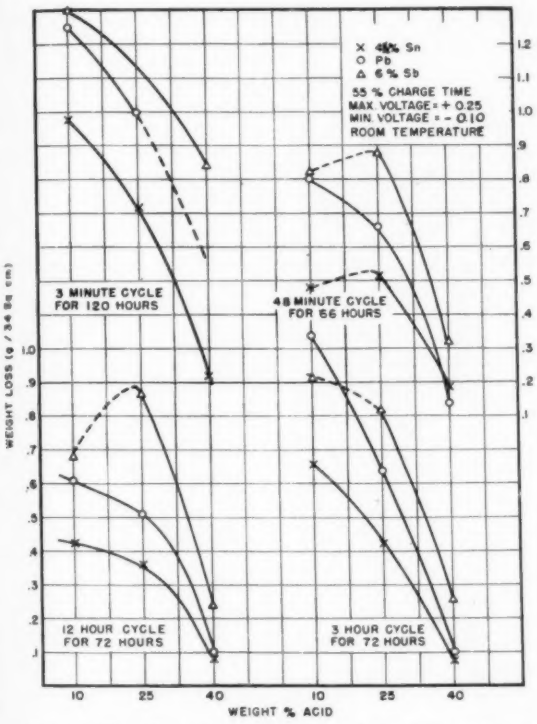

FIG. 4. The effect of acid concentration on corrosion of Pb and two alloys under various cycling conditions.

at least, that increasing concentration results in a decreased corrosion rate, just as it does under constant potential conditions.

Further examination of these data[3] shows that an increase in corrosion rate occurs as time of cycle is decreased. This is quite understandable when considered in connection with the previous data (2) where it is shown that the protective PbO_2 film is not established for one to eight hours or so, depending to a considerable extent on concentration and temperature. Therefore it should be expected that this factor will operate to a small or negligible extent for very short time cycles and to an increasingly large extent as time duration of cycle increases beyond one to eight hours, depending on conditions.

[3] Log-log plots of weight loss vs. water activity show slopes ranging between about two and four. From this and the previous rate-activity data (2), it might be predicted that a study of corrosion during early PbO_2 formation will show a rate dependency as the fourth power of the water activity.

General Discussion

As a result of this and the previous work (2) the following combination of mechanisms for corrosion at the positive lead grid is proposed. During charge, provided the potential does not become too high, a protective film of PbO_2 is built up more or less gradually at the lead surface. When the charge is stopped, or during discharge, electrons may move from the grid to the PbO_2 film, releasing O^{--} ions for formation of PbO at the Pb-PbO_2 interface. Furthermore, the PbO film becomes porous by fracture or recrystallization, whereupon the metal grid becomes available for reaction with the water of the electrolyte to form more PbO. Thus, on stand or discharge, corrosion of the grid may proceed by the two mechanisms more or less at the same time. At a pure lead grid corrosion during the charge part of the cycle should be slow, except during the initial period necessary to establish the protective film. Corrosion by the solid phase reaction would seem to be of considerably less importance in terms of rate than corrosion by action of the electrolyte through pores in the film, on the basis of the magnitude of the concentration effect.

Application of the concentration effect may prove to be of importance in extending battery life. However, these tests were all run at constant concentration, while in a battery concentration cycles over a considerable range. Thus, during discharge when potentials are shown to be most corrosive (2), water is being produced in the pores of the active material. Furthermore, during the first part of the charge the protective film may not be established and concentration of water in the pores is still at a comparatively high value, so that combination of these several factors may lead to a considerably smaller dependence of life on acid concentration in a cycling cell than might be indicated by the data obtained under constant concentration conditions.

Temperature cycling may also affect the corrosion rate, not only because higher temperatures speed up the rate of reaction, but also because such a cycle may promote cracking of the film thus contributing to its porosity.

On raising acid concentration, it is to be expected that self-discharge at the negative plate will be increased (3, 4), even for pure lead negative grids (5). However, it is indicated (5) that self-discharge is less at negatives with pure lead grids at high gravi-

ties, than at antimonial grids with lower gravities. Charging efficiency would also be expected to be decreased at the negative plate, leading to sulfation or hardening of the negative plate material. This is not necessarily a serious objection because it is expected that sulfated negative plates can be brought back (6, 7), especially if antimony can be excluded from the cell. The foregoing discussion is based on the assumption that the tests conform in a general way at least to conditions in a cycling cell. It also should be considered that even the longest of these tests was of short duration compared to normal battery life.

Summary

PbO_2 undergoes a solid phase reaction with Pb to form tetragonal PbO. A mechanism involving the Volta effect is proposed. A contact potential between Pb and PbO_2 may be an important part of the cell potential and explain self-discharge and the discharge reaction at the positive plate.

An intermediate film of PbO_2 is formed by the corrosion process which does not cycle completely to $PbSO_4$. Because of this it retains its compact nature and may in large measure be responsible for slowing down grid corrosion.

Grid growth appears to be proportional to the depth of corrosion after an initial period. The initial period and the rate of growth are probably characteristic of the tensile strength or creep resistance of the metal.

Electrolyte concentration and cycle time are shown to be important factors in the corrosion process under constant-concentration conditions. These effects are discussed in terms of a cycling cell.

Acknowledgment

The author gratefully acknowledges permission of the Naval Research Laboratory to publish this paper.

Any discussion of this paper will appear in a Discussion Section, to be published in the December 1951 issue of the Journal.

REFERENCES

1. U. B. Thomas, F. T. Forster, and H. E. Haring, *Trans. Electrochem. Soc.*, **92**, 322 (1947).
2. J. J. Lander, *J. Electrochem. Soc.*, **98**, 213 (1951).
3. G. Vinal, "Storage Batteries," 3rd ed., p. 123, John Wiley & Sons, Inc., New York (1940).
4. M. Boyer and R. Friend, Naval Research Laboratory Report No. P-2981, October 11, 1946, Unclassified.
5. A. C. Zachlin, *Trans. Electrochem. Soc.*, **92**, 259 (1947).
6. G. Vinal, "Storage Batteries," 3rd ed., p. 310, John Wiley & Sons, Inc., New York (1940).
7. E. J. Peebles, Naval Research Laboratory, Unpublished work.

Bright Nickel Plating on Metallic Single Crystals in the Absence of Addition Agent[1, 2]

HENRY LEIDHEISER, JR.[3], AND ALLAN T. GWATHMEY

Cobb Chemical Laboratory, University of Virginia, Charlottesville, Virginia

ABSTRACT

Nickel was electrodeposited on electrolytically polished single crystal spheres of copper and nickel under a wide variety of experimental conditions. The deposit which formed on the (100) faces and on faces making a small angle with the (100) plane remained mirror bright to thicknesses of the deposit as great as 0.01 inch. The deposit which formed on the (111) faces and on faces making a small angle with the (111) plane became matte from the very start of deposition. X-ray analysis at grazing incidence indicated that the deposit on the (100) face remained monocrystalline, whereas the deposit on the (111) face was polycrystalline from the very start of deposition. The polycrystalline deposit rapidly assumed a (100) preferred orientation under the experimental conditions utilized. The following comparative characteristics of the two types of deposits were determined: composition by spectrographic analysis, current density and current efficiency during deposition, hardness, ductility, porosity, and corrosion resistance. The results may have application in the growth of nickel single crystals by electrodeposition.

INTRODUCTION

It is known that bright plating of metals is often accompanied by a preferred orientation of the deposit. An outstanding example of this has recently been observed and the facts are presented herein as additional information useful in formulating a mechanism of bright plating.

EXPERIMENTAL

Single crystals of copper and nickel in the shape of spheres, $\frac{5}{8}$ in. in diameter, with a shaft, $\frac{3}{16}$ in. in diameter and $\frac{1}{2}$ in. long, were machined from long crystals grown from the melt (1). The spheres were mechanically polished with emery paper and electrolytically polished. Copper was polished electrolytically in 42.5 per cent by volume phosphoric acid and nickel was electropolished in 70 per cent by weight sulfuric acid. Both methods of electropolishing produced very smooth surfaces as judged by observation, microscopically at 700×.

After removal from the polishing bath and washing under a stream of water, the crystals were immediately placed in the plating bath and electrodeposition started at the desired current density[4]. In this manner grease and oxide films on the surface were reduced to a minimum. In all experiments even plating over the entire surface was obtained.

The plating experiments were conducted in 250-ml beakers or large crystallizing dishes. The anode was a thin sheet of nickel which was shaped to fit the inside surface of the glass container. The electrolyte described as a Watts bath contained $NiSO_4 \cdot 6H_2O$ 240 g/l, $NiCl_2 \cdot 6H_2O$ 45 g/l, and H_3BO_3 30 g/l. The solution was generally used at a *p*H of 3–4. As described later, this electrolyte was prepared from reagents of different purity with exactly the same results.

RESULTS

The majority of experiments were conducted on single crystals of copper but key experiments were also conducted on single crystals of nickel. In all cases the results with the nickel substrate were identical to those observed with the copper substrate. For convenience in discussion the experiments described will be confined to the electrodeposition of nickel on copper crystals.

During these studies two important results were obtained: (*a*) the deposit formed on the (100) faces remained bright and smooth for long periods of time, whereas the deposit on the (111) faces became matte in appearance very shortly after the current was started; and (*b*) the deposit on the (100) face remained monocrystalline to great thicknesses whereas the (111) face became polycrystalline soon after deposition began. The following is a more detailed account of these results.

Fig. 1 is a photograph of the results obtained when nickel was electrodeposited on copper single crystals from a Watts-type bath. The repetition of results on each octant of the surface causes the formation of a pattern from which the various faces may be identi-

[1] Manuscript received October 30, 1950. This paper prepared for delivery before the Washington Meeting, April 8 to 12, 1951.

[2] The research reported in this paper was supported by a grant from the Research Corporation.

[3] Present address: Virginia Institute for Scientific Research, 326 North Boulevard, Richmond, Virginia.

[4] All current densities are given in amp/dm². To convert to amp/ft², multiply by 9.29.

fied. The dark (100) areas (2) are very smooth and thus reflect little light into the camera lens. The light (111) areas are rough on a microscopic scale and thus much diffuse light is reflected into the camera lens.

Similar results were obtained over a wide range of experimental conditions. The same pattern in all respects was obtained over a current density range of 0.10–8.0 amp/dm², a *p*H range of 0.5–5.5, and a temperature range of 20°–60°C, with and without agitation. No experiments were conducted above 8.0 amp/dm², but there is every reason to believe that the highest current density which would give a result similar to that shown in Fig. 1 is considerably above this value. In experiments conducted above 0.8 amp/dm² the electrolyte was vigorously stirred in order to avoid effects of the depletion of nickel ions in the immediate neighborhood of the cathode.

FIG. 1. Typical nickel electrodeposition pattern formed on copper single crystals in a Watts-type bath. View normal to (111).

In experiments conducted at room temperature and a *p*H of 3.3 the (111) areas became matte in appearance approximately 5 minutes after the experiment was begun at 0.10 amp/dm² and immediately in experiments conducted above 2.0 amp/dm². The matte appearance changed to a granular, nodular appearance as the deposit thickened and finally took on a very coarse granular appearance. In contrast to this, the (100) areas remained very bright and shiny for thicknesses of the deposit up to 0.01 in. in some cases. The (100) area required 4 hours at 4.0 amp/dm² to assume a comparable granular appearance that was observed in 15 minutes on the (111) face. In general, after the deposit was approximately 0.005 in. thick, the brightness of the (100) area began to decrease in intensity but even after 24 hours at 1.0 amp/dm² the (100) area was quite smooth and exhibited mirror-like reflections of objects held near the surface. The difference in behavior of these two areas will be discussed later.

Exactly similar results were observed in the Watts-type bath when the electrolyte was prepared from technical grade chemicals, from reagent grade chemicals, and from nickel salts of reagent grade with very low cobalt content. In some cases the plating solutions were heated with nickel carbonate slurry. The solution was filtered and the *p*H was adjusted to the desired value with hydrochloric acid. This additional purification treatment did not have any effect on the deposition pattern which formed on the single crystals. Similar results were also obtained at low current densities from a bath containing $NiSO_4 \cdot 6H_2O$ 120 g/l, NH_4Cl 22.5 g/l, and H_3BO_3 30 g/l. A few experiments were also conducted with electrolytes containing only a pure nickel salt. Electrolytes prepared from either $NiSO_4$, $NiCl_2$, or $Ni(NO_3)_2$ gave the same pattern at very low current densities in the initial stages of deposition, but the eventual pattern formed was dependent on the ions present in the bath.

Preliminary x-ray photographs of the deposit indicated that the deposit in the (111) areas became polycrystalline a very short time after deposition started whereas the (100) areas remained monocrystalline for long periods of time. A series of experiments was conducted at 4.0 amp/dm², room temperature, a *p*H of 3.3, and with moderate agitation to follow the character of the deposit as it increased in thickness. X-ray pictures were taken at grazing incidence with molybdenum white radiation at various times of deposition, and the surface structure was studied at the same points on the surface with a light microscope at a magnification of 700×. In some instances with thick deposits, Laue back reflection photographs were also taken. X-ray photographs were taken after deposition times of 30 seconds, 1½, 5, 10, 30, 90, and 330 minutes. As shown in Fig. 2 and 3 the deposit in the (100) area after 30 minutes was a perfect single crystal and the surface at a magnification of 700× was very smooth. After 90 minutes the (100) area showed signs of a slight decrease in brightness as shown in Fig. 4. The deposit was still essentially a single crystal with polycrystalline inclusions. Rings, indicative of polycrystalline material, first became visible on the x-ray photographs as shown in Fig. 5. The polycrystalline material was largely confined to the outer layers of the deposit as judged by the fact that the polycrystalline rings were much more prominent when copper radiation was used in place of the molybdenum radiation. In the case of the (111) areas the deposit was matte from the very start of deposition. The x-ray picture taken after 30 seconds of deposition indicated that the deposit was highly strained but there was no indication of polycrystalline rings. After 1½ minutes of deposition, the first faint signs of polycrystalline rings were apparent as shown in Fig. 6. Fig. 7 is a photomicrograph of the same area after 1½ minutes of deposition. It will be noted that the (111) area was much rougher after only 1½

minutes of deposition than the (100) area after 30 minutes of deposition. The polycrystalline rings on the x-ray photographs of the (111) area became much more prominent with time and after 10 minutes a definite (100) preferred orientation was detected. Fig. 8 to 10 show the increase in roughness of the (111) area with time. The degree of orientation increased as deposition proceeded and after 330 minutes excellent (100) preferred orientation was observed on deposits in both the (100) and (111) areas. After approximately 330 minutes of deposition the (100) and (111) areas were indistinguishable with the naked eye, microscopically, or from the x-ray photographs.

The results of the x-ray study may be summarized

FIG. 2. Glancing angle x-ray picture of nickel deposit on (100) face after deposition for 30 minutes at 4.0 amp/dm². Note that deposit is a perfect single crystal.

FIG. 3. Photomicrograph of nickel deposit on (100) face after deposition for 30 minutes at 4.0 amp/dm². 700×. Note extreme smoothness of surface.

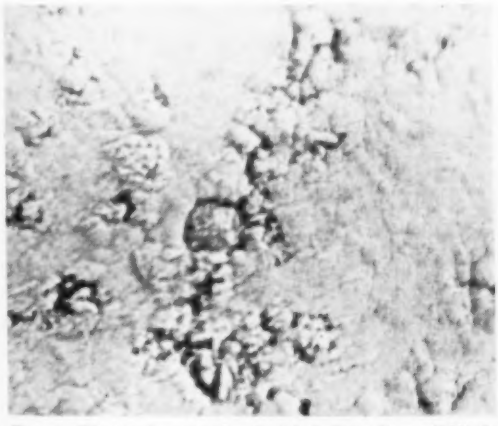

FIG. 4. Photomicrograph of nickel deposit on (100) face after deposition for 90 minutes at 4.0 amp/dm². 700×. The illumination was oblique to bring out the slight roughness.

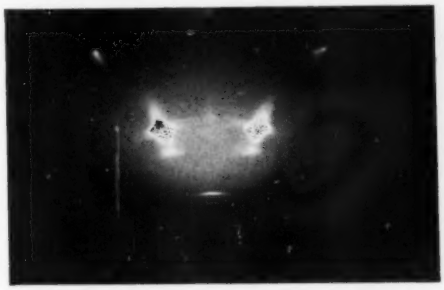

FIG. 5. Glancing angle x-ray picture of nickel deposit on (100) face after deposition for 90 minutes at 4.0 amp/dm².

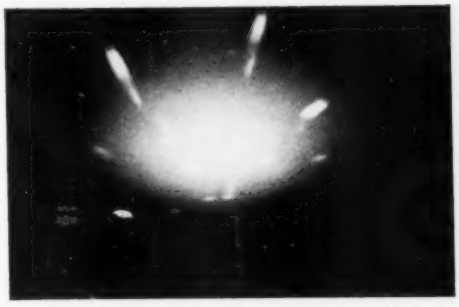

FIG. 6. Glancing angle x-ray picture of nickel deposit on (111) face after deposition for 1½ minutes at 4.0 amp/dm². Note first faint sign of polycrystalline ring.

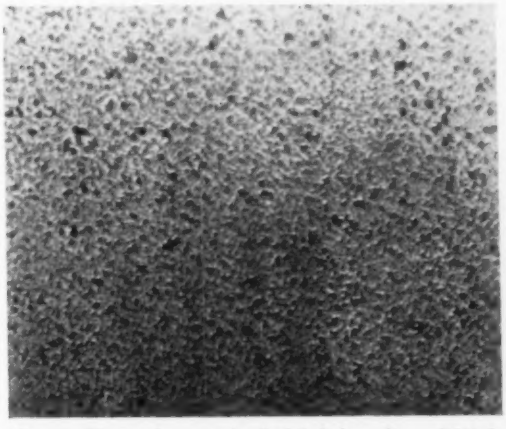

FIG. 7. Photomicrograph of nickel deposit on (111) face after deposition for 1½ minutes at 4.0 amp/dm². 700×.

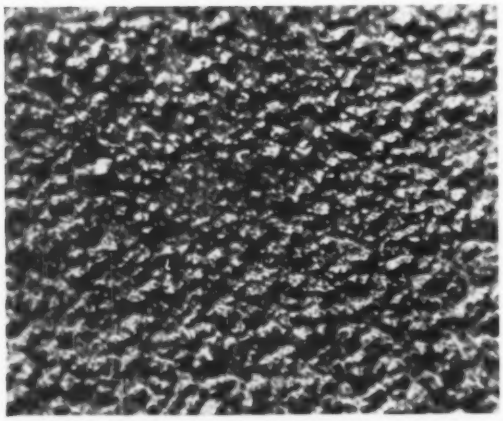

FIG. 8. Photomicrograph of nickel deposit on (111) face after deposition for 30 minutes at 4.0 amp/dm². 700×.

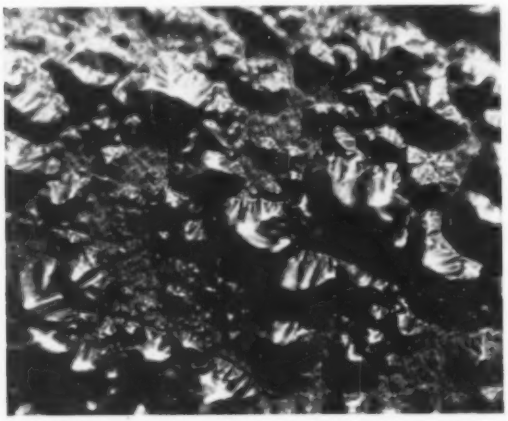

FIG. 9. Photomicrograph of nickel deposit on (111) face after deposition for 90 minutes at 4.0 amp/dm². 700×.

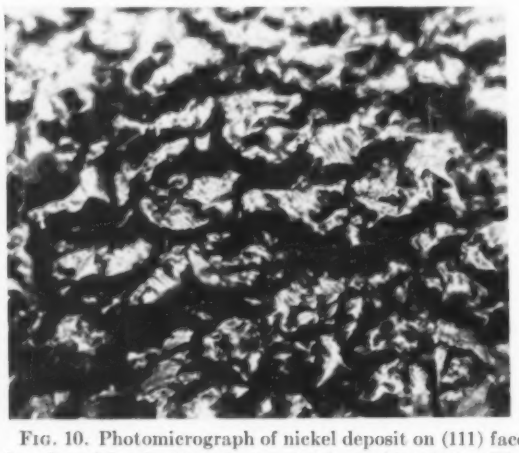

FIG. 10. Photomicrograph of nickel deposit on (111) face after deposition for 330 minutes at 4.0 amp/dm². 700×. The (100) area was the same in appearance.

as follows: The deposit on the (100) area, which remained bright for long periods of time, continued the orientation of the substrate and remained monocrystalline. The disappearance of brightness after extended deposition times on the (100) face coincided with the first appearance of polycrystalline rings on the x-ray pictures. The deposit on the (111) face became polycrystalline immediately or very soon after deposition began. The formation of polycrystalline material coincided with the development of a rough, matte surface.

It was next of interest to determine the factor which was responsible for the different plating characteristics of the (100) and (111) areas. The following experiments were conducted to obtain a measure of the comparative current densities on the (100) and (111) faces during deposition. Plating experiments were conducted at various current densities for periods of time until the very first signs of nickel were observed on the copper surface. In all instances it was observed that there was no detectable difference in the initial rate of deposition on the (100) and (111) faces. As judged also from the following experiments it appears that the average current density per apparent cm² was approximately the same on the (100) and (111) faces during the over-all deposition time. During the course of this research several hundred plating experiments were conducted. In all instances it was necessary to abrade the nickel deposit away before conducting another experiment. This was accomplished by clamping the shaft of the sphere in a chuck attached to an electric motor and holding strips of metallographic polishing papers against the sphere as it revolved. In each abrasion it was observed that the deposit was removed at the same over-all rate from both the (100) and (111) areas. In another experiment a sphere was plated at 4.0 amp/dm² to a thickness of approximately 0.001 inch. The sphere was then cut in half through the center of two (100) and four (111) areas. The hemisphere was mounted in sealing wax to protect the edges during polishing, and the specimen was mechanically polished and electrolytically etched. The thickness of the deposit was then determined under the microscope with the aid of a calibrated scale in the eyepiece of the microscope. It was observed that within the limits of measurement the thickness of the deposit was uniform over the entire surface. Rough measurements were also made of the thickness of the deposit by the use of the chord method and it was found that the deposit was the same thickness in both the (100) and (111) areas.

Experiments were carried out at room temperature and 1.0 amp/dm² at a *p*H of 2.0 and a *p*H of 4.0 on flat slices cut parallel to the (100) and (111) faces in order to determine the current efficiency on these faces. The copper single crystal slices were electrolytically polished and the edges were stopped off

with a water proof varnish. The weight gain of the specimen was used as a measure of the current efficiency. The current efficiencies were approximately the same on both faces under these conditions, approximately 88 per cent at *p*H 2, and approximately 96 per cent at *p*H 4.

As would be expected on the basis of grain size, the monocrystalline deposit in the (100) area was much softer than the polycrystalline (111) areas. Pin prick and pin scratch experiments indicated this in a qualitative manner. The appearance of slip lines in the (100) areas and the nonappearance of slip lines in the (111) areas offered evidence that the (100) area was monocrystalline and the (111) area was polycrystalline in many experiments in which x-ray analysis was not made.

Spectrographic analysis of the deposit in the two areas indicated that the type of metallic trace impurities in the (100) and (111) areas were essentially the same, but the (111) areas contained slightly larger amounts of some foreign metals. It should be pointed out, however, that the spectrographic analysis would give no indication of constituents or impurities adsorbed on the copper surface before deposition was begun.

Experiments were also conducted using half-wave rectified alternating current. The 115-volt line voltage was stepped down with a variable transformer and then passed through a copper-copper oxide rectifier. Experiments conducted at 0.1–0.4 amp/dm^2 indicated that as with direct current the (111) area became polycrystalline and the (100) area remained monocrystalline. However, the results differed in one important respect. In the case of the half-wave rectified current the deposit in the (100) area did not remain bright for more than approximately 10 minutes. Brilliant light reflections then became visible from the (100) areas when a flashlight beam was directed normal to (100). Under the microscope small facets parallel to the (100) planes were observed. Thus in the case of direct current the deposit remained smooth without the development of facets, whereas facets developed rapidly on the (100) face when the current was interrupted 60 times a second.

Several experiments were conducted to note the comparative corrosion resistance of the two surfaces. The following corroding environments were used: 10 per cent HCl, action of an alternating current in the Watts-type bath, and electrolytic etching in HNO_3-acetic acid solution. In all instances the (111) area possessed the least corrosion resistance. It was observed after sectioning and microscopic examination that channels were rapidly etched through the deposit to the copper substrate. In some instances the copper substrate deposited on the nickel surface in the (111) areas by metal replacement reaction.

Discussion

The plating characteristics of the bright (100) areas differed in one major respect from those obtained with typical bright plating baths. The deposit in the (100) area would remain bright when deposition was carried out on a bright copper or nickel substrate, but the bath did not have the ability to increase the brightness and smoothness relative to the substrate. Thus if the (100) area were purposely roughened by etching before deposition, the deposit did not become brighter with thickness of the deposit. This fact suggests that the mechanism of bright plating with addition agents is different in principle than that observed on the (100) face. However, we feel that experiments such as these may help in understanding the mechanism of bright plating in general or in developing a new type of bright plating.

The comparative properties of the nickel electrodeposit formed on the (100) and (111) faces are given in Table I.

TABLE I

Property of deposit	(100)	(111)
Surface appearance	Smooth and mirror-bright	Matte and rough
Crystallinity	Single crystal	Polycrystalline
Current density	Same on both faces	Same on both faces
Current efficiency	Same on both faces	Same on both faces
Hardness	Soft	Harder than (100)
Ductility	Excellent	Less than (100)
Porosity	Compact plate	Comparatively porous
Corrosion resistance	Excellent	Comparatively poor

It is well known that deposits from a Watts-type bath tend to assume a (100) preferred orientation in many instances. It is not entirely unexpected to find that a (100) substrate possesses great power for orienting the deposit to the maximum amount—thus complete monocrystalline continuity between the substrate and the deposit. Copper and nickel both possess the same crystal structure, face-centered cubic, and the lattice constants are very similar. It would not be expected then that much strain would be present at the interface between copper and nickel in the (100) areas. This is borne out by the sharpness of the spots on the x-ray diffraction photographs. For as yet unknown reasons the Watts-type electrolyte causes the crystals to orient so that (100) planes tend to lie parallel to the surface. This tendency presumably originates from the interaction of the electrolyte, or components in the electrolyte, with the surface because different orientations are obtained in other electrolytes (3). It is interesting to

note that in a previous study of the electrodeposition of copper on copper single crystals (2) the deposit on the (111) face remained monocrystalline whereas the deposit on the (100) face became polycrystalline as the deposit thickened. In the case of copper the monocrystalline deposit lost its bright appearance as the deposit increased in thickness. The relative tendencies of the deposits on the (100) and (111) faces to remain monocrystalline are different for nickel and copper in the plating solutions used in these studies.

The results suggest strongly that the difference in plating characteristics of the (100) and (111) faces cannot be accounted for on the basis of differences in initial current density on the two faces or differences in average current density on the two faces during the course of deposition. The fact that appreciable strain, as judged from the x-ray results, was present in the nickel deposit on the (111) face after 30 seconds of deposition at 4.0 amp/dm^2, when the deposit was only approximately 4000 Å thick, suggests that the first few atom layers may be deposited in a strained or polycrystalline manner. It should be pointed out that electron diffraction methods are best suited for the study of very thin deposits and that x-ray results represent an integration of effects over a considerable thickness. It appears that nickel atoms depositing on the (111) face meet a resistance of some sort which prevents them from assuming the stable position in layers continuing the structure of the substrate. It is impossible with the experimental data at hand to determine if this resistance is an abstract energy barrier or a barrier imposed by steric factors resulting from preferred adsorption of constituents of the electrolyte on the geometric configuration representative of the (111) face of a face-centered cubic structure.

The striking lack of smoothness of the (100) area when half-wave rectified alternating current was used was unexpected. It is known that in some cases of commercial plating half-wave rectified current gives essentially the same results as direct current. The essential difference between the two types of current is that in the case of the half-wave rectified current 1/120 of a second elapses between current pulses. During this short interval the neutralized cations (nickel atoms) presumably have time to migrate to the most stable position. Many thousands of experiments on metallic single crystals in hundreds of different environments indicate that the stable state of a metal surface undergoing change is one containing facets. The crystal faces that develop depend on the metal, the crystal face at the geometric surface, and the environment. In the case of direct current additional discharged cations would be continually striking the surface and thus would offer obstacles to the mobility of atoms already present on the surface. Nickel, with a high melting point and a high recrystallization temperature (*ca.* 600°C), would not be expected to have the mobility of lower melting metals such as copper and silver. This fact may be a partial explanation of why the phenomenon of a smooth surface in the absence of addition agent has not been observed previously in many experiments conducted on the electrodeposition of copper, silver, zinc, cadmium, indium, and lead on various metallic single crystals. In partial verification that the phenomenon of bright deposition on the (100) face is one of lack of mobility is the qualitative fact that the tendency to form facets on the (100) face after several hours increased somewhat as the current density was decreased. In a few experiments, conducted below 0.10 amp/dm^2, very small but recognizable facets were faintly visible under the microscope at 700× after 5 hours or more. However, even in these cases the (100) areas had a bright appearance.

The results obtained in this study suggest that nickel single crystals may be prepared by electrodeposition. It is essential, however, that deposition be carried out on a copper or nickel seed crystal with a smooth, strain-free (100) surface. A few preliminary experiments indicated that the high temperature oxidation properties of monocrystalline nickel prepared by electrodeposition were essentially the same as those of a massive nickel single crystal prepared from the molten metal.

Any discussion of this paper will appear in a Discussion Section, to be published in the December 1951 issue of the JOURNAL.

REFERENCES

1. ALLAN T. GWATHMEY AND A. F. BENTON, *J. Phys. Chem.*, **44**, 35 (1940).
2. H. LEIDHEISER, JR., AND A. T. GWATHMEY, *Trans. Electrochem. Soc.*, **91**, 95 (1947) (Summary of the conventions used in describing results on spherical single crystals).
3. C. S. BARRETT, "Structure of Metals," p. 439, McGraw-Hill Book Co., New York (1943).

Amperometric Titrations of Sn^{IV} and Hg^{II} with Tetraphenylarsonium Chloride[1]

I. M. Kolthoff

University of Minnesota, Minneapolis, Minnesota

AND

Ralph A. Johnson

University of Illinois, Urbana, Illinois

ABSTRACT

Sn^{IV} and Hg^{II} can be titrated amperometrically with tetraphenylarsonium chloride using the dropping mercury electrode as the indicator electrode. Procedures are given and the limitations of the method are discussed.

The use of tetraphenylarsonium chloride (denoted as TPAC) as a reagent in the indirect determination of mercuric, stannic, cadmium, and zinc ions has been described by Willard and Smith (1). These determinations involve formation of insoluble tetraphenylarsonium salts of the chloro-complexes of the metal ions and subsequent determination of the excess TPAC by potentiometric titration with iodine (2).

Certain features of the reactions of TPAC with stannic and mercuric chlorocomplexes suggest their use in amperometric titrations. First, attainment of equilibrium is rapid. Second, the precipitates have a low solubility. Third, both mercuric and stannic ions yield suitable diffusion currents.

The amperometric titration permits a direct determination of the metal ions and represents a considerable saving in time over the indirect method.

Determination of Stannic Ion

This determination of tin is based on the reaction

$$2(C_6H_5)_4As^+ + SnCl_6^{--} \rightarrow [(C_6H_5)_4As]_2SnCl_6.$$

Current before the end point is derived from the stannic-stannous wave, which is catalyzed by TPAC (3). In 3*N* hydrochloric acid, the current may be measured at −0.3 volt vs. S.C.E.

Because tin must be in the form of the hexachlorostannate complex to react with tetraphenylarsonium ion, a certain lower limit of chloride concentration is indicated for the titration. Furthermore, the acidity must be high enough to prevent hydrolysis of the hexachloro-complex. If both the acidity and chloride concentrations are less than 2*N*, quantitative precipitation does not occur and the attainment of equilibrium is slow. If the concentration of chloride is 2–4*M*, good precipitation lines and precision are obtained even when the concentration of hydrogen ion is as low as 1*N*. Above 4*M* chloride, the points on the precipitation line are not linearly related; in particular, currents obtained in the beginning of the precipitation are less than theoretical, but closer to the end point the current approaches the expected values. For best results, the chloride concentration should be maintained at approximately 3–4*M*.

The effects of variation in hydrogen-ion concentration are not as marked as the effects associated with chloride variations. In mixtures containing 2–3*M* chloride which are 1*N* in acid the results are slightly higher and the titration curves are not as well defined as in 2*N* acid. In 5*N* acid the results tend to be a little low. The best range of acidity is between two and four normal. This acidity can be lowered to 1*N* without seriously affecting the results, at a total chloride concentration of 2–3*N*.

Procedure

Take for analysis a sample containing 60 to 180 mg of tin in the stannic state. Add sufficient hydrochloric acid to make the solution 2–4*N* in hydrogen ion when it is diluted to 100 ml. Note that the final chloride concentration should be 3–4*N*. Finally, dilute the mixture to volume in a 100-ml volumetric flask. Pipet 25.00 ml into a polarographic cell.

Titrate with 0.05*M* TPAC solution added from a calibrated 10-ml buret. Make the first addition of reagent immediately after assembling the titration unit and beginning the flow of nitrogen through the cell. Continue passage of nitrogen through the system for ten minutes to remove oxygen. Measure the current at −0.30 volt vs. S.C.E., and add a second portion of reagent. After passing nitrogen through for two minutes, make a second reading. Obtain three to five points on either side of the end point. Correct the observed currents for dilution and plot

[1] Manuscript received December 14, 1950.

the titration lines to determine the end point. Standardize the reagent by the above procedure against 0.01*M* stannic solution.

Results

The results of several determinations are shown in Table I. The standard deviation of these results is ±0.13 mg; the mean deviation ±0.11 mg. The errors approach a random distribution about zero in the range 15–35 mg of tin. In the higher concentrations, viz., 35–50 mg of tin, a definite trend toward more negative results has been observed. The coefficient of regression (4) of this trend has been determined to be −0.24 relative per cent error per millimolar concentration unit. Considerable improvement in precision is possible in the higher range if correction is made for this regression.

TABLE I. *Amperometric titrations of stannic tin*
(25.00 ml Sn^{IV} solutions titrated in 3*N* HCl with 0.0453*M* TPAC. Currents measured at −0.3 volt vs. S.C.E.)

Tin taken	Tin found	Difference
mg	mg	mg
14.83	14.98	+0.15
17.80	18.09	+0.29
20.77	20.88	+0.11
23.73	23.64	−0.09
26.70	26.73	+0.03
29.67	29.88	+0.21
35.60	35.60	0.00
	35.54	−0.06

Interfering Substances

Substances which interfere with the amperometric titration of tin may be divided into three classes: (*a*) those that give polarographic currents at −0.3 volt, (*b*) those that react with tetraphenylarsonium ion, and (*c*) those that complex tin to form ions which are not precipitated by the reagent.

A list of ions which yield interfering polarographic currents includes ferric, mercuric, bismuth, antimony$^{III \text{ and } V}$, arsenious, cupric, uranyl, molybdate, vanadate, and selenite ions. Lead, though reduced at a potential more negative than −0.3 volt, interferes by causing the reduction of tin to begin at more negative potentials (3). If lead is present in concentrations of 0.005*M* or less, the titration may be made by measuring currents at −0.4 volt.

Ions that precipitate tetraphenylarsonium ion and which must be absent include perchlorate, tungstate, permanganate, perrhenate, molybdate, iodide, bromide, fluoride, thiocyanate, bismuth, platinum, zinc, cadmium, thallic, and mercuric ions. Separation of tin from these ions with phenylarsonic acid is suggested, but the feasibility of this procedure has not been investigated.

A number of organic acids form stable complexes with stannic tin which are not precipitated by tetraphenylarsonium ion and thus interfere with the amperometric titration. Citrate and oxalate are particularly troublesome in this respect. However, Willard and Smith (1) found that moderate amounts of tartrate and acetate did not interfere with their method. Nitrate, sulfate, potassium, and sodium ions are without effect in the method. Phosphate interferes through a complexing action.

Determination of Mercuric Ion

The amperometric titration of mercuric ion is based on the reaction

$$2(C_6H_5)_4As^+ + HgCl_4^{--} \rightarrow [(C_6H_5)_4As]_2HgCl_2.$$

The current before the end point is due to the two-electron reduction of chloromercuriate ion. The lower limit of potential for good mercuric diffusion current measurements is set by the potential at which the anodic chloride wave appears. In 3*N* hydrochloric acid, this is −0.10 volt vs. S.C.E. At this potential only a small fraction of the oxygen dissolved in a solution is reduced. It is not necessary, therefore, to remove oxygen in the titration.

As in the titration of stannic ion, so in this titration the concentrations of hydrogen and chloride ions must be considered. At chloride concentrations below 2*N*, the results are low. The concentration of hydrogen ion has an effect upon the crystallinity of the precipitate. When $[H^+]$ is below 2*N*, the precipitate is always voluminous and results tend to be low. Good accuracy and precision are obtained only when both chloride and hydrogen ion concentrations are greater than 2*N*. Best results are obtained in 3*N* hydrochloric acid. If the concentration of hydrochloric acid is increased much above 3*N*, the attainment of equilibrium is too slowly reached and the titration curves are not so well defined.

In making the above investigation, ammonium chloride, nitric acid, and hydrochloric acid were used to prepare the various hydrogen ion-chloride ion mixtures.

Procedure

Take for analysis a sample containing 120 to 480 mg of mercury in the mercuric state. Add sufficient hydrochloric acid to bring the concentration of this acid to 3*N*. (Note that, in special cases, hydrogen and chloride ions may be added independently through nitric acid and ammonium chloride, respectively, in order to bring $[H^+]$ and $[Cl^-]$ up to 3*N*.) Dilute the mixture to 100 ml in a volumetric flask. Pipet 25.00 ml into a 50-ml beaker. Add 0.05*M* TPAC from a 10-ml buret, and stir well. Allow 3 to 4 minutes for the system to come to equilibrium after

the first addition of reagent before reading the current. After subsequent additions, 1 to 2 minutes is sufficient time for equilibrium to be reached. Establish the titration lines with 4 or 5 points on either side of the end point. Correct the observed currents for dilution and plot the points to determine the end point. Standardize the reagent by the above procedure against 0.01*M* mercuric solution.

TABLE II. *Amperometric titrations of mercuric ion* (25.00 ml Hg^{II} solutions titrated in 3*N* HCl with 0.05*M* TPAC. Currents measured at −0.3 volt vs. S.C.E.)

Hg^{II} taken	Hg^{II} found	Difference
mg	*mg*	*mg*
30.1	29.9	−0.2
	29.6	−0.5
35.1	34.5	−0.6
	35.4	+0.3
40.1	39.0	−1.1
	39.8	−0.3
45.1	45.2	+0.1
	45.2	+0.1
50.2	50.6	+0.4
	50.4	+0.2
55.2	55.2	0.0
	55.8	+0.6
60.2	60.0	−0.2
	60.0	−0.2
65.2	64.3	−0.9
	64.8	−0.4
70.2	70.7	+0.5
	69.9	−0.3
75.2	74.6	−0.6
	75.7	+0.5
80.2	80.1	−0.1
	80.5	+0.3

Results

The results of several determinations are shown in Table II. The standard deviation of these results is ±0.47 mg; the mean deviation is ±0.38 mg. The errors are randomly distributed around zero in the range 30–80 mg; however, in samples containing more than 80 mg, the errors are significantly negative.

Interfering Substances

Ions which yield cathodic currents at −0.10 volt, thus interfering with the mercury determination, include ferric, bismuth, cupric, uranyl, molybdate, vanadate, and selenite. As in the determination of tin, ions which precipitate with TPAC in 3*N* hydrochloric acid interfere. Nitrate and sulfate are without effect.

Cadmium and Zinc

Attempts to determine cadmium accurately by amperometric titration with TPAC were unsuccessful. In a systematic study of the titration in various hydrogen ion-chloride ion mixtures, no conditions were found which yielded well-defined titration curves and reproducible results. Equilibrium was much more slowly attained in cadmium titrations than in mercuric and stannic titrations.

Since zinc does not yield a diffusion current under conditions necessary to its titration with TPAC, this determination is not feasible.

Any discussion of this paper will appear in a Discussion Section, to be published in the December 1951 issue of the Journal.

REFERENCES

1. H. H. Willard and G. M. Smith, *Ind. Eng. Chem., Anal. Ed.*, **11**, 269 (1939).
2. *Ibid.*, **11**, 186 (1939).
3. I. M. Kolthoff and R. A. Johnson, *Anal. Chem.* (In press).
4. G. W. Snedecor, "Statistical Methods," Iowa State College Press, Ames, Iowa (1946).

The Mechanism and Rate of Dissolution of Titanium in Hydrofluoric Acid[1]

M. E. Straumanis and P. C. Chen

University of Missouri, School of Mines and Metallurgy, Department of Metallurgy, Rolla, Missouri

ABSTRACT

Titanium dissolves rapidly in hydrofluoric acid according to the reaction: $2Ti + 6HF \rightarrow 2TiF_3 + 3H_2$. The formation of the trifluoride was confirmed by titration with potassium permanganate solution and by measurement of the volume of hydrogen evolved. The rate of dissolution, V, of titanium in hydrofluoric acid of concentrations between $0.02N$ and $0.2N$ conforms with the empirical equation: $V = 459N^{2/3}$ mm³/cm²min. For the acid between $0.2N$ and $10N$ the equation becomes $V = 88 + 473N$ mm³/cm²min. Metal salts added to the acid during the dissolution of titanium increased the rate in the following order: Fe^{2+}, Ni^{2+}, Ag^{+}, Cu^{2+}, Au^{3+}, Pt^{4+}, that is, nearly the order of decreasing overvoltage of the corresponding metals. Mg^{2+} proved to be inactive while Pb^{2+} hampered the dissolution reaction. The open-circuit potential of titanium became more anodic as the concentration of hydrofluoric acid varied from $0.0125N$ to $0.2N$. The potential remained practically constant with concentrations higher than $0.2N$ (-0.768 volt, hydrogen scale). A visible grayish blue film was formed on titanium in concentrations below $0.5N$. The dissolution of titanium in hydrofluoric acid is probably an electrochemical process, based on the activity of local elements.

Introduction

The literature covering corrosion data on titanium is limited, especially for comparatively pure titanium, and such data concern mostly the impure brittle metal (1). Except for two papers (2, 3), references are generally qualitative statements: for instance, it has been reported that titanium is very soluble in hydrofluoric acid. None of the papers published thus far have dealt with the mechanism of dissolution.

The present paper reports a quantitative study on the dissolution of titanium in hydrofluoric acid. The study includes the basic reaction of dissolution, rates of dissolution, effects of added salts, potential measurements, and a discussion of the mechanism of dissolution.

Three kinds of titanium were used for this study: titanium I, obtained from Remington Arms in form of a rolled sheet 1.5 mm thick (nominal purity over 99 per cent); titanium II, received from the Bureau of Mines as a sheet 1 mm thick, sintered from sponge by the Bureau (over 99.1 per cent); and titanium III, obtained from Battelle Memorial Institute in form of a rod 1.5 cm in diameter, made by the iodide process (over 99.9 per cent). The purity is given according to the data of current literature (3, 4). Samples for the experiments were cut from these metals.

[1] Manuscript received September 11, 1950. This paper, based on a thesis submitted by P. C. Chen in partial fulfillment of the requirements for the Ph.D. degree to the Graduate School of the University of Missouri, prepared for delivery before the Detroit Meeting, October 9 to 12, 1951.

The Reaction of Dissolution

As the metal dissolves quickly in hydrofluoric acid, the best method of evaluating the rate of dissolution is the measurement of hydrogen evolved. To do this, it is important to know the basic reaction. Two possibilities are:

$$2Ti + 6HF \rightarrow 2TiF_3 + 3H_2 \qquad (I)$$

and

$$Ti + 4HF \rightarrow TiF_4 + 2H_2. \qquad (II)$$

According to reaction (I), one gram atom of titanium would evolve 1.5 gram moles of hydrogen, whereas, for reaction (II), 2 gram moles should be evolved. Thus it is possible to distinguish between the reactions by means of the hydrogen volume.

This question arose because our qualitative tests showed that titanium ions of lower valency than 4 are formed during the dissolution in hydrofluoric acid, but it is reported to be reaction (II) (5–7). Ruff and Ipsen (8), however, stated that titanium reacted according to reaction (II) when anhydrous hydrogen fluoride gas was used at about 700°C. Because of the ambiguity it seemed advisable to investigate the true nature of the reaction in question.

Two methods of approach were used: (*a*) direct titration of the oxygen-free solution with potassium permanganate, and (*b*) measurement of the hydrogen volume obtained during the dissolution reaction.

The volumetric titration of the titanium solution.—If the titanium metal dissolves in hydrofluoric acid to form trifluoride under the protection of an inert atmosphere, the trivalent ions thus obtained could be oxidized to tetravalent ions by a potassium permanganate solution in the presence of sulfuric acid. The complete ionic and molecular equations of the titration reaction would be as follows:

$$MnO_4^- + 8H^+ + 5e \rightarrow Mn^{2+} + 4H_2O$$
$$5Ti^{3+} \rightarrow 5Ti^{4+} + 5e$$

$$5Ti^{3+} + 8H^+ + MnO_4^- \rightarrow 5Ti^{4+} + Mn^{2+} + 4H_2O \quad (III)$$

$$5TiF_3 + 8HF + KMnO_4 \rightarrow 5TiF_4 + MnF_2 + KF + 4H_2O. \quad (IV)$$

Therefore, if the dissolution of titanium occurs according to reaction (I), the titration reaction (IV) should be correct. The titrations of solutions of titanium I showed a discrepancy of −3.62 per cent (average of 6 determinations) between the sample weight and the titanium determined by titration.

It was important to know whether the discrepancy of −3.62 per cent was the result of the presence of oxygen in the apparatus, although CO_2 used as inert gas was passed through a $CrCl_2$ solution, or because of impurities in the titanium.

A weighed sample of titanium was dissolved in the presence of zinc amalgam in a small bulb (9). Two ml of 6*N* sulfuric acid were added to the 15 ml of 1*N* hydrofluoric acid to insure the reducing activity of the amalgam. Separate tests showed that titanium goes into solution also in sulfuric acid with lower valency than 4. After the titanium metal had completely dissolved in the acid, the greenish-yellow solution was transferred into an Erlenmeyer flask and the amalgam was washed. The whole apparatus was airtight and no oxygen could enter the flask or bulb. The titration was carried out with a 0.1*N* $KMnO_4$ solution (1 ml of the solution was equivalent to 47.90×10^{-4} g Ti) while a stream of CO_2 was turned on. The titanium solution was kept in motion by a magnetic stirrer.

The results of 4 titrations showed that there is still a discrepancy of −2.34 per cent. To check this result the volume of hydrogen evolved was measured.

The gasometric determination of titanium; purity of titanium.—As the dissolution of titanium in hydrofluoric acid occurs most likely according to reaction (I), one mg titanium is equivalent to 0.702 ml H_2 gas at standard conditions (atomic weight of Ti = 47.90). This ratio must be checked by experiments. On the other hand, the purity of the titanium under question can be determined from the deviations, if any, from the ratio mentioned.

The apparatus used for this purpose is shown in Fig. 1. A previous experiment revealed that 1.5*N* hydrofluoric acid attacked Pyrex glass at a rate of 0.57 mg/cm² hr, for the first 24 hours. Although the rate of attack decreased gradually in the course of time, the inside walls of the reaction flask were lined with paraffin to protect them as well as possible from this attack. The rotational speed of the stirring rod was about 250 revolutions per minute. The hydrogen evolved was collected over water. The reaction flask was placed in a water bath at 25° ± 0.1°C.

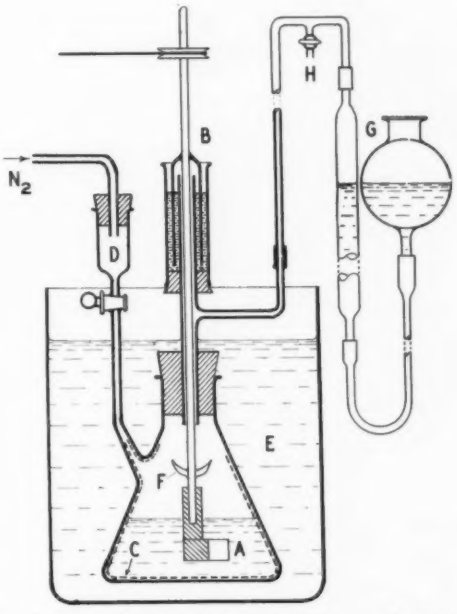

FIG. 1. Apparatus for determining the ratio between titanium dissolved and hydrogen evolved and also for determining the rate of dissolution of titanium in hydrofluoric acid. A—Ti sample on the ebonite foot of the stirrer, B—stirrer with mercury closure, C—paraffin lining, D—funnel for introducing pure N_2 and reagents, E—constant temperature water bath (25°C), F—rubber cap, G—gas buret with leveling bulb, H—valve for the outlet of gas.

The first runs showed that it is necessary to remove the oxygen from the apparatus, since the following reaction occurred with a contraction in volume:

$$4TiF_3 + 4HF + O_2 \rightarrow 4TiF_4 + 2H_2O. \quad (V)$$

In addition, titanium may act catalytically in the formation of water from oxygen and liberated hydrogen. Therefore, the air in the apparatus (Fig. 1) was replaced by nitrogen before the experiment. Qualitative tests showed that the nitrogen contained only traces of oxygen.

A sample of titanium I, polished and cleaned, was accurately weighed and glued to the ebonite foot of the stirrer by means of plastic cement. The flask was filled with 75 ml of 1*N* hydrofluoric acid (C.P.

analyzed) and the stirrer B inserted. This was held temporarily in an elevated position so that the sample was above the acid level. Nitrogen was introduced through D for a period of at least 10 minutes (it escaped through the valve H). When the flask reached the temperature of the water bath, the stirrer was lowered and put into rotation, the valves were closed, and the hydrogen measured by lowering of the level bulb. The volume of gas was reduced to standard dry conditions (see Table I).

These results show clearly that during the dissolution only trivalent titanium ions are formed (Ti^{3+}). The discrepancy might be less by approximately 0.3 per cent because of some loss of hydrogen and probably because of some oxygen remaining in the nitrogen and in the acid, which caused the decrease in volume due to reaction (V). If the estimated 0.3 per cent is added to the discrepancy values of Table I, one will get a lower discrepancy of −2.2 per cent for titanium I, which agrees well with the value obtained by direct titration, −2.34 per cent. The titanium samples may not have the purity claimed. The presence of impurities could even be observed in the first two samples of Table I: some black residue always remained after the dissolving of titanium, most likely consisting of carbon according to the literature (3, 4). The fluctuations of results in different runs (Table I) can be explained well by the variation in purity of separate samples.

TABLE I. *Volume of hydrogen obtained by dissolution of titanium in HF. Volume calculated from equation (I)*

Titanium	Loss in weight	H_2 observed	H_2 calculated	Discrepancy
	mg	*ml*	*ml*	%
I	208.92	145.10	146.65	−1.06
	257.00	176.12	180.41	−2.38
	200.00	135.86	140.93	−3.60
	231.05	157.39	162.20	−2.96
Average				−2.50
II	228.50	157.15	160.41	−2.03
	214.75	149.45	150.75	−0.86
	207.38	143.58	145.58	−1.37
	216.55	149.62	152 02	−1.58
Average				−1.46
III	125.00	87.36	87.75	−0.44
	213.90	148.89	150.16	−0.84
	237.30	166.97	166.58	+0.23
	216.00	150.47	151.63	−0.78
	240.50	168.56	168.83	−0.16
Average				−0.39

The Rate of Dissolution of Titanium in Hydrofluoric Acid

The investigation of the rate of dissolution was based solely on the collection and measurement of the volume of hydrogen gas liberated. The method applied was described earlier (10). The apparatus shown in Fig. 1 was used. Squares were cut from titanium I, filed down to the exact dimension of 1 cm^2, and mounted in Bakelite in such a manner as to expose only the 1 cm^2 face. Superfluous Bakelite was ground away. The surface to be exposed to the acid was ground with emery paper and polished with a polishing wheel and levigated aluminum oxide. Two titanium samples were used for each concentration of the acid to give the average rate of dissolution. The rate (V) was calculated in mm^3/cm^2min from the gas volume (v_0) reduced to standard conditions:

$$V = \frac{\Delta v_0}{\Delta t F}. \qquad (1)$$

Titanium I was used in all runs because of the plentiful supply on hand.

Fourteen different concentrations of hydrofluoric acid were used: 0.02, 0.04, 0.08, 0.2, 0.5, 1, 2, 3, 4, 5, 6, 7, 8, and 10N. Each run started with an induction period, which was shorter in acids of lower concentration. After a flat maximum, lasting for a longer period of time in more concentrated acids, the reaction rate decreased slowly. For instance, in the case of dissolution in 0.02N acid the maximum rate was reached in 30 minutes. The maximum was sharp and the average rate of two runs was 34.6. In 5N acid the induction period lasted 60–80 minutes, the maximum was flat, and the average rate was 2540 mm^3/cm^2min. The sample surfaces, after dissolution in dilute acids (0.02 to 0.5N), exhibited a dark bluish gray film.

In Fig. 2 the average maximum rates were plotted against the concentration of the acid. The curve consisted of two separate parts: a straight line representing rates in acid of concentrations higher than 0.2N and a curve for the lower concentrations. For these concentrations (0.02, 0.04, and 0.08N) the rate of dissolution conforms to the following empirical expression:

$$V = 459(N)^{2/3}. \qquad (2)$$

For acids more concentrated than 0.2N, the rate of dissolution can be expressed by

$$V = 88 + 473N. \qquad (3)$$

The comparison between the rates calculated by equations (2) and (3) and those observed are shown in Table II. The curve obtained resembles the disso-

lution curves of other metals, e.g., Al in NaON, KOH, or $Ba(OH)_2$ (10, 11).

Influence of Foreign Ions in the Acid on the Rates of Dissolution

The process of dissolution of titanium in hydrofluoric acid might be of chemical or of electrochemical nature. There are several experimental methods to distinguish between these two possibilities: (*a*) by measuring the rate of dissolution of titanium in the presence of metallic impurities more noble than titanium itself; (*b*) by potential measurements of the dissolving metal; and (*c*) by the statement of the presence of the difference effect.

To investigate the first possibility, the change in the rate was observed when a metallic salt solution was introduced to the acid during the dissolution process in the apparatus shown in Fig. 1. One ml of

TABLE II. *Observed and calculated rates of dissolution V of titanium I in HF of various concentrations at 25°C*

Normality of HF	found mm³/cm²min	calc mm³/cm² min	Δ	* Δ%
0.02*	34.4	33.9	+0.5	+1.4
0.04	50.5	53.7	−3.2	−6.3
0.08	89.0	85.3	+3.7	+4.2
0.2‡	183	183	±0.0	±0.0
0.5	332	325	+7	+2.2
1	588	561	+27	+4.5
2	1047	1034	+13	+1.3
3	1659	1507	+152	+10.0
4	1970	1980	−10	−0.5
5	2540	2453	+93	+3.8
6	2954	2926	+28	+0.9
7	3490	3399	+91	+2.6
8	3490	3872	−382	−9.9
10	4660	4818	−158	−3.5

* Equation (2).
‡ Equation (3).

0.1*M* metallic salt solution was added through the funnel D when the rate of dissolution of the titanium sample was decreasing. This moment was chosen in order to be quite sure about the effect produced by the salt. Only 1*N* hydrofluoric acid was used throughout this series of tests (at 25°C). To avoid the dilution of the acid by the additional reagent, an equal amount (1 ml) of 2*N* hydrofluoric acid was premixed with the salt solution (1*N*, fresh acid, added alone did not influence the rate). Immediately after introduction of the mixture into the reaction flask, the valves were closed and readings of the gas volume started. The stirring mechanism was working all the time during these operations. Eight different additional reagents were used: $PtCl_4$, $AuCl_3$, $CuSO_4$, $AgNO_3$, $NiSO_4$, $FeSO_4$, $Mg(CH_3COO)_2$, and $Pb(NO_3)_2$. Two typical runs are shown in Table III. The platinum increased the rate by 364 per cent but it dropped very rapidly, while the nickel increased it only by 23 per cent and the rate decreased slowly. The effects of the eight additions are summarized in Table IV. The percentages obtained are averages of 2 to 4 runs.

TABLE III. *The effect of addition of $PtCl_4$ and of $NiSO_4$ to 1N HF on the velocity of dissolution of titanium I at 25°C*

Salt	Time min	v_0 ml	V mm²/cm² min
$PtCl_4$	165	90.6	542
	180	98.7	540
	195	106.8	540
	0	0	—*
	15	37.6	2508
	30	49.5	794
	45	60.5	733
	60	70.2	648
	75	79.9	648
$NiSO_4$	120	69.4	565
	135	78.2	586
	150	86.8	573
	0	0	—‡
	15	10.6	708
	30	21.3	713
	45	31.5	680
	60	41.8	686
	75	51.9	674

* $PtCl_4$ solution added.
‡ $NiSO_4$ solution added.

TABLE IV. *The effect of salts, added to 1N HF, on the rate of dissolution of titanium. Hydrogen overvoltage in volts*

Ions of the salts	Change in rate (%)	Hydrogen overvoltage of metals in volts (12)	
		1 amp/dm²	10 amp/dm²
Pt^{4+}	364	0.03	0.04
Au^{3+}	72.9	0.39	0.59
Cu^{2+}	67.9	0.58	0.85
Ag^{+}	30.8	0.76	0.88
Ni^{2+}	24.1	0.76	1.05
Fe^{2+}	5.4	0.56	0.82
Mg^{2+}	−2.7		
Pb^{2+}	−5.5*	1.09	1.18

* PbF_2 partly precipitated from the solution; but it is believed that there were Pb^{++} enough to be plated out on the Ti.

Table IV shows the relationship between the velocity of dissolution and the overvoltage of the nobler metal (13) precipitated on titanium: the highest acceleration in the rate is obtained by Pt^{4+} (low hydrogen overvoltage on platinum), and the lowest by Pb^{2+} (high overvoltage on lead). Only iron is slightly out of the series. The overvoltage is a function of current density and in some cases (lead) it rises very rapidly with the current, in other cases

(silver) not. But the overvoltage of a local cathode is always less anodic than the potential of the dissolving metal. The influence of the anion seems to be without effect, if the salts are present in small quantities, because $Mg(CH_3COO)_2$ and KCl, added to the acid, did not change the rate of dissolution.

Potential Measurements and the Surface Film on Titanium

Potential measurements and observations on the current density produced by a metallic electrode are of great value for the explanation of the mechanism of dissolution.

The potential developed by titanium in dissolving to Ti^{3+}, equation (I), was measured in hydrofluoric acid of various concentrations up to 1*N* (see Table V). The determinations were made by measuring the emf of the cell

TABLE V. *Dissolution potential ϵ' of titanium in HF in the presence of air*

N of the acid	Hydrogen scale ϵ' in volts	
	1st reading	Max negative reading
0.0125	−0.160	−0.646
0.025	−0.187	−0.637
0.05	−0.587	−0.656
0.1	−0.665	−0.699
0.2	−0.778	−0.778
0.3	−0.769	−0.769
0.4	−0.758	−0.758
0.5	−0.767	−0.767
0.6	−0.761	−0.770
0.8	−0.768	−0.768
1.0	−0.769	−0.769

$$Ti \mid\mid HF \mid 1N\ KCl \mid 1N\ KCl,\ Hg_2Cl_2 \mid\mid Hg.$$

The measurements were performed in the presence of air since some tests made in nitrogen revealed that the difference in readings is within the error limits (±0.005 volt). The figures in Table V represent dissolution potentials, since the titanium dissolved during the measurements and ϵ', being a function of the rate of dissolution, fluctuated, because the rate was not constant during the measurements.

Table V shows further that in acids of low concentrations the reading obtained just after dipping the metal into the acid was considerably less anodic than the values obtained some hours later. Further, above 0.2*N* acid the potential of titanium was independent of the concentration of the acid (in hydrochloric and sulfuric acid the behavior of titanium was different). These facts speak in favor of the presence of a film on dissolving titanium as already mentioned above. The film became just visible in 0.5*N* acid, darkened with decreasing concentration of the acid, and showed a grayish blue color in 0.2*N* acid. That is the point where the potential started to become more noble. Further, the presence of a film could be proved by the following experiment, which also can be taken as a proof of the electrochemical conception of dissolution of metals in acids. The maximum current produced by a milliammeter short-circuited Ti | HF | Pt cell came just after the circuit was closed and when the acid was less than 0.2*N*. The current decreased rapidly to zero. For 0.2*N* acid and above, the current reached its maximum only after approximately one hour and then decreased gradually in the course of time. In 1*N* acid a current of 0.1 amp could be drawn from the small cell. The polarization affects the current appreciably only below 0.2*N*, where the dark film could be observed on the metal surface. The nature of the film was not established.

Conclusions

All the facts mentioned and the experiments just described showed that the dissolution of titanium in hydrofluoric acid might be an electrochemical process, the velocity of which is determined by the activity of local cells. Thus, the picture of the dissolution of titanium in hydrofluoric acid is as follows. The dissolving metal is covered by a porous film the thickness of which decreases considerably (the pores widen simultaneously) when the concentration of the acid is above 0.2*N*. The dissolution process of titanium occurs in these pores through the activity of local elements, the cathodes of which are the impurities in titanium. The film on the metal may act as cathode only in case it has a low electrical resistance and a low overvoltage. Since the emf of a local cell is $\epsilon' - \eta$ and its total resistance is r the average current produced by a cell is:

$$i = \frac{\epsilon' - \eta}{r}.$$

η is the hydrogen overvoltage. The three variables ϵ', η, and r are functions of the current i. If there are z' active elements on unit area of dissolving titanium the total current produced will be

$$I = z' \frac{\epsilon' - \eta}{r}.$$

z' is the number of local elements in the pores not shielded by the protective film (z is the total number of elements per cm²). In this z' is incorporated the whole theory of W. J. Müller (14). To express the rate of dissolution according to equation (1), a factor k must be added (15, 16):

$$V = kz' \frac{\epsilon' - \eta}{r} \qquad (4)$$

This equation explains the observations described in the present paper. For example, platinum (Table IV) acted so violently because of the low overvoltage of the cathodes of the local cells. The platinum precipitated rapidly because of the reaction[2]

$$Pt^{4+} + 4Ti^{3+} \rightarrow Pt + 4Ti^{4+}. \qquad (VI)$$

However, only part of the platinum precipitated in the pores of the film on the titanium:

$$3Pt^{4+} + 4\,Ti \rightarrow 3Pt + 4Ti^{3+}. \qquad (VII)$$

And even this part fell down quickly because of the poor adhesion or undermining. Therefore, the number of acting local cathodes in the pores decreased the rate of dissolution rapidly and simultaneously. The precipitate was on the bottom of the vessel. The same occurred in the case of Au^{3+}, Cu^{2+}, and Ag^{2+}. Of course, the influence on the rate of dissolution of titanium was lower because of the decreasing emf of the local elements. In the case of Ni-, Fe-, and Pb-cations only the titanium metal served as reducing agent, equation (VII). The precipitation of these metals on the surface of titanium was, therefore, slow and the acceleration effect small but continuous (constant and low z', low emf). No precipitate was observed on the bottom of the vessel. The Pb^{++} even hampered the dissolution process. Magnesium, being more anodic than titanium, did not influence the rate, which decreased in the normal way.

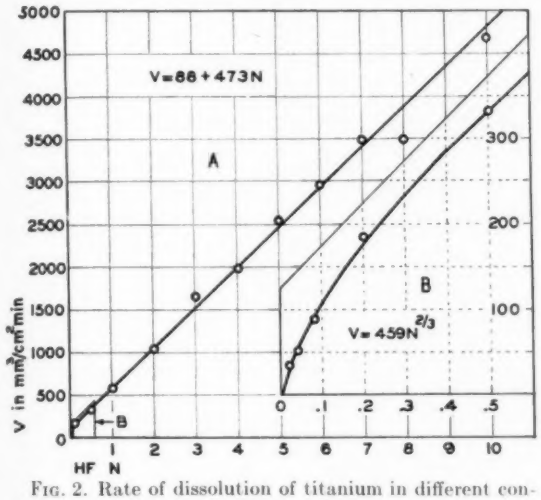

FIG. 2. Rate of dissolution of titanium in different concentrations of HF. A: 0–10N; B: 0–0.5N.

The curve of Fig. 2 can be explained as follows: at low concentrations of the acid the rate is low (small z', low emf, high r). With increasing acid concentrations two things happen: the pores of the film widen (increasing z') and the emf of the local cells rises (increasing ϵ', Table V), both contributing to the velocity of dissolution (curved part of Fig. 2). At concentrations higher than 0.2N, ϵ' remains nearly constant (Table V), so that only the widening of the pores (increasing z') in the film increases the rate, resulting in the straight line part of Fig. 2. The thickness of the film and, therefore, the width of the pores depend on the concentration of the acid, since at higher concentrations the breakdown or the solubility of the film in the acid is better. The resistance of the acid is of minor importance, because hydrofluoric acid is weak and has, therefore, as compared with hydrochloric acid, a high resistance (17), the changes of which do not influence appreciably the current produced by the local elements.

A further proof in favor of the local element theory, to be published later, is the difference effect observed on titanium.

Some experiments showed that the pure titanium III had a higher rate of dissolution than did titanium I. This is not in contradiction with the theory, because titanium I evidently contains an alloying element which slows down the rate of dissolution of pure titanium (18, 19).

ACKNOWLEDGMENT

The authors wish to express their thanks to Dr. A. W. Schlechten, Chairman of the Department of Metallurgical Engineering, to the Battelle Memorial Institute, Columbus, Ohio, to the U. S. Bureau of Mines, and to the Remington Arms Company for supplying the titanium used in this investigation.

Any discussion of this paper will appear in a Discussion Section, to be published in the December 1951 issue of the JOURNAL.

REFERENCES

1. W. J. KROLL, "Corrosion Handbook" (H. H. Uhlig, Editor), p. 329, John Wiley & Sons, Inc., New York (1948).
2. E. A. GEE, L. B. GOLDEN, AND W. E. LUSBY, *Ind. Eng. Chem.*, **41**, 1668 (1949).
3. G. E. HUTCHINSON AND P. H. PERMAR, *Corrosion*, **5**, 319 (1949).
4. E. A. GEE, W. H. VAN DERHOEF, AND C. M. WINTER, JR., *J. Electrochem. Soc.*, **97**, 49 (1950).
5. R. M. CAVEN, "Textbook of Inorganic Chemistry" (G. N. Friend, Editor), Vol. **V**, p. 237, Griffin, London (1921).
6. W. H. LATIMER AND J. H. HILDEBRAND, "Reference Book of Inorganic Chemistry," p. 314, Macmillan Co., New York (1940).
7. J. W. MELLOR, "A Comprehensive Treatise on Inorganic and Theoretical Chemistry," p. 19, Longmans, Green & Co., New York (1927).
8. O. RUFF AND R. IPSEN, *Ber.*, **36**, 1777 (1903).

[2] The side reaction $3Ti^{4+} + Ti \rightarrow 4Ti^{3+}$ can proceed only with a low velocity because of the low concentration of Ti^{4+}.

9. W. H. Thornton, Jr., "Titanium," p. 142, Chemical Catalog Co., New York (1927).
10. M. E. Straumanis and N. Brakšs, *J. (and Trans.) Electrochem. Soc.*, **95,** 98 (1949).
11. M. E. Straumanis and N. Brakšs, *Ibid.*, **96,** 21 (1949).
12. M. Knobel, C. Caplan, and M. Eiseman, *Trans. Electrochem. Soc.*, **43,** 55 (1923).
13. M. Straumanis, *Z. physik. Chem.*, **A129,** 370 (1927).
14. W. J. Müller, "Die Bedeckungstheorie der Passivität der Metalle," Verlag Chemie, Berlin (1933).
15. M. Straumanis, *Korrosion u. Metallschutz*, **9,** 1, 29 (1933).
16. M. Straumanis, *Ibid.*, **14,** 81 (1938).
17. E. G. Hill and A. P. Sirkar, *Proc. Roy. Soc. (London)*, **A83,** 144 (1910).
18. M. Straumanis, *Z. physik. Chem.*, **A148,** 112 (1930).
19. U. R. Evans, "Metallic Corrosion, Passivity and Protection," p. 203, Longmans, Green & Co., New York (1948).

The Kinetics of the Oxidation of Cobalt[1]

EARL A. GULBRANSEN AND KENNETH F. ANDREW

Westinghouse Research Laboratories, East Pittsburgh, Pennsylvania

ABSTRACT

The kinetics of oxidation of cobalt is a complex problem since the metal forms two or more oxides and the metal itself has a phase transition from hexagonal to face-centered cubic at a temperature between 300° and 500°C.

The vacuum microbalance method is used to study the effect of time, temperature, pressure, pretreatment, etc., on the rate of the reaction at temperatures below 700°C. The hexagonal (cold-worked) form of cobalt was found to oxidize more rapidly than the cubic (annealed) form. The rate of reaction was found to increase abruptly between 600° and 700°C. The rate data are interpreted in terms of the transition state theory and the energy and entropy of activation for the reaction calculated.

Valensi has discussed the oxidation mechanism above 700°C in terms of diffusion of oxygen through the oxide lattice. Electron diffraction studies on the solid phase reaction of $Co_3O_4 + Co$ to give 4CoO indicate that the cobalt diffuses through the oxide at temperatures as low as 450°C. An alternate mechanism to that proposed by Valensi is suggested to account for the reaction based on the diffusion of cations and electrons.

INTRODUCTION

This paper presents the results of a kinetic study of the oxidation of cobalt over the temperature range of 200° to 700°C. Such a study is of interest since a number of high temperature and high strength alloys contain cobalt. It is also of interest from a scientific and theoretical point of view since cobalt is one of a number of metals forming multiple oxides and one of a few metals having a structural transformation occurring in the temperature region most important in oxidation.

One may predict that cobalt has some degree of oxidation resistance since the volume ratio of the oxide to the metal is greater than unity (27). The other favorable factor in its general behavior with gases is that the metal does not react with nitrogen or hydrogen. However, a number of unfavorable factors are: (*a*) the oxides are readily reduced by hydrogen or carbon monoxide, (*b*) the oxides Co_2O_3 and Co_3O_4 are unstable at elevated temperatures, (*c*) solid phase reactions of the oxide with the metal are favorable thermodynamically at all temperatures, and (*d*) the crystal structure transformation of the hexagonal close-packed structure to the face-centered cubic structure occurs at 430°C.

Literature Survey

Kinetics.—The reaction of cobalt with oxygen above 600°C has been studied by a number of workers. Hatfield (16) found that oxygen reacted with cobalt between 700° and 1000°C at a faster rate than it did with nickel but slower than with iron. Dunn and Wilkins (5) found the reaction to follow the predictions of the parabolic rate law and the Arrhenius law. Valensi (31) showed that the oxidation of cobalt above 600°C followed the parabolic rate law, corrected for the speed of an interface reaction, for freshly cleaned specimens up to 900°C. Contamination of the samples by the atmosphere was found to be a major effect. Correlation of the data with those of Johns and Baldwin (19) indicates a definite change in the mechanism of reaction. Valensi (31) interprets the data in terms of an oxide predominately CoO above 700°C and Co_3O_4 below 700°C. Oxygen is assumed to diffuse through the oxide and no cation movement is indicated.

The velocity of oxidation of CoO to Co_3O_4 has been studied by Chauvenet (4) and by Johns and Baldwin (19). Chauvenet (4) finds the data to fit the parabolic rate law and calculates an energy of activation of 23,950 calories per mole. The data for this reaction have been analyzed by Valensi (31) and by Johns and Baldwin (19) in terms of Valensi's theory (32) but they do not fit the theory.

McAdam and Geil (22) have studied the rate of oxidation by observing the time for the appearance of the several temper colors at different temperatures. At 300°C cobalt oxidizes at a slower rate than iron but faster than nickel, aluminum, tungsten, and vanadium.

Stability and structure of the oxides.—Natta and Strada (25) have shown the existence of the three oxides CoO, Co_3O_4, and Co_2O_3. CoO has the face-centered cubic structure (NaCl type) with $a = 4.22$ Å; Co_3O_4 (17) has the spinel type of structure

[1] Manuscript received December 28, 1950. This paper prepared for delivery before the Buffalo Meeting, October 11 to 13, 1950.

with $a = 8.108$ Å; and Co_2O_3 (25) has a hexagonal structure with $a = 4.64$ Å and $c/a = 1.24$.

LeBlanc and Mobius (21) have studied CoO and its system with oxygen. Co_3O_4 is formed only if CoO is reacted above 100°C and below the decomposition temperature for Co_3O_4 with O_2. Co_3O_4 in turn can react with O_2 to form $Co_3O_4 \cdot mO_2$ without forming Co_2O_3. Co_2O_3 can be prepared only through precipitation of a solution of Co^{+++} with OH^- and not by dry oxidation.

An x-ray study of cobalt oxidized in air (385°–800°C) (2) shows that the main part of the oxide layer consists of CoO in contact with the metal and a small amount of Co_3O_4 on the surface. At low temperatures the relative amount of Co_3O_4 increases. Arkharov and Graevskii (1) noted the lattice spacings for CoO at the boundary with Co to be 4.2508 Å, while at the boundary with air a value of 4.2548 Å was observed. They conclude that the growth of CoO occurs by the diffusion of oxygen inward.

Arkharov and Lomakin (3) show that below 890°C the film consists of a thin layer of Co_3O_4 and a thicker film of CoO, while above 890° C only CoO is present.

Crystal structure transformation in cobalt.—Hull (18) first showed that cobalt exists in both the face-centered cubic and hexagonal close-packed modifications. Edwards and Lipson (7) in an x-ray study have shown that above 500°C the cubic form is stable. Upon cooling to 300°C the hexagonal structure is formed to a small extent. As the temperature is lowered to room temperature about equal amounts of the two phases form. The authors conclude that the free energy of the two phases are almost equal below 500°C and that the approach to equilibrium is governed by other factors including crystal grain size.

In a recent study Troiano and Tokich (30) show that heat treatment above the transition temperature suppresses the cubic to hexagonal transformation on cooling to room temperature for rapid quenches and that it is possible to prepare essentially cubic cobalt. Cold working of cobalt produces the hexagonal phase indicating that deformation is involved in the transformation mechanism.

Nishiyama (26) has studied the effect of polishing on the crystal structure of the cobalt. It is shown that the effect is greatest at the surface in that the hexagonal phase is formed while the interior retained the cubic phase.

Thermodynamic Calculations

Several types of reactions are of interest in this study. These are (*a*) the direct formation of the several oxides, (*b*) the equilibrium between the several oxides and oxygen, (*c*) the equilibrium between the several oxides and the metal, and (*d*) the reduction of the oxides by hydrogen.

The free energy of the reaction $CoO \rightleftarrows Co + \frac{1}{2}O_2$ is calculated from an equation given by Shibata and Mori (28):

$$\Delta F^\circ = 57{,}423 + 2.00\ T \log_{10} T - 0.00025\ T^2 - 24.74\ T.$$

The free energy of the reaction $Co_3O_4 \rightleftarrows 3CoO + \frac{1}{2}O_2$ is calculated from an equation given by Watanabe (35):

$$\Delta F^\circ = 38{,}972 + 1.73\ T \log_{10} T - 0.00025\ T^2 - 36.07\ T.$$

The second equation based on observations at temperatures between 800° and 970°C has been essentially checked by Gulbransen and Andrew (9) in the temperature range of 600° to 740°C using McLeod gauge pressure measurements.

TABLE I. *Equilibrium calculations on cobalt reactions*

Reaction	References
1. $Co(s) + \frac{1}{2}O_2(g) \rightleftarrows CoO(s)$	29
2. $3Co(s) + 2O_2(g) \rightleftarrows Co_3O_4(s)$	9, 35
3. $Co_3O_4(s) \rightleftarrows 3CoO(s) + \frac{1}{2}O_2(g)$	9, 29, 35
4. $Co_3O_4(s) + Co(s) \rightleftarrows 4CoO(s)$	9, 29, 35
5. $CoO(s) + H_2(g) \rightleftarrows Co(s) + H_2O(g)$	20, 29
6. $Co_3O_4(s) + 4H_2(g) \rightleftarrows 3Co(s) + 4H_2O(g)$	9, 20, 35
7. $Co_3O_4(s) + H_2(g) \rightleftarrows 3CoO(s) + H_2O(g)$	9, 20, 29, 35

Temp °C	(1) $-\log p_{O_2}$	(2) $-\log p_{O_2}$	(3) $-\log p_{O_2}$	(4) $+\log K$	(5) $-\log p_{H_2O}/p_{H_2}$	(6) $-\log p_{H_2O}/p_{H_2}$	(7) $-\log p_{H_2O}/p_{H_2}$
25	75.4	67.35	43.2	16.1	2.38	6.41	18.5
200	44.5	38.92	22.2	11.15	2.10	4.89	13.26
400	28.84	24.54	11.64	8.60	1.91	4.06	10.51
600	20.42	16.78	5.88	7.27	1.74	3.56	9.01
800	15.10	11.89	2.26	6.42	1.63	3.23	8.05
1000	11.48	8.57	−.166	5.82	1.53	2.99	7.35

Table I shows the equations for which the free energy is calculated together with the results and literature references for the other data used in the calculations. The logarithms of the decomposition pressures or pressure ratios of water to hydrogen are tabulated as a function of the temperature in °C for the several reactions. The logarithms of the equilibrium constant K are tabulated for the solid phase reaction of the metal with the oxide.

The results show the following: (*a*) CoO is stable to direct decomposition over the temperature range 25° to 1000°C and in high vacua, (*b*) Co_3O_4 decomposes to CoO and O_2 in vacua of the order of 10^{-9} atm at temperatures of 500°C or greater, (*c*) the solid phase reaction of Co_3O_4 with cobalt is feasible at all temperatures, and (*d*) the reduction of CoO and Co_3O_4 with hydrogen is feasible even in atmospheres containing large amounts of water vapor.

Experimental Procedures

Samples

The cobalt metal was prepared here from commercial cobalt rondels obtained from the African Metals Corporation. The rondels were melted to an ingot deoxidizing with 0.2 per cent CaSi. Table II shows chemical analyses of the ingot.

TABLE II. *Chemical analyses of cobalt*

Chemical analyses (Nominal)	%
Si	0.05
Mn	0.08
P	0.001
S	0.012
Fe	0.21
Ni	0.45
Cu	0.05
Al	0.05
Pb	<.01
O_2	0.005 (approx.)
C	0.01
Co	remainder

TABLE III. *Preparation procedures and crystal structure of cobalt specimens*

Group	Abrading procedures	Annealing procedures	Crystal structure
1	Ground and abraded 1/0 to 4/0 under kerosene. Washed with soap and water, distilled water, petroleum ether and absolute alcohol.	None	Hexagonal close-packed
2	Same as above	24 Hours at 475°C in vacuum 10^{-6} mm of Hg	Face-centered cubic plus small amount of hexagonal
3	Same as above	6 Hours at 885°C in vacuum 10^{-6} mm of Hg	Equal mixture of two phases
4	Same as above	Exposed to contamination for 2 weeks in room atmosphere	Hexagonal close-packed

A section was cut from the bottom of the ingot and hot rolled to 0.0762 cm. The strip was ground on both sides to 0.050 cm and the specimens cut out and machined to size. The specimens weigh 0.6500 g and have projected surface areas of 3.4 cm^2.

To test the influence of the crystal structure and the effect of atmospheric contamination several groups of specimens were prepared. The abrading and preparation procedures are shown in Table III. The samples cannot be abraded after annealing if the formation of the hexagonal phase is to be prevented. The crystal structure of the several groups of specimens was determined by x-ray diffraction analyses and tabulated in Table III.

Apparatus and Methods

The vacuum microbalance (10) and associated equipment was used for all of the kinetic measurements. The sensitivity of the balance was 0.91 divisions per microgram and the weight change was estimated to 0.25 microgram. The methods used for carrying out the experiments and the purification of the gases have been described (11–13).

Results and Discussion

High Vacuum Reaction

The procedures used for minimizing the initial film formation prior to reaction have been described (12). In brief, the specimens are heated to the reaction temperature, as rapidly as possible, in the apparatus at 10^{-6} mm of Hg or less. No weight gain is observed on heating the cobalt specimens to 850°C over a period of 2 hours so it is possible to heat the cobalt to the reaction temperature without forming more than a few angstroms of oxide.

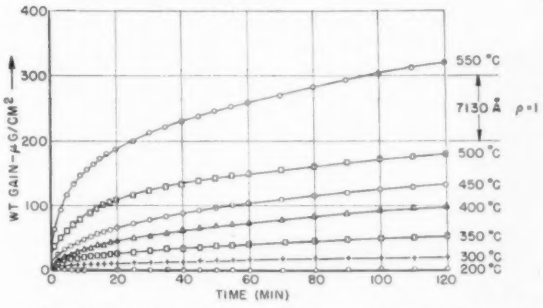

Fig. 1. Reaction of Co with 7.6 cm of Hg of O_2; effect of temperature (200°–550°C).

Reaction with Oxygen

The reaction is studied as a function of time, temperature, pressure, and pretreatment. The results are shown in Fig. 1 to 5 and Fig. 8, and in Tables IV to VII. Assuming the ratio of the real to measured area to be unity ($\rho = 1$) and the oxide to be CoO, the thickness in angstroms is related to the weight gain in micrograms per cm^2 by the factor 71.3. Since the oxide is not CoO alone, but a mixture of CoO and Co_3O_4 whose composition is not known, this factor may be in error by 1 to 10 per cent.

Time and temperature—hexagonal structure.—Fig. 1 and 2 show the time course of the oxidation for the cold-worked samples (hexagonal at start) over the temperature range of 200° to 550°C and 500° to

750°C, and for a pressure of 7.6 cm of Hg. Typical oxidation rate curves are found except for the 750°C curve of Fig. 2. After an initial period this oxidation experiment shows an increasing rate of reaction over the time range studied. Table IV shows a correlation of the film thickness, the color of the oxide,

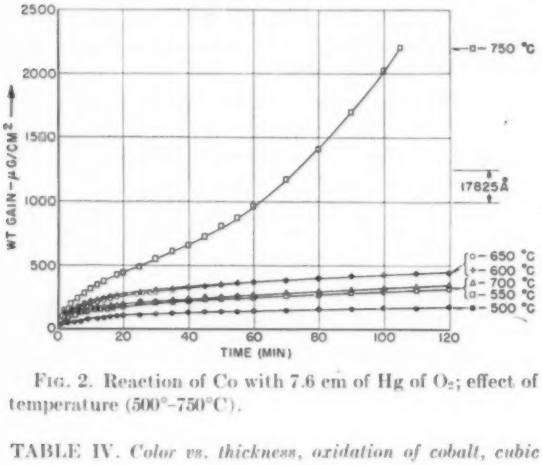

FIG. 2. Reaction of Co with 7.6 cm of Hg of O_2; effect of temperature (500°–750°C).

TABLE IV. *Color vs. thickness, oxidation of cobalt, cubic and hexagonal forms*

Temp °C	Thickness (2 hours) μg/cm²	Thickness (2 hours) Angstrom (ρ = 1)	Color	Stability to cracking on cooling
A. Hexagonal form at start				
200	1.73	122	bright	stable
300	20.4	1,442	blue-pink	stable
350	52.0	3,680		
400	97.7	6,910	blue-straw	stable
450	132	9,340	metallic gray	stable
500	179	12,680		
550	320	22,600	dark gray	stable
600	419	22,960	gray-black	unstable
650	443	31,300	gray-black	unstable
700	347	24,600	gray-black	unstable
750	3200	156,000	brown	stable
B. Cubic form + small amount of hexagonal form—annealed 475°C, 24 hr				
300	8.75	619	blue-green	stable
350	23.6	1670	pale blue	stable
400	30.0	2120	pale blue	stable
500	124.0	8760		
600	310.0	21925	gray-black	unstable
700	435.0	30800	gray-black	unstable

and the stability of the film to cracking on cooling for 2-hour experiments.

The oxide layer is stable to cracking on cooling for those oxidations carried out below 600°C. For the 2-hour oxidations carried out between 600° and 750°C the oxides flake off of the surface on cooling. At 750°C the oxide which was formed appeared to be stable to cracking on cooling.

The oxidation reaction between 550° and 700°C has a small temperature dependence. Above 700°C the rate of reaction changes rapidly as the temperature is increased.

Fig. 3 shows a comparison of the oxidation of cobalt with that for iron, zirconium, titanium, and beryllium. At 400°C and for a pressure of 7.6 cm of Hg the hexagonal form of cobalt oxidizes faster than the other metals. Except for iron this comparison is in agreement with the results of McAdam and Geil (22).

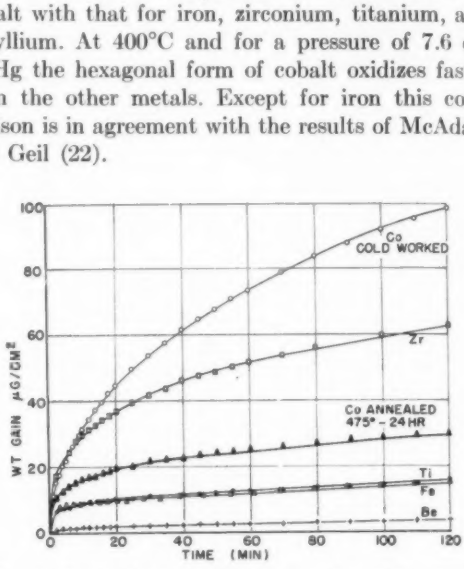

FIG. 3. Comparison of oxidation reaction of Co, Fe, Ti, Be, and Zr; 7.6 cm of Hg of O_2, 400°C.

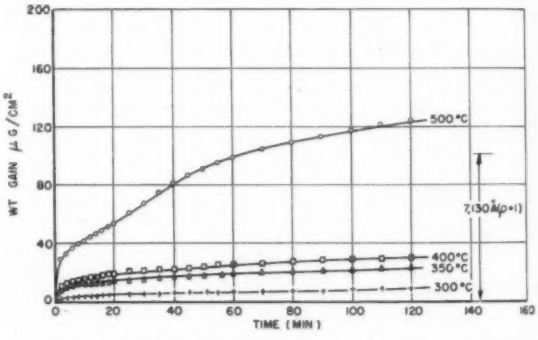

FIG. 4. Reaction of annealed Co with 7.6 cm of Hg of O_2; effect of temperature (300°–500°C).

Time and Temperature—Face-Centered Cubic Structure

Fig. 4 and 5 show the time course of the oxidation for the group of samples annealed at 475°C for 2 hours, for a pressure of 7.6 cm of Hg. The crystal structure of the cobalt is largely the cubic structure plus a smaller amount of the hexagonal structure. The cubic modification has a slower rate of reaction than the hexagonal form over the temperature range of 200° to 550°C.

The curves for the 500° and 600°C oxidations in Fig. 5 show an S-shaped curve after the initial oxygen uptake. This effect is not observed for the cold-

worked samples (hexagonal structure) or for the specimens annealed at 875°C for 6 hours which consist of an equal mixture of the hexagonal and cubic forms of cobalt. The reason for this effect is not understood although it is probably related to the crystal structure transformation occurring in this temperature region.

Film thickness, color of the oxide, and stability of the oxide to cracking on cooling with the cubic cobalt are given in Table IV. The oxides formed at 600° to 700°C are unstable upon cooling. In this sense the two preparations of cobalt behave in a similar manner.

Fig. 3 shows the comparison of the oxidation behavior of the two preparations of cobalt with the oxidation curves of a number of other metals.

A question may be raised as to whether the reactivity of the two forms of cobalt is due to the crystal structure or to an effect of the annealing procedure used in preparing the samples. In addition to changing the crystal structure the annealing procedure may: (*a*) add an oxide film, (*b*) cause a change in the crystal size and orientation of the crystals, and (*c*) relieve the stresses caused by the cold working of the cobalt. Several experiments are made to test the presence or absence of these disturbing effects.

One annealed specimen is treated with H_2 at 600°C for one hour to remove any oxide film formed in the vacuum annealing procedure. A comparison of the oxidation at 350°C with a regular annealed sample shows a similar oxidation curve. The parabolic rate law constants differ by 30 per cent. This may be compared to a difference of 400 per cent between the two forms of cobalt.

A set of samples was annealed at 885°C for 6 hours to form a mixture of the two forms of cobalt. Oxidation experiments carried out between 400° and 700°C are in essential agreement with the results on the samples annealed at 475°C for 24 hours.

One annealed sample was abraded and then oxidized at 400°C. The oxidation curve found was intermediate between the cold-worked and annealed samples.

The results of these experiments show that the difference in reactivity of the two preparations of cobalt cannot be interpreted in terms of an oxide film and must be attributed to changes in the crystal structure, crystal size and orientation, and stresses in the surface.

Time and Temperature Equations

The parabolic rate law (23, 27) and its several modifications (31, 33), the linear rate law, and the logarithmic rate law (29) have been used to interpret the time variation of the oxidation rate. The parabolic rate law when corrected for the velocity of the interface reaction, AW, is given by the equation $W^2 + AW = Kt + C$. Here W is the weight gain, t the time, K the rate constant, and C a constant.

The temperature variation of the parabolic rate law constant may be interpreted by either the Arrhenius equation (6) or the transition state theory (15). The latter theory gives the following expression for K:

$$K = 2\frac{kT}{h}\lambda^2 e^{\Delta S^*/R} e^{-E/RT}.$$

The significance of the terms has been described (15).

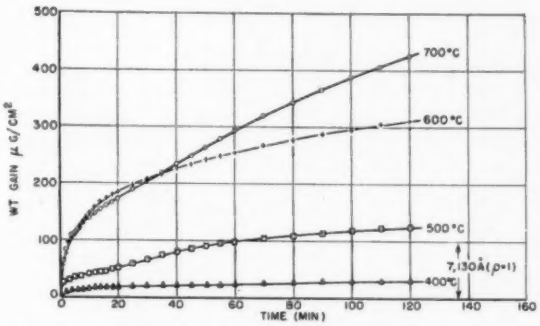

FIG. 5. Reaction of annealed Co with 7.6 cm of Hg of O_2; effect of temperature (500°–700°C).

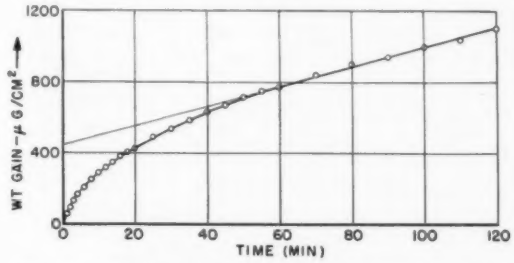

FIG. 6. Oxidation of Co, 400°C, 7.6 cm of Hg of O_2; parabolic plot; annealed 885°C, 6 hours.

The linear rate law and the logarithmic rate law do not fit the data. The parabolic rate law corrected for the velocity of interface reaction does not apply in the temperature range studied here. Although a number of empirical equations may be found to fit the data, we propose to apply the parabolic rate law which is based on a fundamental physical process and to study the nature of the deviations.

Fig. 6 shows a typical parabolic rate law plot in which W^2 is plotted againt t for the oxidation of cobalt at 400°C and 7.6 cm of Hg. The data fit the parabolic rate law after an initial deviation during which the reaction proceeds faster than the law would predict. Similar fits are found for both forms of cobalt.

The initial deviation from the parabolic rate law may be expected because of a number of disturbing phenomena which are difficult to include in any equation. These phenomena are: (*a*) the influence of the decrease in roughness or surface area as the reaction proceeds, (*b*) the influence of the heat evolved in the reaction on the rate of reaction, (*c*) the influence of the solution of oxygen in the metal on the rate of reaction, (*d*) the influence of the concentration of impurities in the oxide during the early stages of the reaction, (*e*) the change in oxide composition, and (*f*) the influence of potential fields at the gas-oxide interface due to adsorbed oxygen ions according to the mechanism of Mott (24).

TABLE V. *Parabolic rate law constants oxidation of cobalt*

Temp °C	$1/T \times 10^3$	K (g/cm²)²sec⁻¹	K'/T cm²/sec/°C
Cold-worked abraded			
200	2.1142	4.17×10^{-16}	4.48×10^{-19}
250	1.9121	7.50×10^{-15}	7.28×10^{-18}
300	1.7452	4.03×10^{-14}	3.57×10^{-17}
350	1.6051	3.06×10^{-13}	2.50×10^{-16}
400	1.4859	1.222×10^{-12}	9.23×10^{-16}
450	1.3831	1.915×10^{-12}	1.348×10^{-15}
500	1.2937	2.80×10^{-12}	1.84×10^{-15}
500	1.2937	2.97×10^{-12}	$1\ 955 \times 10^{-15}$
550	1.2151	10.30×10^{-12}	6.36×10^{-15}
575	1.1793	9.25×10^{-12}	5.55×10^{-15}
575	1.1793	11.95×10^{-12}	7.17×10^{-15}
585	1.1655	13.35×10^{-12}	7.91×10^{-15}
600	1.1455	8.05×10^{-12}	4.68×10^{-15}
*600	1.1455	11.66×10^{-12}	6.80×10^{-15}
600	1.1455	19.2×10^{-12}	11.18×10^{-15}
650	1.0834	10.84×10^{-12}	5.98×10^{-15}
700	1.0278	13.33×10^{-12}	6.96×10^{-15}
†700	1.0278	19.45×10^{-12}	10.15×10^{-15}
‡700	1.0278	12.22×10^{-12}	6.39×10^{-15}
§650	1.0278	14.43×10^{-12}	7.54×10^{-15}
300	1.7452	8.06×10^{-15}	7.14×10^{-18}
350	1.6051	4.83×10^{-14}	3.94×10^{-17}
¶350	1.6051	6.80×10^{-14}	5.55×10^{-17}
400	1.4859	1.628×10^{-13}	1.23×10^{-16}
500	1.2937	1.61×10^{-12}	1.06×10^{-15}
600	1.1455	9.3×10^{-12}	5.42×10^{-15}
700	1.0278	25.8×10^{-12}	13.48×10^{-15}
Annealed 885°C, 6 hours			
400	1.4859	8.90×10^{-14}	6.71×10^{-17}
500	1.2937	1.582×10^{-12}	11.97×10^{-16}
600	1.1455	5.83×10^{-12}	3.39×10^{-16}
700	1.0278	21.93×10^{-12}	11.47×10^{-16}
Exposed to atmosphere 2 weeks			
500	1.2937	1.054×10^{-12}	6.94×10^{-16}
600	1.1455	10.0×10^{-12}	5.82×10^{-15}
700	1.0278	16.0×10^{-12}	8.37×10^{-15}

* Freshly abraded
† Held 45 min before reaction
‡ Small sample
§ Small sample
¶ Initial oxide reduced in H_2 at 600°C

Time and Temperature Correlation

The K values used in the analysis of the temperature effects are calculated from parabolic rate law plots in the time interval of 60 to 120 minutes where the law is found to hold. The temperature is involved in the transition state theory as part of the exponential term $e^{-E/RT}$ and also directly as T. The energy of activation E is evaluated from a plot of log K/T vs. $1/T$. The parabolic rate law constants are given in Table V.

Fig. 7 shows a plot of log K/T vs. $1/T \times 10^3$. The data can best be fitted by two straight lines.

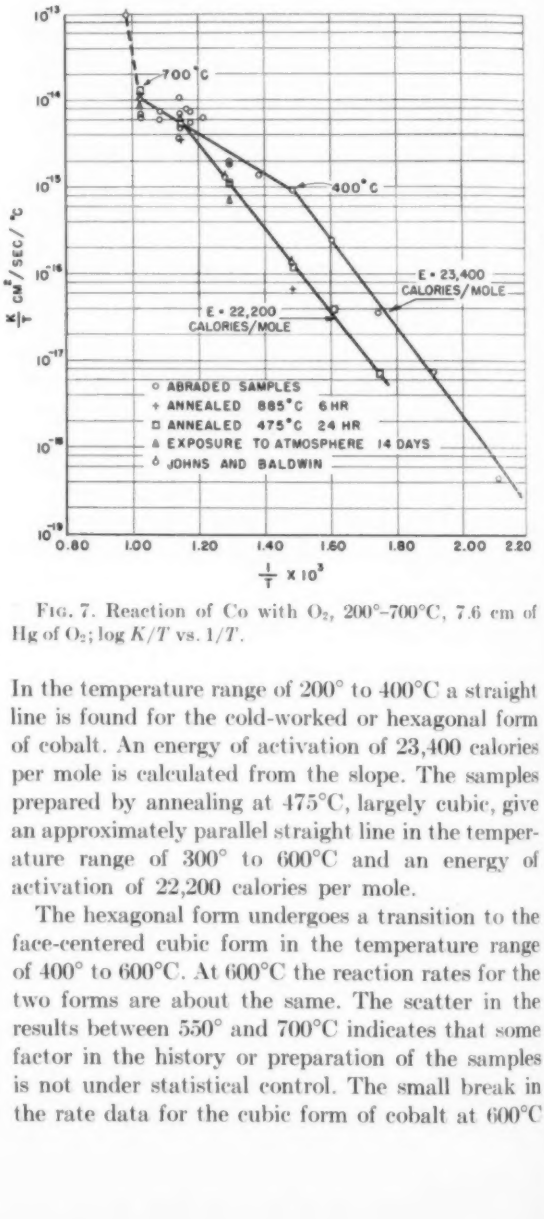

FIG. 7. Reaction of Co with O_2, 200°–700°C, 7.6 cm of Hg of O_2; log K/T vs. $1/T$.

In the temperature range of 200° to 400°C a straight line is found for the cold-worked or hexagonal form of cobalt. An energy of activation of 23,400 calories per mole is calculated from the slope. The samples prepared by annealing at 475°C, largely cubic, give an approximately parallel straight line in the temperature range of 300° to 600°C and an energy of activation of 22,200 calories per mole.

The hexagonal form undergoes a transition to the face-centered cubic form in the temperature range of 400° to 600°C. At 600°C the reaction rates for the two forms are about the same. The scatter in the results between 550° and 700°C indicates that some factor in the history or preparation of the samples is not under statistical control. The small break in the rate data for the cubic form of cobalt at 600°C

may be due to the presence of the small amount of hexagonal form which is transforming to the cubic structure at this temperature.

The data of Johns and Baldwin (19) are also included in Fig. 7. Good agreement is found with our data.

An analysis of the available data above and below 700°C indicates a marked change in the rate of reaction at this temperature and it is reasonable to assume that this is due to a change in the mechanism of the reaction or to a sudden change in one of the important variables governing the reaction.

Table VI shows the values of the parabolic rate law constants and the energies, entropies, and free energies of activation of the rate-controlling process in the oxidation of cobalt. The temperature independent factors $e^{\Delta S^*/R}$ are evaluated from the transition state theory equation for K.

Table VII shows a comparison of the parabolic rate law constants and the energies, entropies, and free energies of activation for the two forms of cobalt and the values for iron, titanium, and zirconium. From an oxidation resistance viewpoint cobalt at 400°C appears to be inferior to iron, beryllium, and titanium. Zirconium is superior to the hexagonal form of cobalt but inferior to the cubic form.

It is of interest to note that the two forms of cobalt have practically the same temperature dependence of the reaction rate. The difference in the actual values of the reaction rate must be interpreted, therefore, in terms of the temperature independent term $e^{\Delta S^*/R}$. Since the oxide is probably the same in both cases it appears that the difference in the $e^{\Delta S^*/R}$ term is in the process of forming the cation or electrons at the metal-oxide interface. Although the energy required may be nearly the same, the probability factor appears to differ for the two forms of cobalt.

Pressure

The effect of pressure of the oxygen gas on the rate of reaction is shown in Fig. 8 for a temperature of 550°C. The pressure is varied from 0.38 to 7.6 cm of O_2 or by a factor of 20. The results show that the rate of reaction increases as a small power of the pressure. After two hours the total reaction differs by about 30 per cent. At this temperature the data are not of sufficient reproducibility to determine the precise pressure dependence.

Effect of Atmospheric Contamination

Valensi (31) has observed that atmospheric contamination has a critical effect on the rate of reaction. A series of measurements are made to check this observation. Specimens of cold-worked and abraded cobalt were exposed to the laboratory atmosphere for two weeks. Oxidation experiments were then carried out at 500°, 600°, and 700°C. The data can be fitted to the parabolic rate law. The 600° and 700°C oxidation curves agree well with the curves for the regular cold-worked specimens which were not exposed. However, at 500°C the oxidation rate was considerably reduced. This is expected since the effect would be most marked at low temperatures.

The fact that the effect is a small one in these experimental procedures may indicate that exposing

TABLE VI. *Parabolic rate law constants, entropies, energies, and free energies of activation for the oxidation reaction*

Temp °C	K cm²/sec	ΔS^* cal/mole/°C	E cal/mole	$T\Delta S^*$ cal/mole	ΔF^* cal/mole
		A. Hexagonal			
200	2.12×10^{-16}	−14.26	23,400	−6750	30,150
250	3.81×10^{-15}	−13.45	23,400	−7030	30,430
300	2.05×10^{-14}	−14.24	23,400	−8140	31,540
350	1.555×10^{-13}	−13.58	23,400	−8450	31,850
400	6.21×10^{-13}	−13.73	23,400	−9260	32,660
		B. Essentially cubic			
300	4.09×10^{-15}	−19.50	22,200	−11,180	33,380
350	2.455×10^{-14}	−19.17	22,200	−11,930	34,130
400	8.27×10^{-14}	−19.58	22,200	−13,180	35,380
500	8.18×10^{-13}	−19.56	22,200	−15,110	37,310
600	4.73×10^{-12}	−19.57	22,200	−17,100	39,300

TABLE VII. *Comparison of the parabolic rate law constants and the energies, entropies, and free energies of activation* (400°C and 7.6 cm O_2 pressure)

	Co		Fe	Ti	Zr
	Cubic	Hexagonal			
K cm²/sec	8.27×10^{-14}	6.21×10^{-13}	4.09×10^{-15}	6.67×10^{-15}	1.32×10^{-12}
E cal/mole	22,200	23,400	22,600	26,000	18,200
ΔS^* entropy units	−19.58	−13.73	−24.6	−18.8	−25.2
ΔF^* cal/mole	35,380	32,660	39,150	38,100	35,200

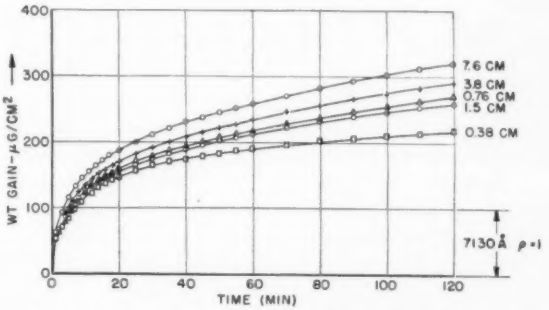

FIG. 8. Reaction of Co with 0.38 to 7.6 cm of Hg of O_2; effect of pressure (550°C).

the specimens to high vacuum before reaction removes the contaminating film for the 600° and 700°C experiments.

Studies on the Mechanism of the Reaction

Valensi (31) has proposed on the basis of the visual appearance of completely oxidized samples of cobalt (CoO) that the reaction occurs by the diffusion of oxygen inward. This mechanism is also suggested by Arkharov and Graevskii (1) from a study of the lattice parameters of CoO at the Co and at the oxygen interface. Valensi (31) has suggested that the oxidation of CoO should lead from his theory to

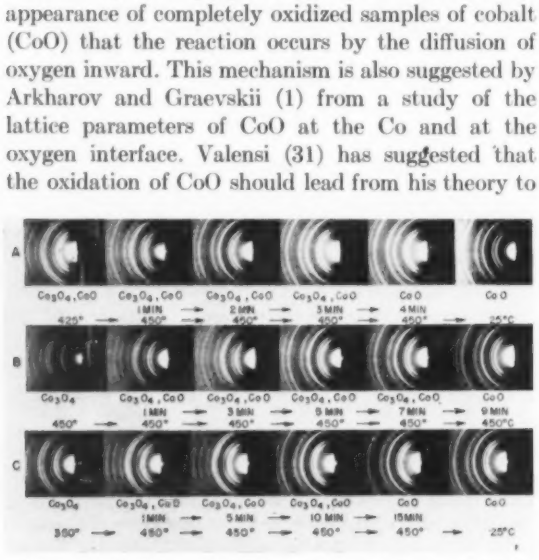

FIG. 9. Heating and cooling oxide films on cobalt in vacuo. A—Oxidized at 425°C, 1 mm of Hg of O_2, 1 min; B—sample A continued, 450°C, 1 mm of Hg of O_2, 1 min; C—sample B continued, 350°C, 1 mm of Hg of O_2, 60 min.

TABLE VIII. *Effect of temperature on solid phase reactions in oxides on cobalt, oxidation pressure = 1 cm O_2*

Temp °C	Additional time of oxidation	Total oxidation time	Time for transformation
500	1	1	245 sec
	10	11	1330 sec
600	1	1	220 sec
	10	11	280 sec
650	1	1	250 sec
	10	11	580 sec
	100	111	2230 sec

a rate of reaction one fourth times that for the corresponding reaction of cobalt. This has not proved to be the case. Oxidation of CoO, however, is not a good test for the theory since the crystal size, orientation, particle size and shape, and the nature of the stresses present in preparations of CoO are not characteristic of CoO when present on the metal.

Cobalt oxide was prepared according to the method of Valensi by oxidizing a 0.050-cm thick specimen for 8 days at 950°C and cooling in high vacuum. The composition of the oxide was determined to be $CoO_{0.99}$. The specimens had the same shape as the original cobalt specimen but enlarged to the volume of oxide. Oxidation studies made on these specimens at 7.6 cm of Hg showed parabolic rate law constants 4500 times as large at 300°C as for the cobalt metal specimen. This and other experiments made in the temperature range of 200° to 500°C showed that the oxidation rate is extremely fast when compared to the reaction of cobalt.

The evidence in favor of the oxygen diffusion picture appears weak, although most of our knowledge concerning the nature of the diffusing species has to date been indirect. It is well to examine the evidence for the alternative mechanism for reaction, namely, the diffusion of the cation and electrons outward. Interesting indirect evidence for the elucidation of the mechanism is the solid phase reactions occurring in the oxide under vacuum conditions. A brief description will be given of these studies.

Electron diffraction studies of solid phase reactions.—Gulbransen and Hickman (8), using the electron diffraction method at high temperatures, observed the formation of CoO on the surface of Co at 300° and 400°C for short periods of oxidation at 1 mm Hg. For longer periods of oxidation Co_3O_4 is formed. These experiments must be interpreted by one of the following reactions: (I) $Co_3O_4 \rightarrow 3CoO + \frac{1}{2}O_2$ or (II) $Co_3O_4 + Co \rightarrow 4CoO$. The influence of reaction (I) to form CoO at 400°C must be small since the equilibrium pressure of O_2 over Co_3O_4 and CoO is $10^{-11.64}$ atmospheres. Stability studies on Co_3O_4 present on CoO showed that decomposition is very slow at 600°C and lower. It is necessary to assume that the solid phase reaction (II) explains the appearance of CoO at 300° and 400°C in high vacuum.

Fig. 9 shows a new study of the solid phase reaction occurring in high vacuum. Cobalt is oxidized in part A for 1 minute at 425°C using 1 mm of O_2. Co_3O_4 and CoO diffraction patterns are first observed in the camera. On heating to 450°C the transformation of Co_3O_4 to CoO occurred in 4 minutes. Parts B and C show the same reaction occurring for other oxidation conditions. The first picture in these experiments is Co_3O_4 since an attempt was made to take the picture immediately on reaching a pressure of 0.7 microns. The transformation of Co_3O_4 by the solid phase reaction with Co occurs in a few minutes.

Table VIII shows additional evidence that the solid phase reaction (II) is occurring in the oxide. In these experiments the metal is oxidized for 1 minute at 1 cm of O_2 for the three temperatures. The system is evacuated. After reaching a pressure of 0.7 microns the electron beam is turned on and the pattern observed on the fluorescent screen. The first structure noted was Co_3O_4 for the three temper-

atures. The time for transformation is taken as the elapsed time after a pressure of 0.7 microns is achieved until the pattern has transformed completely to CoO. Longer oxidation times require longer periods for transformation. This may be explained as due to the thicker CoO layer which decreases the diffusion gradient for the transfer of the cation and o the greater amount of Co_3O_4 to be transformed. From this point of view the solid phase reactions occurring in the oxides of cobalt are similar to those occurring in the oxides of iron above 570°C (14).

These experiments give direct evidence to support the case for the diffusion of cations and electrons through the oxide. The rate of the diffusion of cations and electrons is of the right magnitude to account for the velocity of the oxidation reaction over a large temperature range 350° to 600°C. Since this is the mechanism suggested by Wagner and coworkers (33, 34) and since the solid phase reactions support this mechanism, this mechanism is suggested for the oxidation reaction. It is of interest to express this analytically and to show the relationships between the solid phase reaction in high vacuum and the oxidation reaction. Valensi (32) has also considered this problem from a different point of view and has developed the necessary equations.

Discussion of the Mechanism of Reaction

Fig. 10 shows the interpretation of the oxidation and solid phase reactions occurring in the oxidation process for temperatures below 700°C.

At the left, the metal-oxide interface is shown at point 0. The concentration C_0 is the concentration of Co in the oxide CoO while the concentration of Co in CoO at the Co_3O_4 interface is given by C_1. The concentration of Co in Co_3O_4 at the CoO interface 1 is given by C_1' while C_2 is the concentration at the gas-oxide interface at 2. The thickness of the CoO phase is given by X_1 and the Co_3O_4 phase by X_2. Both thicknesses are a function of the time t.

The concentrations C_0, C_1, C_1', and C_2 may vary, the values being limited only by the range of homogeneity of the particular oxide. In general, the concentrations observed are determined by the equilibrium values modified by whether the reaction is controlled by the interface reactions at 0, 1, or 2, or by diffusion.

The quantity of Co transferred through the CoO layer is given by the expression

$$\frac{dQ}{dt} = K_1 D_{CoO} \frac{(C_0 - C_1)}{X_1(t)}$$

and the quantity transferred through the oxide Co_3O_4 is given by

$$\frac{dQ}{dt} = K_2 D_{Co_3O_4} \frac{(C_1' - C_2)}{X_2(t)}.$$

Here D_{CoO} and $D_{Co_3O_4}$ are the diffusion coefficients of Co in CoO and Co_3O_4, respectively, and are probably a function of the concentration of Co. K_1 and K_2 are numerical constants.

From material balances at 1 and 2 growth of the CoO layer, the Co_3O_4 layer, and the total oxide can be expressed in terms of the equations shown in Fig. 10.

As long as oxygen is reacting at 2 and both oxides are stable, the two oxides will coexist. The relative amounts being determined by the diffusion constant for the particular oxide and the diffusion gradient. The presence of interface rate-controlling reactions determines in part the concentrations of the diffusing species in the oxide and thus effects the quantity of cobalt diffusing through the oxide.

If the oxidation is stopped at 2 by removing the oxygen, the concentration C_2 will increase to the

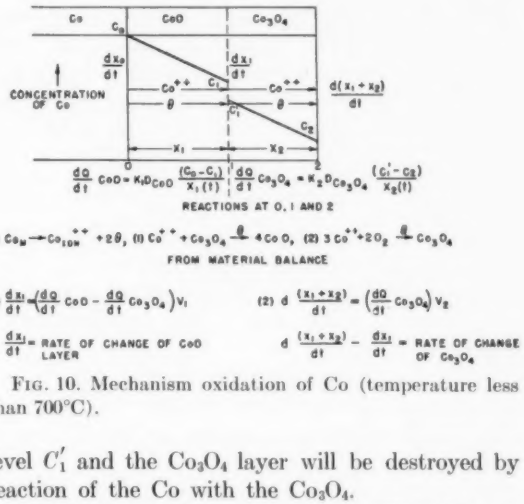

FIG. 10. Mechanism oxidation of Co (temperature less than 700°C).

level C_1' and the Co_3O_4 layer will be destroyed by reaction of the Co with the Co_3O_4.

This picture explains the electron diffraction observations in all details.

At temperatures above the decomposition point for the formation of the Co_3O_4 layer the process is much simpler. In this case the reaction is either controlled by the interface reactions at 0 and 1 or by the diffusion of Co through the oxide.

Discussion of the Change in the Reaction Rate at 700°C

A marked change in the reaction rate at 700°C (19, 31) is confirmed in this study. Valensi (31) interpreted this change in terms of the oxide composition alone. This is perhaps too simple an explanation since CoO can coexist with Co_3O_4 at temperatures as low as 300°C while the decomposition temperature of Co_3O_4 is nearly 1000°C for 1 atm pressure of O_2. At 700°C the decomposition pressure is less than 10^{-4} atm.

Valensi's suggestion should be modified in that

below 700°C the rate-controlling factor is the diffusion of cations and electrons through the Co_3O_4 layer while above 700°C the rate-controlling factor is the diffusion of cations and electrons through the CoO layer. Further studies on the mechanism of the reaction, including micrographs of the oxide layer, must be made before the inflection point in the rate of reaction is adequately explained.

The reason for the instability of the oxide at 600° to 700°C cannot be explained adequately at present. However, two facts should be noted. These are as follows: (*a*) The oxide starts to dissolve a little into the metal at temperatures of the order of 600°C. This removes the original transition layer between the oxide and metal. The presence of this layer helps to prevent cracking of the oxide from the metal. The solution of the oxide into the metal has been noted by electron diffraction studies. (*b*) The solid phase reactions also remove the transition layer completely at 600° and 700°C while at lower temperature the transition zone is maintained even though a crystal structure transformation occurs. This effect has been noted in a study of the epitaxy relationships in the oxidation of single crystals of iron (9).

Summary

Thermodynamic calculations are made on (*a*) the equilibrium between the metal, the several oxides, and oxygen; (*b*) the equilibrium between the several oxides and the metal; and (*c*) the reduction of CoO and Co_3O_4 with H_2.

The reaction of cold-worked cobalt (hexagonal form) and annealed cobalt (largely face-centered cubic form) was studied over the temperature range of 200° to 750°C. Colored oxides were formed except at 200°C. In the temperature range of 600° to 700°C the oxide films cracked on cooling while at temperatures below 600°C the oxide appeared coherent. A comparison of the rate of oxidation of the cold-worked samples with the annealed samples showed that the cold-worked samples oxidized much more rapidly than the annealed samples. This is attributed to the crystalline structure of the cobalt.

A comparison of the oxidation rates of a number of metals showed that cobalt oxidizes more rapidly than iron, titanium, and beryllium and cannot be classed as an oxidation-resistant material. A modified form of the parabolic rate law fits the data. Activation energies of 23,400 and 22,200 calories per mole were calculated for the cold-worked and annealed samples, respectively. The difference in the reaction rate of the two structures was attributed to the entropy term $e^{\Delta S/R}$.

The effect of contamination of the atmosphere was studied and found to be important only at low temperatures.

The solid phase reactions occurring in the oxide were studied using the high temperature electron diffraction camera. The experiments show that the solid phase reaction $Co_3O_4 + Co \rightarrow 4CoO$ occurs readily in the oxide at 450°C. The effect of length of oxidation and temperature on the solid phase reaction is determined.

A mechanism of the oxidation of cobalt and the solid phase reactions occurring within the oxide is suggested based on the diffusion of cations and electrons through the oxide from the metal to the gas oxide surface.

Any discussion of this paper will appear in a Discussion Section, to be published in the December 1951 issue of the JOURNAL.

REFERENCES

1. V. I. Arkharov and K. M. Graevskii, *J. Tech. Phys. (U.S.S.R.)*, **14**, 132 (1944); *C.A.*, **39**, 2726[8] (1945).
2. V. I. Arkharov and S. A. Voroshilova, *J. Tech. Phys. (U.S.S.R.)*, **6**, 781 (1936); *C.A.*, **33**, 5310[8] (1939).
3. V. I. Arkharov and G. D. Lomakin, *J. Tech. Phys. (U.S.S.R.)*, **14**, 155 (1944); *C.A.*, **39**, 4834[1] (1945).
4. G. Chauvenet, *Compt. rend.*, **209**, 886 (1939).
5. J. S. Dunn and F. J. Wilkins, "Review of Oxidation and Scaling of Heated Metals," p. 67, H. M. Stationery Office, London (1935).
6. J. S. Dunn, *J. Chem. Soc.*, **1929**, 1149.
7. O. S. Edwards and H. Lipson, *J. Inst. Metals*, **69**, 177 (1943).
8. E. A. Gulbransen and J. W. Hickman, *Trans. Am. Inst. Mining Met. Engrs.*, **171**, 306 (1947).
9. E. A. Gulbransen and K. Andrew, Unpublished measurements.
10. E. A. Gulbransen, *Trans. Electrochem. Soc.*, **81**, 187 (1942).
11. E. A. Gulbransen, *Rev. Sci. Instruments*, **15**, 201 (1944).
12. E. A. Gulbransen and K. Andrew, *Trans. Am. Inst. Mining Met. Engrs.*, **185**, 515 (1949); *J. Metals* (Aug. 1949).
13. E. A. Gulbransen and K. Andrew, *Ind. Eng. Chem.*, **41**, 2762 (1949).
14. E. A. Gulbransen and R. Ruka, *Ind. Eng. Chem.*, **43**, 697 (1951).
15. E. A. Gulbransen, *Trans. Electrochem. Soc.*, **83**, 301 (1943).
16. W. H. Hatfield, *J. Iron Steel Inst.*, **115**, 483 (1927).
17. S. Holgersson and A. Karlson, *Z. anorg. Chem.*, **183**, 384 (1929).
18. A. W. Hull, *Phys. Rev.*, **17**, 571 (1921).
19. C. S. Johns and W. M. Baldwin, Jr., *Trans. Am. Inst. Mining Met. Engrs.*, **185**, 720 (1950).
20. K. K. Kelley, *U. S. Bur. Mines Bull. 38*, (1935).
21. M. LeBlanc and E. Möbius, *Z. physik. Chem.*, **142**, 151 (1929).
22. D. J. McAdam and G. G. Geil, *J. Research Natl. Bur. Standards*, **28**, 593 (1942).

23. N. F. Mott, *Trans. Faraday Soc.*, **36,** 472 (1940).
24. N. F. Mott, *J. Inst. Metals*, **12,** 367 (1946).
25. G. Natta and M. Strada, *Gazz. chim. ital.*, **58,** 419 (1928).
26. Z. Nishiyama, *Nippon Kinzoku Gakukai-Shi*, **2,** 202 (1938); *C.A.*, **32,** 7381[3] (1938).
27. N. B. Pilling and R. E. Bedworth, *J. Inst. Metals*, **29,** 529 (1923).
28. E. Shibata and J. Mori, *Z. physik. Chem.*, **A142,** 151 (1929).
29. G. Tammann and W. Köster, *Z. anorg. u. allgem. Chem.*, **123,** 196 (1922).
30. A. R. Troiano and J. L. Tokich, *Trans. Am. Inst. Mining Met. Engrs.*, **175,** 728 (1948).
31. G. Valensi, *la metallurgia italiana*, no. 3, marzo (1950).
32. G. Valensi, "Pittsburgh International Conference on Surface Reactions," p. 156, Corrosion Publishing Co., Pittsburgh (1948); *Rev. mét.*, **45,** 208 (1948).
33. H. H. von Baumbach and C. Wagner, *Z. physik. Chem.*, **B24,** 59 (1934).
34. C. Wagner and K. Grüenewald, *Z. physik. Chem.*, **40B,** 455 (1938).
35. M. Watanabe, *Sci. Repts. Tôhoku Imp. Univ., First Ser.*, **23,** 89 (1934).

Discussion Section

THE ANODE LAYER IN THE ELECTROLYTIC POLISHING OF COPPER

H. F. Walton (pp. 219–226)

P. A. Jacquet[1]: Dr. H. F. Walton's excellent work brings much useful information on the phenomena connected with the electropolishing of copper in phosphoric acid baths. As far as the anodic layer thickness is concerned, it is most remarkable that the *calculated* value of 0.06 mm is in such good agreement with the *experimental* data which I obtained by direct measurement with an adequate optical device[2]. Actually I found a thickness of 0.05 mm in equilibrium conditions corresponding to polishing, without agitation, the voltage being set at 1.8 volts. A moderate agitation brings it down to 1.3 volts and the thickness of the anodic layer decreases to 0.035 mm. A more violent agitation brings the voltage down to 1.2 volts and the layer thickness down to 0.028 mm. By such a process the copper is not polished, but etched. This proves a close correlation between the anodic layer thickness and the voltage on the one hand, and between the voltage and the polishing quality on the other.

DUCTILE CHROMIUM

W. J. Kroll, W. F. Hergert, and L. A. Yerkes (pp. 258–264)

Bruce Gonser[3]: Have you noted any differences in ductility or ease of forming according to the type of work imposed? That is, does the speed or way in which the chromium is deformed seem to exert much influence?

W. J. Kroll: We have not tried different speeds when rolling chromium but it is possible that low speed has a favorable influence on the malleability. The relative ease with which chromium can be pressed cold would confirm this supposition. I thank Dr. Gonser for his valuable suggestion.

STUDIES ON GALVANIC COUPLES, I

H. D. Holler (pp. 271–276)

J. M. Pearson[4]: The bridge circuit as designed by Dr. Holler in this study is a distinct improvement for making precise measurements of the internal emf and of variations of internal resistance as functions of the external current passing through the electrode under observation. It has the advantage that it can be applied to a half-cell or to a dry cell (of two half-cells) with equal facility, and with nearly equal precision.

Where the bridge is used on the terminals of a dry cell as in Fig. 3, the measurements of internal emf and resistance can be precise to the same order as the precision of the bridge components, if the stability of the measured quantities permits complete adjustment.

Where the bridge is used to measure the half-cell potential of a single electrode (or galvanic couple) as in Fig. 6, there are two points of difference with the first case which merit attention. The first is one of definition, viz., what is the meaning of the "half-cell potential" of a galvanic couple? A good definition is given in operational form on page 275 of the text in the discussion of the proper position (outside the field of the local action current) for the observing half-cell S.

The second point is the inaccuracy introduced by the internal resistance (let us call it "y") of the half-cell S, which is in series with the bridge arm Q. The result of adding this resistance to the circuit is to make $E_G \pm 2V_g$, and $r \pm x$ when the bridge is at null for emf and for resistance balance. A simple analysis shows the relations in this case to be

$$E_G = 2V_g\left(\frac{Q}{D} + \frac{y}{D}\right) = 2V_g\left(1 + \frac{y}{D}\right) \quad \text{if} \quad Q = D$$

$$r = x\left(\frac{Q}{D} + \frac{y}{D}\right) = x\left(1 + \frac{y}{D}\right) \quad \text{if} \quad Q = D.$$

If the ultimate precision of the bridge is to be realized, either $y/D \ll 1$ (the usual case) to the degree of the tolerable error, or y is measured independently (by another bridge) and the corrections applied, or Q is adjusted to make $Q + y = D$. In each case, high precision is available to the experimenter using this bridge.

Ordinarily $Q + D$ is so large a resistance that a negligible fraction of the test current I will by-pass the electrode. If this is suspected not to be the case, an ammeter in series with the wire from G to x (Fig. 6) can be used at the point of total balance (both for emf and resistance) to measure the true applied current. If this is done, the resistance of the meter must be added to x to get the correct internal resistance of the cell. Also, the meter used must have an internal resistance less than that of the cell, to allow for adjustment of x.

There is one implication, on page 276, to which exception may be taken. It is contained in the statement: "Then

$$\frac{I_a}{I_c} = \frac{r_c}{r_a}\frac{(E - e_a)}{(E - e_c)} \qquad \text{(XXIV)}$$

which shows that the partition of current I is determined by the opposing emf as well as by the resistance of each path." This conclusion arises from the direct interpretation of the explicit form of equation (XXIV); actually both I_a and I_c contain the local action current implicitly; hence they do not represent simply the partition of I. When the local action current is recognized and made explicit in the equation, the partition of I is seen to be

---

This Discussion Section includes discussion of papers appearing in the Journal of The Electrochemical Society, **97**, No. 7–12 (July–December 1950).

[1] 1bis Avenue de Lowendal, Paris, France.

[2] P. A. Jacquet, *Compt. rend.*, **202**, 402 (1936); *Bull. soc. chim. France*, 5e Série, **3**, 705 (1936).

[3] Battelle Memorial Institute, Columbus, Ohio.

[4] Sun Physical Laboratory, Sun Oil Company, Newtown Square, Pennsylvania.

independent of both e_c and e_a. This point is correctly emphasized in the text below equation (XV) on page 274, but is contradicted by the implications of the statement under question. The matter can be clarified as follows:

From the text

$$E_G = e_a - i_o r_a \quad \text{(IX)}$$

$$E_G = e_c + i_o r_c \quad \text{(X)}$$

$$I_a = \frac{E - e_a}{r_a} \quad \text{(XII)}$$

$$I_c = \frac{E - e_c}{r_c} \quad \text{(XIII)}$$

$$e_a - e_c = i_o(r_a + r_c) \quad \text{(XV)}$$

$$\frac{E - E_G}{I} = \frac{r_a r_c}{r_a + r_c} \quad \text{(XVII)}$$

Using these equations:

Solve (XVII) for $E = E_G + I\,\frac{r_a r_c}{r_a + r_c}$ (1)

Substitute i_o from (XV) in (IX) to get

$$E_G = e_a - i_o r_a = e_a - \frac{e_a - e_c}{r_a + r_c}\, r_a$$

$$= \frac{r_c}{r_a + r_c}\, e_a + \frac{r_a}{r_a + r_c}\, e_c. \quad (2)$$

Substitute (2) in (1) and obtain

$$E = \frac{r_c}{r_a + r_c}\, e_a + \frac{r_a}{r_a + r_c}\, e_c + I\,\frac{r_a r_c}{r_a + r_c} \quad (3)$$

showing that E contains e_a and e_c implicitly along with I.

Substitute (3) in (XII) for

$$I_a = \frac{E}{r_a} - \frac{e_a}{r_a} = \frac{r_c}{r_a + r_c}\,\frac{e_a}{r_a}$$

$$+ \frac{r_c}{r_a + r_c}\,\frac{e_c}{r_a} + I\,\frac{r_c}{r_a + r_c} - \frac{e_a}{r_a}.$$

Collecting terms

$$I_a = \frac{e_c - e_a}{r_a + r_c} + I\,\frac{r_c}{r_a + r_c} = -i_o + I\,\frac{r_c}{r_a + r_c} \quad (4)$$

Similarly,

$$I_c = \frac{e_a - e_c}{r_a + r_c} + I\,\frac{r_a}{r_a + r_c} = +i_o + I\,\frac{r_a}{r_a + r_c}. \quad (5)$$

Equations (4) and (5) show that I_a and I_c are composed of the algebraic sum of i_o, the local action current, and fractions of I, each according to the law of shunts for the respective branches. The second terms of each expression are the respective partitions of I which now are seen to be independent of e_a and e_c. e_a and e_c uniquely determine i_o, as per equation (XV). If $I = 0$, $I_a = -i_o$ and $I_c = +i_o$, which must be the case since i_o is independent of I, as pointed out on page 274.

I hope that this very excellent technique will be generally used by experimenters to study polarization phenomena by resolving them in terms of emf and resistance components as functions of the applied currents. Data of this kind are useful for analysis and understanding of many complex relations, as in electrolytic corrosion circuits.

H. D. Holler: The comments by Dr. Pearson are appreciated.

Perhaps the simplest way to make allowance for y, the resistance of the half-cell, is to add an equal resistance to the other arm D.

The interpretation of equation (XXIV) depends on how one wishes to define the partition of current. The Müller idea, as expressed in Dr. Pearson's equations (4) and (5), concerns the mathematical components, $I(r_c/r_a + r_c)$ and $I(r_a/r_a + r_c)$. Partition of current I into these components is, of course, their ratio, or r_c/r_a. However, if one is interested in the actual currents I_a and I_c, the true partition of current is that represented by equation (XXIV).

PHASE RELATIONSHIPS IN THE BINARY SYSTEMS OF NITRIDES AND CARBIDES OF ZIRCONIUM, COLUMBIUM, TITANIUM, AND VANADIUM

Pol Duwez and Francis Odell (pp. 299–304)

John W. Graham[5]: It has been shown in this paper that values for the a_0 crystal dimension of TiC, listed from various studies over the past few years, have gradually increased, presumably due to increased purity. It is expected that, as the oxygen content decreases, the a_0 dimension would more nearly approach the theoretical value.

Lately in the Kennametal Laboratory, some TiC, prepared by the Menstrum process, was observed by preliminary x-ray diffraction analysis to have an a_0 crystal dimension of 4.338 Å or 4.329 kx units, somewhat higher than values listed in this paper.

Pol Duwez and Francis Odell: The authors believe that Dr. Graham is correct in saying that the greatest uncertainty in the value of the lattice parameter of TiC is due to differences in carbon content.

Gordon R. Finlay[6]: The value of 4.60 Å for the lattice constant of TiC which is listed by Karl Becker leads to an extremely low calculated density, viz., 4.08 g/ml. All the variations in composition suggested earlier by Dr. Norton would seem to decrease the lattice dimension from the upper limit of 4.338 kx units proposed by Dr. Graham. Can any explanation be offered for the high value reported by Becker? In our experience, all preparations of TiC have a real density in the range of 4.8 to 4.9 g/ml.

Pol Duwez and Francis Odell: The value given by Becker (4.60 Å) is definitely too high, but it is impossible to determine exactly whether this abnormal value was due to a specimen deficient in carbon or to careless x-ray diffraction work.

PREPARATION OF DUCTILE VANADIUM BY CALCIUM REDUCTION

R. K. McKechnie and A. U. Seybolt (pp. 311–315)

W. J. Kroll[7]: I join Dr. Marden in congratulating Mr. McKechnie and Mr. Seybolt for the splendid work

[5] Research Laboratory, Kennametal Inc., Latrobe, Pennsylvania.

[6] Norton Company, Chippawa, Ontario, Canada.

[7] U. S. Department of the Interior, Bureau of Mines, Albany, Oregon.

they have accomplished. I used the same process fourteen years ago[8] but the metal obtained was brittle in the cold state in spite of its high purity of 99.8 per cent.

I doubt that commercial grade of calcium metal, electrolytic or aluminum reduced, could be used for a large-scale reduction of vanadium oxide because of its high cost and relative impurity. It usually contains too much carbon and nitrogen and would have to be redistilled. Whether low-nitrogen calcium metal can be made directly in Pidgeon retorts is questionable because of the porosity of the cast retorts. Also, due to the high reduction temperature of at least 1200°C, at which retort life is short, the aluminum-reduced calcium will remain expensive. Redistilling adds to the cost. Preference should go to attempts at reducing the chlorides of vanadium with magnesium under noble gas, magnesium being purer and cheaper than calcium.

A. C. Loonam[9]: The use by the authors of a mixture of calcium chloride and calcium iodide as a flux instead of the chloride alone is very interesting and may add significantly to the utility of this type of flux. The iodide mixture should have all the advantages of pure calcium chloride, namely, high solvent power for metallic calcium and calcium oxide and low vapor pressure and, in addition, should have a considerably lower melting point. Calcium chloride (mp 773°C) and calcium iodide (mp 740°C) should form a simple eutectic system with a minimum melting point, perhaps around 500°C or even lower. There may be other advantages as well. Calcium bromide (mp 765°C) probably cannot be substituted for the iodide as it should form a continuous series of solid solutions with the chloride with all melting points between those of the pure salts.

R. K. McKechnie and A. U. Seybolt: We wish to thank Dr. Kroll and Dr. Marden for their very kind commendation.

We agree with Dr. Kroll that commercial calcium would be unsatisfactory for large-scale reductions according to the process we have described. The use of magnesium as a reductant has been satisfactorily demonstrated with vanadium trifluoride, although in these reductions we believe that there was a high residual oxygen content in the metal. We have not been attracted by the vanadium chlorides for bomb reduction since the chlorides are generally hygroscopic.

In reply to Dr. Loonam we should merely like to emphasize that we did very little with the calcium chloride-calcium iodide fluxes since we found that the ability to charge additional active ingredients brought greater dividends than were obtained by the use of calcium chloride as a fluxing agent.

HEAT RESISTANCE OF ZIRCONIUM IN SEVERAL MEDIUMS

E. T. Hayes, A. H. Roberson, and R. H. Robertson (pp. 316-323)

R. M. Treco[10]: This work is very timely and clarifies many points concerning the reactivity of zirconium metal produced by the Bureau of Mines with the common gas atmospheres. The reactions of zirconium with hydrogen are of particular interest since the production of zirconium powder depends on the formation of a brittle hydride which can be mechanically comminuted into powder. In this connection I would be interested in the amount of residual hydrogen after the 700°C desorption treatment in vacuum. The second paragraph on page 320 in reference to the softening effect of hydrogen appears to be at variance with our experience and does not agree with the authors' following statement concerning the embrittling effects of hydrogen. Possibly the softening observed can be attributed to annealing of the sheet stock. Finally, if hardness data are available for inclusion with the tensile data they would constitute a valuable addition.

E. T. Hayes, A. H. Roberson, and R. H. Robertson: The data given in the second paragraph on page 320 do present an anomaly in that, although the metal is embrittled by hydrogen at 800°C, it is at the same time softened, suggesting that the embrittlement is truly an intergranular phenomenon. These statements were checked by heating in dry hydrogen at 800°C for 18 hours a sheet of zirconium which previously had been heated at 1500°C for six hours and furnace cooled. Before the hydrogen treatment the Rockwell hardness was B 74. Post treatment Rockwell hardness could not be determined because the specimen was shattered by the ball penetrator. However, Knoop hardness determined with a Tukon hardness tester showed that a decrease from 237 to 176 resulted from hydrogenation. This definitely rules out the possibility of strain relief, since the specimen was fully annealed and the grains were extremely large, having an average diameter of at least $\frac{1}{8}$ inch.

The amount of residual hydrogen after the 700°C desorption treatment was not determined.

Complete hardness data are not available for inclusion with the tensile data.

STUDIES ON ALTERNATING CURRENT ELECTROLYSIS, I

Manuel Shaw and A. Edward Remick (pp. 324-334)

S. Barnartt[11]: During electrolysis of sulfuric acid and some other aqueous solutions, hydrated PtO_2 is formed at platinum anodes. Is it possible that the polarization capacity at platinum electrodes in sulfuric acid solutions during a-c electrolysis could result from irreversible oxide formation rather than from adsorption of hydrogen ion? The drift of polarization capacity with time, which increases as the sulfuric acid concentration increases, might then be correlated with the solubility of anodic platinum oxides, which also increases with sulfuric acid concentration.

A. Edward Remick: The possibility that platinum oxide formation at the electrodes may have an effect on polarization capacity seems very likely, especially in view of our observation that reproducibility of polarization capacity measurements is improved by cathodic cleaning of the electrodes. It is not clear to me, however, how our observed drifts of capacity can be related to the solubility of platinum oxides. I suppose these oxides would be most

[8] W. Kroll, *Z. Metallkunde*, **28**, 30 (1936).

[9] Deutsch and Loonam, 70 East 45th Street, New York, New York.

[10] Sylvania Electric Products Inc., Bayside, Long Island, New York.

[11] Westinghouse Research Laboratories, East Pittsburgh, Pennsylvania.

apt to be formed electrolytically and since, in making our drift studies, the current was turned on only long enough to make each capacitance measurement, it is hard to understand how the combined effect of a steady rate of solubility and the irregular periods of electrolysis could result in a smooth curve when capacitance is plotted against time.

MORRIS FEINLEIB[12]: Is the peak value of the a-c potential corresponding to the capacity elevation point of the same order of magnitude as the d-c decomposition potential of water (in the systems investigated here)? This would lend support to the authors' theory that the capacity elevation point is associated with the electrolysis of water.

Were any electrodes other than platinum tried in these investigations, and, if so, does the choice of electrode affect the capacity elevation point or the polarization capacity at a given frequency and current density?

A. EDWARD REMICK: The peak value of the a-c potential corresponding to the capacitive elevation point varies from 0.113 to 0.124 volt over the frequency range from 400 to 1000 cycles per second. This is the potential drop across the double layer as calculated from equation (VIII) and presumably corresponds to the overvoltage. Adding to this value the reversible potential of the hydrogen-oxygen cell, viz., 1.23 volts, gives us about 1.35 volts for the decomposition potential of water. The accepted value of 1.67 volts for said decomposition potential includes the so-called "bubble overvoltage" of water. Certainly our overvoltage is not a bubble overvoltage inasmuch as we never observed any gas bubbles on our electrodes. Our value of the decomposition potential thus might reasonably be supposed to be lower than 1.67 volts and on the whole seems to support the idea that the capacitive elevation point corresponds to the onset of the reaction $H_3O^+ + e \leftrightarrows H_2O + H$. No electrodes other than platinum were used in determining the capacitive elevation point.

G. W. THIESSEN[13]: As a corollary of capacity being a minimum when ratio of oxidant/reductant = ∞ or 0, and a maximum when it is unity, it would follow that an electrometric location of end point in a redox titration could be located by capacitance measurement.

A. EDWARD REMICK: Yes, it could, but due consideration would have to be given to the effect of variable concentration, as shown in Fig. 8.

N. F. MURPHY[14]: Apparently, the capacities given were the combined chemical and physical capacities of the cell. Is this correct?

A. EDWARD REMICK: The values of C_S represent the total capacity, as shown by the equation $C_S = C_o + C_h + C_P$ given on page 331.

J. V. PETROCELLI[15]: This is a very interesting paper and represents an approach to the study of electrode reactions which should prove fruitful.

It may be worthwhile to point out that we have been concerned with similar techniques and measurements in our laboratory for some time, and that our results also show extremely high capacitance values for some electrode systems. Thus, in solutions about 0.25 molar in ferric and ferrous chloride, we have obtained polarization capacitance values as high as 800 microfarads/cm^2.

I should like to ask Dr. Remick if he has made any attempt to explain his results on the basis of concentration polarization effects such as the treatment given by Randles[16].

A. EDWARD REMICK: Randles treats the concentration polarization effect in terms of Fick's diffusion law, much as Warburg did years ago. As is evident from our paper, we did give some consideration to the Warburg equation, as shown on page 329. We have not attempted any further quantitative correlation of our results with the diffusion law although, of course, we used the idea qualitatively throughout our paper.

There are two errors which appear in the printed version of the paper. In Table II the frequencies listed for system 2 are all ten times too large. Equation (V) should have been printed as follows:

$$I = \frac{\pi q_2^{\frac{1}{2}} f}{\sqrt{2}}.$$

STUDIES ON ALTERNATING CURRENT ELECTROLYSIS, II

Jacob Silverman and A. Edward Remick (pp. 335–345)

G. W. THIESSEN[17]: At Monmouth College, we did "slow motion" electrolysis, running current (I) from 0 to arbitrary maximum (I_0), down to 0, reverse to previous numerical maximum ($-I_0$), and back to 0, and corresponding voltages (E) were read. I was set equal to $I_0 \sin(wt)$ or $I_0 \sin\alpha$, and α was calculated for each I, and α was made the X axis. Against $\alpha = wt = X$ was plotted I in one curve, E in the other. The displacement between maximums of E and I curves was taken as measuring phase angle of lag, from which it was intended to calculate the "capacitance" of the cell. Poor reproducibility on successive cycles led us to abandon the idea. The oscillograph was not available to us then (1932). But perhaps the oscillograms could be retranslated to this plot. The poor cyclic reversibility was to be shown by polar coordinates, letting $P = I$ and E, and the polar angle = α; but we never did it. This plot might make the electrical engineers happier!

A. EDWARD REMICK: I would not expect that a-c oscillograms could be retranslated to Thiessen's plot. The effect of concentration polarization would be very different in the two cases—so also might be the kind and concentration of material deposited on the electrode.

ELECTRODEPOSITION OF METAL POWDERS

Gustaf Wranglen (pp. 353–360)

G. L. PUTNAM[18]: The experiments described by Dr. Wranglen are of interest in that they qualitatively present the conditions necessary for metal powder deposition.

One or two of the theoretical interpretations, however, may be open to some criticism. There is no evidence, for example, that low metal overvoltage, per se, is responsible for metal powder formation. It would seem equally correct

[12] Armour Research Foundation, Chicago, Illinois.
[13] Monmouth College, Monmouth, Illinois.
[14] Virginia Polytechnic Institute, Blacksburg, Virginia.
[15] The Patent Button Company, Waterbury, Connecticut.
[16] J. E. B. RANDLES, *Disc. Faraday Soc.*, **1**, 11 (1947).
[17] Monmouth College, Monmouth, Illinois.
[18] University of Washington, Seattle, Washington.

to say that low recrystallization temperature[19], low melting point, or low tensile strength promote powder deposition.

The author's emphasis on cathode film conditions is well taken. Conditions at the site of the reaction, the cathode surface, control the reaction, bulk electrolyte compositions, temperature, etc., being important only insofar as they affect conditions at the cathode surface. Thus for a given current density and natural convection, the metal ion concentration in the cathode-electrolyte interface will increase as the size of the cathode increases, as quantitatively shown by Wagner[20]; and in the deposition of cadmium and copper powders, alkali salts may greatly influence the result by altering the metal ion concentration at the cathode surface, since the salt can sometimes cause large increases in the *p*H at the cathode surface.

Progress is being made toward the calculation of the conditions obtaining at electrode surfaces[21, 22] and it is hoped that it will eventually be possible to describe industrial processes in terms of such conditions.

Gustav Wranglen: I am very much obliged to Dr. Putnam for his valuable discussion. Dr. Putnam is right that it is doubtful whether low metal overvoltage should be put up as a factor responsible for metal powder formation. It is certain, however, that the metals with low overvoltage are much more easily obtained in powder form than the high overvoltage metals. It seems a matter of taste as to how this fact should be expressed. As for the other properties mentioned by Dr. Putnam, it was pointed out by Tammann and Jaachs[23] that they coincide with low metal overvoltage.

Although the conditions favoring metal powder deposition seem rather clear, much work is still to be done (or at least to be published) to obtain quantitative relationships. It is still not possible to say which conditions should be used to get a certain desired screen analysis and good flow, structure, and density properties without subsequent heat treatment, ballmilling, etc., of the powder. However, in the case of copper, the recent work by Putnam and collaborators[24] has done much to clarify the situation. It is not certain, however, and for other reasons than those mentioned in the paper, that in a case as this the traditional electrolyte, slightly modified from refining, is the best. Gassing in a strongly acid solution is always very troublesome in a technical plant. For the problem of separating metal powder and anode slimes, be it done by revolving cathodes and scrapers or by anode bags, a less corrosive electrolyte is also desirable. Finally, there is the problem of washing and drying the powder without oxidation, which in most cases is a difficult one.

[19] R. S. Williams and V. O. Homerberg, "Principles of Metallography," 4th ed., p. 77, McGraw-Hill Publishing Co., Inc., New York (1939).

[20] C. Wagner, *J. (and Trans.) Electrochem. Soc.*, **95**, 161 (1949).

[21] T. R. Beck and G. L. Putnam, *Ind. Eng. Chem.*, **43** (1951).

[22] C. S. Lin, H. S. Gaskill, E. B. Denton, and G. L. Putnam, *Ind. Eng. Chem.*, **43** (1951).

[23] G. Tammann and H. Jaachs, *Z. anorg. u. allgem. Chem.*, **227**, 249 (1936).

[24] D. W. Drumiler, R. W. Moulton, and G. L. Putnam, *Ind. Eng. Chem.*, **42**, 2099 (1950).

PLATING EXPERIMENTS WITH AQUEOUS SOLUTIONS AT HIGH TEMPERATURES

Seymour Senderoff and Abner Brenner (pp. 361-366)

M. L. Holt[25]: If an atmosphere of hydrogen were used in these high pressure, high temperature cells, would it not be possible in the case of copper solutions that the metal in the bottom of the cell was the result of displacement by hydrogen? There are cases mentioned in the literature of displacement of Cu^{++} by hydrogen under high pressure.

Semour Senderoff and Abner Brenner: Although Ipatieff reported that copper ion was replaced by hydrogen at high temperature and pressure, this could not have occurred in this case since the run was made under nitrogen.

R. A. Schaefer[26]: The authors spoke of "complete and instantaneous polarization" in their experiment work. I would appreciate further explanation of this phrase, including how the measurements were made.

Seymour Senderoff and Abner Brenner: On page 364, column 2, we refer to "almost instantaneous polarization." We mean by this phrase that the potential drop between the anodes and solution equaled the applied potential of 12 volts, and that no appreciable current passed. By instantaneous we mean that it occurred too rapidly for us to measure the time of build-up of polarization by ordinary methods, i.e., ammeter and voltmeter.

On page 366 we refer to "completely passive" anodes. We mean that no current would pass at 12 volts using an ordinary ammeter and voltmeter for measurement.

INSTRUMENTATION IN A MODERN CHLORINE HANDLING PLANT

J. M. Hildyard (pp. 367-376)

Leonard A. Harris[27]: What has been your experience with motor valves in liquid chlorine service? Is there a type which is comparatively trouble-free, yet reasonably leakproof?

J. M. Hildyard: We do not have many applications for using motor valves on liquid chlorine, therefore our experience is rather limited. The valves we do have, however, are of the same construction as those we use for gaseous chlorine. The only difference is that the stuffing boxes give less trouble on liquid service.

It is important that the action of the valve and the superstructure be chosen so that the packing gland is on the high pressure side of the valve port. This is the opposite of normal valve operation. The reason for this is that sometimes flashing will occur in the downstream portion of a valve body. Flashing will reduce the temperature of the chlorine and may permit dissolved materials to drop out and coat the downstream parts of the valve body. The

[25] University of Wisconsin, Madison, Wisconsin.

[26] Cleveland Graphite Bronze Company, Cleveland, Ohio.

[27] Columbia Chemical Division, Pittsburgh Plate Glass Company, Barberton, Ohio.

reversal of the valve body permits the stem to operate at a higher temperature.

RUSSELL E. CUSHING[28]: With reference to the valves which you employ for controlling the pressure in the individual cell rooms, what type of valve is used? Are they commercially available or are they of your own design and construction?

J. M. HILDYARD: The motor valves we use in our cell rooms are of our own design and construction. We have tried both slide and butterfly types. Either type operates satisfactorily if the correct materials of construction are chosen.

THE KINETICS OF THE REACTIONS OF BERYLLIUM WITH OXYGEN AND NITROGEN AND THE EFFECT OF OXIDE AND NITRIDE FILMS ON ITS VAPOR PRESSURE

Earl A. Gulbransen and Kenneth F. Andrew (pp. 383–395)

W. C. LILLIENDAHL[29]: Since the vapor pressure of beryllium is affected by oxide films, does the data which are in agreement with other authors indicate that the solid solubility of oxygen in Be is very low since the metal used was supposed to contain an appreciable per cent of BeO?

EARL A. GULBRANSEN AND KENNETH F. ANDREW: We don't think one can draw any definite conclusions from the data on the solubility of oxygen in beryllium since one would need to know how sensitive the vapor pressure of beryllium is to the solubility of oxygen. The conclusion we draw is that volatile impurities are the critical factor affecting the vapor pressure.

C. H. TOENSING[30]: Does the surface roughness influence the entropy term in the equation

$$K = \frac{2kT}{h} \lambda^2 e^{\Delta S^*/R} e^{-E/RT}$$

EARL A. GULBRANSEN AND KENNETH F. ANDREW: We have not studied this point. It is rather difficult to say whether the surface roughness affects E or S since a variation in surface roughness alone is difficult to achieve experimentally. Thus, changing the surface roughness changes the orientation and state of subdivision of the crystallites of the metal in the surface as well as influencing the oxide film formation. In using the rate equation it is advisable not to use it in the thickness region where the surface roughness factor is changing rapidly, i.e., during the initial stage of the reaction.

SIDNEY BARNARTT[31]: Preliminary formation of a nitride film accelerated the rate of oxidation. Did a solid solution of oxide and nitride form on the surface during the oxidation? If not, the accelerated oxidation is probably due to the formation of a cracked film of mechanically mixed oxide and nitride phases on the surface.

EARL A. GULBRANSEN AND KENNETH F. ANDREW: We have not investigated whether a solid solution of oxide and nitride is formed. The mechanism suggested by Dr. Barnartt is a possible one although stated in too simple a form. It is of interest to note that the acceleration of the rate of reaction extends to the initial stage of the reaction. No visible evidence of cracking was found on the film although this may have occurred microscopically.

ALAN U. SEYBOLT[32]: If the reaction temperature were increased to between 1200° and 1400°C instead of in the region of 600°C, then the form of the weight gain - time curves might be different. This could occur because of some of the oxygen or nitrogen going into solid solution, in cases where there was an appreciable solid solubility.

EARL A. GULBRANSEN AND KENNETH F. ANDREW: The weight gain vs. time curves would probably be very different in the temperature range of 1200° to 1400°C. Above a certain temperature range in the oxidation of aluminum and magnesium we have found that the familiar parabolic rate law shifts to a linear rate law. This is in the temperature range where the vapor pressure of the metal is becoming appreciable. The same phenomena may occur with beryllium above 1000° to 1100°C where the vapor pressure is becoming appreciable.

THE KINETICS OF THE REACTIONS OF VANADIUM WITH OXYGEN AND NITROGEN

Earl A. Gulbransen and Kenneth F. Andrew (pp. 396–404)

W. C. LILLIENDAHL[33]: To obtain a clear picture of the process of nitrogen or oxygen pickup, it would appear that we should consider two basic reactions: (1) the surface oxidation or nitriding of the surface, and (2) the rate of solution of these films into the metal lattice. Thus, exceeding a critical temperature for each metal, the weight gain might be expected to be related to the rate of diffusion into the metal lattice as well as surface film formation.

EARL A. GULBRANSEN AND KENNETH F. ANDREW: We are in agreement with your picture. It is well illustrated in the oxygen pickup by zirconium.

ROBERT L. HADLEY[34]: In connection with increased rate of nitrogen solution after solution of an oxide film at 850°C, it seems likely that the presence of the oxygen would significantly increase the lattice parameter of the vanadium. This might tend to make nitrogen solution more rapid.

EARL A. GULBRANSEN AND KENNETH F. ANDREW: We think this is a possible interpretation.

REFINING OF MAGNESIUM BY VAPORIZATION AT EXTREMELY LOW PRESSURE

R. R. Rogers and G. E. Viens (pp. 419–424)

A. W. SCHLECHTEN[35]: The authors have made a contribution to a subject, the vacuum distillation of metals, which is of great current interest. The removal of zinc from lead bullion by vaporization under vacuum has been

[28] Pennsylvania Salt Manufacturing Company, Wyandotte, Michigan.

[29] Westinghouse Electric Corporation, Bloomfield, New Jersey.

[30] The Brush Beryllium Company, Cleveland, Ohio.

[31] Westinghouse Research Laboratories, East Pittsburgh, Pennsylvania.

[32] Knolls Atomic Power Laboratory, Schenectady, New York.

[33] Westinghouse Electric Corporation, Bloomfield, New Jersey.

[34] General Electric Company, Schenectady, New York.

[35] School of Mines and Metallurgy, University of Missouri, Rolla, Missouri.

a decided commercial success, and there may be many other applications such as the one suggested in this paper.

The very low pressures recorded in this paper are a tribute to the excellent construction of the apparatus and also to the pumping capacity of the large diffusion pump which was used. A question arises as to whether the results obtained at 0.05 microns are any different than those that would be obtained at 5 or even 50 microns. This point is of importance because the 0.05 micron pressure would be very difficult to maintain on a commercial scale.

The use of a vacuum in distillation has two main purposes: to protect the metal or metals from oxidation and to increase the rate of evaporation. Pidgeon reported that in the ferrosilicon-dolomite process no improvement in yield was noted at two microns as compared with 100–200 microns. St. Clair and Spendlove of the U. S. Bureau of Mines have reported careful determinations on the rate of evaporation of zinc versus residual gas pressures; one series of tests showed no increase in rate below pressures of 100 microns. A second series of tests are not as conclusive; there seems to be some improvement below 100 microns but the data are scattered.

P. C. Carman writing in the 1948 *Transactions of the Faraday Society* states that in the distillation of liquids or the evaporation of solids the following equation gives the relation between rate of evaporation and the residual gas pressure when P is less than π.

$$W = W_o\left(1 - \frac{P}{\pi}\right)$$

where W = rate of evaporation, W_o = the maximum rate, P = the pressure above the liquid or solid, and π is the saturation vapor pressure of the solid or liquid.

Taking Run No. 4 as an example, at 600°C the vapor pressure of magnesium would be close to 880 microns. The distillation rate under a residual gas pressure of 0.05 microns according to the above equation would be 99.9944 per cent of the maximum rate. At a residual gas pressure of 5 microns the measured rate would be 99.44 per cent maximum, and at 50 microns it would be 94.4 per cent maximum.

This loss of 5.6 per cent in the evaporation rate resulting from operation at 50 microns rather than 0.05 microns is not very serious as it could be compensated for by a temperature increase of 2°C.

At lower temperatures the difference in evaporating rates between operating pressure of 0.05 and 50 microns would be greater; at higher temperatures it would be less.

R. R. Rogers and G. E. Viens: Dr. Schlechten's remarks deal largely with the effect of pressure on evaporation rate and yield. Since only one pressure was used in the work which we have reported, our paper does not contain any conclusions with regard to the effect of pressure. We were concerned particularly with the efficiency with which the alloying metals could be removed from the magnesium, i.e. with the efficiency with which the magnesium could be refined. We also wished to determine the lowest temperature at which the process could be operated satisfactorily. Obviously the success of the process would be determined to a considerable extent by these two considerations.

DETECTION OF SOIL REMOVAL IN METAL CLEANING BY THE RADIOACTIVE TRACER TECHNIQUE

J. C. Harris, R. E. Kamp, and W. H. Yanko (pp. 430–432)

Abner Brenner[36]: The paper shows that the appearance of water break on a metal surface is second only to the radioactive method in sensitivity. I believe that the method of employing water break which was used by the authors could have been made much more sensitive if they had immersed the cleaned and rinsed specimen in a weak acid dip before examining it. Frequently a metal specimen may be removed from an alkaline cleaner and rinsed without showing a water break, but as soon as it is acid dipped it will develop a water break.

The radioactive method of examining a surface for soil removal is satisfactory for many purposes, but I believe that for purposes of electrodeposition the final test is to electrodeposit a coating on the surface and then make an adhesion test. A standardized test of this kind would be the most practical test for electroplating.

J. C. Harris, R. E. Kamp, and W. H. Yanko: It is agreed that subjecting the specimen to a weak acid dip might have removed any hydrophilic film, to show water break if present. However, in practice, the specimen would not necessarily be so treated and would therefore appear to be clean. We agree that an electrodeposited coating is the best test for cleanliness of surfaces to be electroplated.

Walter B. Kleiner[37]: Is the C_{14} sufficiently radioactive to determine the distribution on the surface by self-photographing? This would answer some of the previous questions as to distribution.

J. C. Harris, R. E. Kamp, and W. H. Yanko: The suggestion concerning radiography as a means for determination of distribution of radioactive tracer is an excellent one and should be followed.

W. A. Raymond[38]: First, I would like to compliment the authors on having done a very fine job in this paper. I believe it is the best paper on cleaner evaluation in recent years.

Their results on the sensitivity of various cleaning tests now in wide usage is especially interesting (Table II). The fact that both the water-break test and Hogaboom's copper sulfate test are shown to be more sensitive than the fluorescent dye technique is probably contrary to common thinking, and, therefore, quite significant.

I think that, with radioactive tracer techniques, we at last have a method sensitive enough to permit accurate and reproducible cleaning test results.

Table II also points out the relative insensitivity of the fluorescent dye technique discussed in Morgan and Hoyt's paper. For instance, 0.26 per cent of residual soil gave a negative fluorescent dye test (Mr. Hoyt would have called this "perfect" cleaning), but the samples still showed water break and lack of complete coppering in the Hogaboom copper sulfate test. Experience has shown that such a condition would not permit good quality, adhesive electrodeposits.

This paper would indicate that residual soil should not

[36] National Bureau of Standards, Washington, D. C.

[37] Central Research Laboratory, American Smelting & Refining Company, Perth Amboy, New Jersey.

[38] *Metal Finishing*, New York, New York.

exceed 0.10 per cent (or $2\text{–}2.4 \cdot 10^{-6}$ g/cm^2) if adherent plating of acceptable commercial quality is to be guaranteed.

M. L. Holt[39]: The authors mention that one of the limitations of the technique described is the small amount of surface that can be used due to the area of the counter window. Would it not be possible to use a larger surface area and cut it into sections small enough for the counter, thus also solving the problem of counting over the whole larger surface area?

J. C. Harris, R. E. Kamp, and W. H. Yanko: Perhaps it might be possible to cut the soiled or washed specimens for examination, but an even better procedure would be to use the same or a slightly larger specimen which could be introduced as a complete sample into a counting chamber. Further sensitivity of method could be attained through the use of a proportional counter.

J. J. Bikerman[40]: It should be possible to utilize the excellent method worked out by Harris, Kamp, and Yanko also for estimating the surface roughness of a specimen. Spread a standard amount of the standard soiling composition on the specimen surface. Rub this with some bibulous material, again in a standardized manner. The amount of soil remaining on the surface certainly will, as a rule, be greater the rougher the surface.

J. C. Harris, R. E. Kamp, and W. H. Yanko: Dr. Bikerman's suggestion that the tracer method be used for estimating surface roughness is an interesting one and might prove of much value in such work.

STUDIES OF TIME-POTENTIAL CHANGES ON AN ELECTRODE SURFACE DURING CURRENT INTERRUPTION, I

Sigmund Schuldiner and Roger E. White (pp. 433–447)

Herbert C. Cocks[41]: I realize that the investigations described are preliminary, but it appears to me that the authors have concentrated on the decay, rather than the build-up, of polarization. Would the authors care to comment on the speed of build-up relative to that of decay, and would they give their views on the relative values of electrode potential, which exists when the polarizing current is interrupted, compared with that when the current is continuous, i.e., does the fact that the current is interrupted, for however short a time, affect the value of the potential? Glasstone[42] apparently found that, at least at low current densities, the value for the two types of current was the same.

In this connection, it may be of interest to note that measurements of the deposition potential of zinc-nickel alloys gave approximately the same value whether the polarizing current was a simple direct current or a pulsating direct one of approximately the same value. The pulsating current was a 50 cycle/sec one. The measurements referred to[43] were, however, made by the "direct" method.

Sigmund Schuldiner and Roger E. White: A typical example of the relative rate of polarization decay to build-up time can be seen in Fig. 10 of the paper. From this figure the decay time was approximately 50 microseconds whereas the build-up time was about 20 microseconds. A relatively faster build-up time is also expected from the electrical analogy of the double layer which we have assumed. This can readily be seen from the discharge and charge equations

$$E_C = Ee^{-t/R_pC} \qquad \text{(I)}$$

$$E_C = E\left(\frac{R_p}{R_s + R_p}\right)(1 - e^{-t/C(1/R_s+1/R_p)}) \qquad \text{(II)}$$

for this electrical analogy. From (I) the time constant for potential decay is R_pC, while the time constant for potential build-up is seen from equation (II) to be $C\left[\frac{1}{1/R_s + 1/R_p}\right]$ which is equal to $C\left(\frac{R_sR_p}{R_s + R_p}\right)$. Since $\frac{R_sR_p}{R_s + R_p}$ is always less than R_p, the rate of build-up will always be faster than the rate of decay.

The interrupter method we have used has been designed to give electrode potentials which are the same as for continuous currents. It has been observed on our potential traces that the potential after interruption builds up to the same value as before decay. The duty cycle of one per cent interruption time and the pulse repetition rate are such that there is sufficient time to bring the electrode potential to the same value as before interruption.

EFFECT OF MAGNETIC TRANSFORMATION AT THE CURIE TEMPERATURES ON OXIDATION RATES OF CHROMIUM-IRON ALLOYS

H. H. Uhlig and Anton de S. Brasunas (pp. 448–452)

Earl A. Gulbransen[44]: (1) Your analysis assumes a reaction rate which is independent of thickness for a given temperature. Has this been experimentally verified?

(2) Have you tried plotting W^2/t or the parabolic rate law constant against $1/T$?

(3) Is it not possible on your plot of the weight gain after 24 hours against $1/T$ that a curve is obtained which gives the appearance of two separate straight lines intersecting more or less at the Curie point?

(4) Do you obtain the same energy of activation on plotting the weight gain after six hours against $1/T$ as you get for the twenty-four hour data?

H. H. Uhlig and Anton de S. Brasunas: (1) Our analysis assumes that the weight gain or thickness of film varies linearly with the logarithm of time of exposure at a given temperature. This relation has been accurately established for thin films by many investigators including Tammann, Vernon, Mehl, and their co-workers. According to the logarithmic relation, the rate of reaction dw/dt, where w is the weight gain proportional to the film thickness, is inversely proportional to the time of exposure t.

[39] University of Wisconsin, Madison, Wisconsin.

[40] 45-35 46th Street, Woodside, Long Island, New York.

[41] "Halfway," Onslow Crescent, Woking, Surrey, England.

[42] S. Glasstone, *J. Chem. Soc.*, **123**, 2926 (1923).

[43] H. C. Cocks, *Trans. Faraday Soc.*, **24**, 354 (1928).

[44] Westinghouse Research Laboratories, East Pittsburgh, Pennsylvania.

Hence the rate is an exponential function of the film thickness since from the relation

$$w = k \log (t + 1)$$ it follows that $dw/dt = ke^{-w/k}$*.

Our analysis, therefore, does *not* assume the rate independent of thickness. In fact, we would not expect such a relation to hold except where the linear rate equation applies as in the oxidation of tungsten[45], molybdenum[46], and the alkali metals.

(2) The parabolic rate equation does not satisfactorily apply to our data nor to similar data obtained by several other investigators. A detailed discussion of this matter for copper is included in "Low Temperature Oxidation of Single Crystals of Copper" by Lustman and Mehl[47].

(3) We do not feel that the two experimental straight lines intersecting at the Curie temperature for each alloy is a matter of accident. In fact the experimental data are convincing evidence that the activation energies for oxidation at the reported temperatures above and below the Curie temperature differ by measurable amounts. Our conclusion, that a change in rate of reaction occurs at the electronic change in the alloy at the Curie temperature, confirms the same earlier conclusion by G. Tammann. Furthermore, the data of McAdam and Geil, plotted in similar form to our data, also support this conclusion.

(4) Although our main conclusion that the Curie temperature divides two activation energies is adequately established by the data, the values of activation energies were reported with no intent that these should be considered of high accuracy. Surface preparation of the specimens, as we mention in the paper, was the main factor making it difficult to closely reproduce slopes of log weight gain vs. reciprocal of the absolute temperature. We have no information, as yet, comparing the activation energies for six hour exposure with twenty-four hour exposure. It is our expectation, however, that with reproducible surface preparation the activation energies would probably be identical. The reason for choosing the two testing times, namely six and twenty-four hours, was to obtain approximately equivalent weight gains corresponding to oxide thicknesses in the interference color region.

It is our hope that other workers in this field will repeat work on thin oxide films for other ferro-magnetic metals, since it is expected that the effect observed by Tammann and by us has considerable significance and bearing on the mechanism of initial oxidation rates.

U. R. Evans[48]: The authors honor me by citing fifteen pages of my book as a reference for the "current theory" of oxidation, which lays emphasis on the part played by the oxide as a diffusion barrier. It is perhaps permissible to point out that the possibility of the oxidation-rate being affected by reactions at the interfaces as well as by movement through the film has, from the first, been emphasized in the views put forward from Cambridge. A paper presented, by invitation, to the Detroit Meeting of The Electrochemical Society twenty-six years ago, developed a modified equation which introduced both chemical and physical effects[49]. This equation may be written

$$\frac{dy}{dt} = \frac{k_0 k_1 C_0}{k_1 y + k_0}$$

where C_0 is the concentration of the nonmetal outside the film, y is the film thickness at time t, k_0 is a physical (diffusion) constant, and k_1 a chemical (reaction) constant. The modified equation is itself parabolic, and the "ordinary" (Pilling-Bedworth) parabolic equation and the rectilinear equation are its two limiting cases. It was afterward found by Fischbeck[50] to be obeyed when steam acts on iron. Meanwhile at Cambridge, Bannister[51] had found that the action of iodine (dissolved in chloroform) on silver, which obeys the "ordinary" parabolic law ($dy/dt = k/y$) at relatively large film thicknesses, departs from it at small thicknesses, while Wilkins and Rideal[52] had found that the action of oxygen on copper, which obeys the "ordinary" parabolic law at normal oxygen pressures, departs from it at very low pressures; in the latter case, the departure is probably due to failure of the oxygen to arrive at the external surface of the film at a rate sufficient to keep up with the velocity at which copper cations could arrive by diffusion—as explained in the section of my book quoted by the authors. The work on platinum by Rideal and Wansbrough-Jones[53], also quoted by them, was carried out at temperatures and pressures chosen to cause the oxide to volatilize immediately; here there could be no question of control by the rate of movement through a film.

There is no difficulty in agreeing with the authors when they say that the base metal cannot always be ignored. The fact that the reaction proceeding either at the internal or external surface of the film may sometimes influence the oxidation rate, can, in the simplest cases, be recognized by a departure from the "ordinary" parabolic law in the direction of a rectilinear law. However, for iron alloys, the position is not simple. Even unalloyed iron forms three layers of oxide; Bénard and Coquelle[54] state that the innermost layer grows according to the parabolic law, and the two others according to the rectilinear law. If the iron contains chromium, there is a gradual accumulation

* Dr. C. Wagner points out that, to be dimensionally correct, the logarithmic equation should be expressed in the form

$$W = k \log (t + \tau) - k \log \tau$$

where τ is a constant with dimensions of time. The same reasoning as is outlined above applies using this equation.

[45] B. Lustman, *Metal Progress*, **57**, 629 (1950).

[46] E. Scheil, *Z. Metallkunde*, **29**, 209 (1937).

[47] B. Lustman and R. F. Mehl, *Trans. Am. Inst. Mining Met. Engrs.*, **143**, 246 (1941).

[48] Cambridge University, England.

[49] U. R. Evans, *Trans. Electrochem. Soc.*, **46**, 269 (1924).

[50] K. Fischbeck, *Z. Elektrochem.*, **40**, 522 (1934).

[51] U. R. Evans and L. C. Bannister, *Proc. Roy. Soc. (London)*, **A125**, 389 (1929).

[52] F. J. Wilkins and E. K. Rideal, *Proc. Roy. Soc. (London)*, **A128**, 394, 407 (1930); F. J. Wilkins, *J. Chem. Soc.*, **1931**, 330; *Phil. Mag.*, **11**, 422 (1931).

[53] E. K. Rideal and O. H. Wansbrough-Jones, *Proc. Roy. Soc. (London)*, **A123**, 202 (1929).

[54] J. Bénard and O. Coquelle, *Compt. rend.*, **222**, 884 (1946); *Métaux & corrosion*, **25**, 241 (1950).

of chromium oxide at the base of the film, as shown by Pfeil[55], and by Portevin, Prétet, and Jolivet[56]; it is generally considered that this layer of chromium oxide provides the protection. The French investigators found the parabolic law to be obeyed by alloys containing 6 per cent chromium, above which value a decision became difficult owing to the slow attack.

It may be difficult to apply a test based on the form of the oxidation-time curve to decide whether control due to surface reactions is responsible for any anomalies observed at either allotropic or magnetic change-points. Until this has been done, the decision must remain in doubt. There are many established cases where an oxidation rate is affected not only by passage through the film, but also by a reaction occurring at one of the film boundaries; it is not, however, quite certain that this is true of the cases described in the paper.

H. H. Uhlig and Anton de S. Brasunas: Dr. Evans points out correctly that iron and the chromium-iron alloys oxidize according to the parabolic equation, presumably where relatively thick films are formed. For thin films, however, as we point out in our paper, data for iron by Tammann and Vernon indicate that the logarithmic equation is obeyed. It is our impression that this is the situation one expects, namely that in the case of thick films the parabolic equation holds, whereas for thin films the logarithmic equation rate is applicable.

Dr. Evans also points out that control of the reaction rate for thin films, such as we were concerned with in our experiments, may occur at one of the film boundaries of the oxide layer. If this were true, there is a question whether one would logically expect the Curie temperature to have any effect on the course of the reaction. It would be possible only if one could demonstrate that the oxide formed just above the Curie temperature significantly differs as a diffusion barrier and electric conductor from oxide formed just below. Perhaps this experiment should be done, whatever the expected results.

It seems more direct to us, however, to ascribe to the metal such changes as occur at the Curie temperature and that these in turn affect electron emission. This model agrees with the mechanism of initial oxidation rate proposed by N. F. Mott.

Admittedly, our paper only indicates where the initial reaction control may be located, but does not prove it. We should like to point out, however, that what we did prove, with some measure of success, is that the Curie temperature, which is an electronic transition within the alloy, significantly affects the initial oxidation reaction of the chromium-iron alloys.

[55] L. B. Pfeil, *J. Iron Steel Inst.* (*London*), **119**, 526 (1929).

[56] A. Portevin, E. Prétet, and H. Jolivet, *J. Iron Steel Inst.* (*London*), **130**, 219, 221, 242, 249 (1934).

DECEMBER 1951 DISCUSSION SECTION

A Discussion Section, covering papers published in the January–June 1951 Journals, is scheduled for publication in the December 1951 issue. Those who plan to contribute remarks for this Discussion Section should submit their comments or questions in triplicate to the Managing Editor of the Journal, 235 West 102nd Street, New York 25, N. Y., not later than August 15, 1951. All discussions will be forwarded to the author, or authors, for reply before being printed in the Journal.

THE ELECTROCHEMICAL SOCIETY, INC.

The Electrochemical Society is an international organization of individuals and companies concerned with or interested in Electrochemistry and allied subjects.

The Society is dedicated to the advancement of the theory and practice of Electrochemistry and related subjects, as shown in the following divisions:

Battery	Electro-Organic
Corrosion	Electrothermic
Electric Insulation	Industrial Electrolytic
Electrodeposition	Theoretical Electrochemistry
Electronics	

Among the means to this end are the holding of meetings for the reading and discussion of professional and scientific papers on these subjects, the publication of such papers, discussions, and communications as may seem appropriate, and cooperation with chemical, electrical, and other scientific and technical societies.

It is an incorporated society without capital stock. The affairs of the Society are managed by a Board of Directors under a Constitution and By-Laws. Officers are nominated by a nominating committee appointed by the Board of Directors and elected by the members.

Direct all general correspondence and inquiries regarding membership to Society headquarters at 235 West 102nd Street, New York 25, N. Y., c/o Mr. W. J. Holian, Assistant Secretary.

Officers of the Society

President ..... RALPH M. HUNTER
Past President ..... CHARLES L. FAUST
Vice-President ..... J. C. WARNER
Vice-President ..... ROBERT J. MCKAY
Vice-President ..... MARVIN J. UDY
Treasurer ..... E. GIDEON WIDELL
Secretary ..... HENRY B. LINFORD